TRANSFORMER PROTECTION BASED ON DYNAMIC STATE ESTIMATION

A Dissertation
Presented to
The Academic Faculty

by

Rui Fan

In Partial Fulfillment
Of the Requirements for the Degree
Doctor of Philosophy in the
School of Electrical and Computer Engineering

Georgia Institute of Technology
August 2016

TRANSFORMER PROTECTION BASED ON DYNAMIC STATE ESTIMATION

Approved by:

Dr. A.P. Meliopoulos, Advisor
School of Electrical and Computer Engineering
Georgia Institute of Technology

Dr. Ying Zhang,
School of Electrical and Computer Engineering
Georgia Institute of Technology

Dr. Maryam Saeedifard
School of Electrical and Computer Engineering
Georgia Institute of Technology

Dr. Andy Sun
School of Industrial and Systems Engineering
Georgia Institute of Technology

Dr. David G. Taylor
School of Electrical and Computer Engineering
Georgia Institute of Technology

Date Approved: July 14, 2016

To my beloved parents Xiancheng and Silun and my wife Xiaoxia

ACKNOWLEDGEMENTS

The doctoral study at Georgia Tech is an exciting and rewarding journey. I would not have accomplished this great achievement without the support and help of countless people. I would like to express my sincere gratitude to all of them.

First of all, I want to specifically thank my professor, Dr. Sakis Meliopoulos, for not just being my advisor, but also a mentor. He is an erudite professor who provide the guidance through my graduate program. His patience and endless support helped me overcome numerous difficulties and I could not have imagined having a better advisor and mentor for my doctorial study. I would also like to thank Dr. George Cokkinides, who always help me with the experimental work during my research. His professional expertise is always excellent and admirable.

Additionally, I would like specially give thanks and appreciation to the members of my committee, Dr. David Taylor, Dr. Maryam Saeedifard, Dr. Andy Sun, and Dr. Ying Zhang, for providing feedback and commentary to my dissertation. Their time, commitment, and expertise have played important roles in my research.

Special thanks go to all my fellows of the Power Systems Control and Automation Laboratory (PSCAL) at Georgia Tech. I would like to thank Bai Cui, Liangyi Sun, Yu Liu, Zhenyu Tan, Dr. Renke Huang, Dr. Dongbo Zhao, Dr. Aniemi Umana, Dr. Evangelos Polymeneas, Yi Du, Boqi Xie, Wenlu Fu and other laboratory students. It is my honor to spend the wonderful years with you. I am also grateful to other power group students for their friendship and support.

I am thankful to all my friends at Georgia Tech. They supported me academically, personally, and especially during difficulties. Among them special thanks go to Jiaming Li, Chong Han and Ke Li who have provided encouragement, friendship, and support throughout my graduate studies.

Last but not least, I would like to thank my family members especially my parents Xiancheng Fan, Silun Xu and my wife Xiaoxia Min. It is your love, support and encouragement that gives me the confidence and motivation to come through those most difficult days and helps me achieve the doctoral degree.

Table of Contents

List of Tables

List of Figures

SUMMARY

Power transformers are key devices that connect power systems of different voltage levels. They are very expensive and critical equipment that impact the stability and reliability of the entire electric power system. High capacity power transformers can be very large and heavy, costing several million dollars. Once a transformer is broken down and replacement is required, it takes a long time to purchase and install a new one. From the prospective of the utility companies, they never want to see a transformer breaking down because it will cost them large amounts of money and time. Moreover, transformer faults may cause more serious problems such as cascade failures or large-area black out. For these reasons, reliable and secure protection schemes for transformers are extremely important.

Nowadays the numerical relay is the centerpiece of all transformer protection schemes. The numerical relay is a microprocessor-based system with software-based protection algorithms for the detection of transformer internal faults. Despite the advancements of the numerical relays, the coordination and settings for the numerical relay functions are very complex, and numerical relays cannot ensure 100% protection reliability for many reasons. For some transformer faults, such as minor inter-turn faults, the existing numerical relay functions are not able to detect them.

The objective of transformer protection is to detect transformer internal faults or transformer overheating and trip the transformer, with immunity to external faults for which tripping of the transformer is not required. The proposed research aims to

develop a new reliable scheme to achieve the protection objectives for power transformers. That is the dynamic state estimation-based protection.

This method has been inspired from differential protection, which does not require coordination with other protection functions. The DSE-based protection method also requires no coordination with other functions and it has only very few simple settings. This method is very sensitive, secure and reliable, it can detect almost any transformer internal fault, even some minor internal faults such as inter-turn faults.

The fundamental idea of the proposed DSE-based method it to check the consistency between the transformer dynamic model and measurements at the terminals and/or inside the transformer. Any mismatch between the model and measurements indicates something wrong inside the transformer, and protection action should be taken. In contrast to present approaches for numerical relays that the trip decision is based on settings and coordinated logics, the proposed method accurately makes the protection decision only based on the operating condition of the transformer. In this case, some unnecessary relay failures due to improper coordination, or improper settings, or even human errors can be avoided.

The transformer electro-thermal models are built in a standard manner, which is referred as the algebraic quadratic companion form (AQCF). The measurements model is also expressed as an object with similar syntax as the AQCF. The proposed DSE-based protection algorithm directly works with the model and measurements expressed in the above AQCF objects, so the DSE-based scheme is object-oriented.

The proposed DSE-based scheme is a model-based scheme. Modeling accuracy of the transformer is fundamental in the DSE-based approach. Some independent parameters are included in the dynamic state estimation as state variables for the purpose of calibrating the transformer parameters. Therefore, the proposed method can also provide better models with validated parameters compared to traditional approaches.

In this dissertation, the proposed DSE-based protection is tested and compared against the legacy methods for a number of "hard-to-detect" faults, such as transformer faults near the neutral, internal faults during energization, and inter-turn faults. The results show much better performance of the proposed method over legacy methods. The proposed method is secure, reliable, more sensitive and faster than legacy protection functions

CHAPTER 1 INTRODUCTION

1.1 Problem Statement

Power transformers are expensive and critical equipment that impact the stability and reliability of the entire electric power system. For this reason, reliable and secure protection schemes for transformers are extremely important. The objective of transformer protection is to detect transformer internal faults or transformer overheating and trip the transformer, with immunity to external faults for which tripping of the transformer is not required [1]-[2]. The proposed research aims to develop a reliable scheme to achieve the protection objectives for power transformers.

Transformer failures may cause many problems. First, internal faults can evolve to fires or even explosions, which are very dangerous to the safety of personnel. Second, a sudden broken-down transformer may cause serious system disturbances or even large-area black out. Third, transformers are very expensive and they may cost several million dollars. Fourth, replacing a transformer is very complicated, expensive and time-consuming. If the transformer is broken down, it takes a long time to rebuild and install a new one. To protect the transformer, legacy relaying protection schemes with high degree of sophistication have been designed. However, these schemes cannot ensure 100% protection reliability and security for three main reasons: (1) improper coordination or improper settings of relays (2) there is the possibility of false trips during inrush or over-excitation situations; (3) relays may not have enough sensitivity

to detect certain internal faults, such as the minor inter-turn faults or faults near the neutral terminal.

Today, commercial transformer relaying schemes are implemented with multiple protective functions, each function requiring complex settings and coordination among the function and with relays for neighboring protection zones. For example a modern numerical relay has an average of 12 protective functions [3]. The coordination of these protective functions are quite complex. This complexity increases the possibility of human error, and many times it leads to inconsistencies and the possibility of improper protection actions [4]. In fact, according to North American Electric Reliability Corporation (NERC), approximately 65% of the relay failures are caused by the improper coordination or improper settings [5].

When the transformer energization or over-excitation happens, false differential currents are generated and they resemble the conditions of internal faults [6]. The currents are distorted currents because of the core saturation. As a consequence, relays might fail to differentiate the distorted current from internal fault current, causing nuisance trips of the transformer.

If inter-turn faults or faults near neutral terminal happen inside a transformer, the resulting differential currents are very small. In contrast, fault currents flowing though the shorted circuit can be unexpectedly high. The high fault currents generate serious heat that causes localized thermal overloading, which ultimately evolves to catastrophic failures [7]. Therefore, inter-turn faults or faults near neutral terminal should be

detected in their earliest stages before further damages occur to the transformers. However, these kinds of faults are very difficult to be detected by legacy transformer relays because of the small differential currents.

1.2 Research Objectives

The dissertation objectives are (1) to propose a transformer protection scheme which requires no coordination with other functions, (2) to reduce or simplify the settings of relays as much as possible, (3) to detect transformer internal faults, including minor internal faults such as the inter-turn faults, with high sensitivity and certainty, (4) to prevent false tripping during transformer energization or external faults, (5) to validate the electro-thermal model of transformers, and (6) to develop high fidelity models by parameter estimation methods.

To realize these objectives, a new protection scheme based on dynamic state estimation (DSE) is proposed in this research. This method has been inspired from differential protection, which does not require coordination with other protection functions. Specifically, the proposed scheme continuously monitors transformer terminal voltages and currents and other measurable quantities such as tap settings, temperatures, etc. The measurement data are utilized in a dynamic state estimator of the transformer protection zone. A chi-square test is performed to determine how well the measured data fit the dynamic model of the transformer. When the fit is within the accuracy of the meters by which the measurements are taking, the dynamic state estimator provides the true operating condition of the transformer. Discrepancies

indicate an internal abnormality. The scheme takes decisions based on the operating conditions of the transformer. This scheme does not require any coordination with other protection functions. The only setting in this case is the maximum permissible hot spot temperature (typically 105 Celsius).

The computational process requires the dynamic model of the transformer, the measurements and the dynamic state estimation algorithm. The analytics have been implemented in an object-oriented manner. Specifically, the dynamic model of the transformer is expressed as an object with specific syntax referred to as the algebraic quadratic companion form (AQCF). The measurements, obtained with traditional relaying instrumentation or via merging units, are also expressed in an object with similar syntax as the AQCF. The dynamic state estimation algorithm operates directly with the measurement models expressed in the above objects. The feasibility of the proposed DSE-based protection algorithm has been tested in the laboratory.

Three dynamic state estimation methods are implemented, namely the unconstrained weighted least square (UCWLS), constrained weighted least square (CWLS) and the extended Kalman filter (EKF) method. Usually, the UCWLS and CWLS methods are often applied for the static state estimation of power system, while the EKF method is used for the dynamic state estimation. However, the introduction of numerical integration method that converts transformer dynamic models into algebraic companion models makes the UCWLS and CWLS methods suitable for dynamic state estimation, and renders the process equivalent to dynamic state estimation [8]. The

electro-thermal model of transformers is built in the algebraic quadratic companion form with the quadratic integration method, so that all the three methods can be applied to solve the dynamic state estimation problem.

UCWLS method is used to find the best estimates for the states that generate the minimum weighted squared error. It works well with a measurement set that represents actual measurements with usual measurement errors. However, when it is used to handle virtual measurements without uncertainty (noiseless), it may generate numerical instabilities due to the large separation between the variances of the actual measurements and the virtual measurements. This is the reason that the CWLS method is also used. The CWLS method is very similar to the UCWLS method, except that virtual measurements are treated as constraints. EKF method linearizes the nonlinear system to its first-order so that the traditional Kalman filter equations can be applied. The EKF method is recursive and it works in a two-step process. In the prediction step, it predicts the estimates of state variables; in the correction step, the estimates are updated with observed measurements for higher accuracy.

The proposed protection scheme provides many advantages versus legacy transformer relays. First, it requires no coordination with other protective relaying functions and has only very few, simple settings. Therefore it avoids unnecessary relay mis-operations caused by improper coordination or settings, or human errors. Second, the proposed scheme is object-oriented using the standard AQCF format, so it can be easily applied to any type of transformer. Third, the proposed scheme provides faster

speed than legacy protection functions. It can detect the existence of faults within a few samples (fraction of one ms) so that this scheme can trip the transformer at the earliest stage of the fault before further damage happens. Forth, the proposed scheme is very secure: mis-operations would not happen when an inrush current or external fault occurs. Finally, the proposed scheme is dependable and sensitive. It can detect almost any transformer internal fault, including inter-turn faults or faults near the neutral terminal, with high sensitivity and then takes correct actions to protect the transformer.

1.3 Thesis Outline

The outline of the remaining parts of this dissertation is as follows.

In Chapter 2, background information is provided along with presently available transformer protection methods that are being used. In addition, a thorough literature survey is presented that summarizes related research work efforts. In particular, this chapter starts with a summary of legacy protection methods that are available in numerical relays. The principles of these legacy protection methods are presented. A literature review on the recently alternative transformer protection methods that have been proposed by other researchers follows. Finally, a summary is provided on both the legacy protection methods and the recently proposed methods.

Chapter 3 presents an overview of the proposed DSE-based protection method. The laboratory hardware implementation of the proposed DSE-based protection algorithm is presented to mimic the actual field application.

Chapter 4 presents the general method of deriving object-oriented electro-thermal models for power transformers. The electro-thermal models of power transformer are written in standard syntax, the algebraic quadratic companion form (AQCF). Examples for how to derive the AQCF electro-thermal models from the original algebraic differential equations are also given for both a single-phase saturable transformer and a single-phase auto-transformer with tertiary winding. In the end of this chapter, the method of combining three single-phase transformers into one three-phase transformer is also introduced.

Chapter 5 presents in detail three different methods of solving the dynamic state estimation (DSE) problem, namely the unconstrained weighted least square (UCWLS) method, the constrained weighted least square (CWLS) method and the extended Kalman filter (EKF) method. This chapter also introduces the protection logic of proposed DSE-based method, with the description of calculating the values of chi-square and confidence level.

Chapter 6 indicates that dynamic state estimation can be utilized to calibrate the parameters of the transformer models with great accuracy. The basic approach is to expand the dynamic state estimation to include independent parameters as state variables. The mathematical formulation of an auto-transformer parameters identification problem is described in this chapter. Demonstration results of the auto-transformer physical parameter identification are also presented in this chapter.

Chapter 7 presents five different events for the power transformer/ auto-transformer. The proposed DSE-based protection method and six legacy protection methods have been implemented to protect the transformer/ auto-transformer in five events, and the corresponding protection results are compared.

Finally, Chapter 8 summarizes the research work and provides future research directions.

There is also one appendix in this dissertation. In Appendix A, the quadratic integration method is summarized.

CHAPTER 2 LITERATURE SURVEY

2.1 Overview

This chapter provides the background information on existing transformer protection schemes related to the proposed research along with a literature review of the research efforts on these topics. From basic fuses to the most advanced numerical relays, various protection schemes have been applied to transformers [9]-[11]. In general, the following legacy relaying methods are applied to protect power transformers:

1. Percentage differential protection
2. Harmonic-restraint differential protection
3. Negative-sequence differential protection
4. Overcurrent protection
5. Volt-over-hertz protection
6. Thermal protection
7. Gas-and-pressure protection

The above protection functions are presently provided with numerical relays. Recently, attempts have been reported to implement these functions with alternate analytics, noticeably:

1. Frequency analysis, ANN, fuzzy logic, and wavelet-based protection
2. Adaptive differential protection

The above relaying methods are reviewed sequentially.

2.2 Legacy Protection Methods

2.2.1 Percentage-differential protection

Among the transformer protection schemes, the most popular (legacy) one is the differential protection scheme [12]-[17]. This scheme is based on a comparison of the sum of currents at primary and secondary sides of transformer. Differential relays are designed to "see" zero differential currents under normal-operating or external-fault conditions. If an internal fault happens, the relay will detect a substantial differential current and then trip the transformer. To illustrate its principle, the application of differential relay to transformers is presented with a single-phase two-winding transformer in Figure 2-1 (a) [18]. The differential relay calculates the operating current $I_{op} = \left|\vec{I}_{s1} + \vec{I}_{s2}\right|$ and restraining current $I_{res} = \frac{1}{2}\left|\vec{I}_{s1} - \vec{I}_{s2}\right|$ of the transformer. Ideally, the operating current I_{op} remains zero unless an internal fault occurs. However, the existence of variable-tap transformers and instrumentation errors make this simple criterion inappropriate for practical applications. To overcome this problem, a minimum pickup current $I_{\min}$ and differential ratio $K = I_{op} / I_{res}$ are introduced. The relay will trip the transformer only if (1) $I_{op} > I_{\min}$ and (2) the ratio *K* exceeds a certain threshold. In the industry, the threshold is typically set to be 20% ~ 40%.

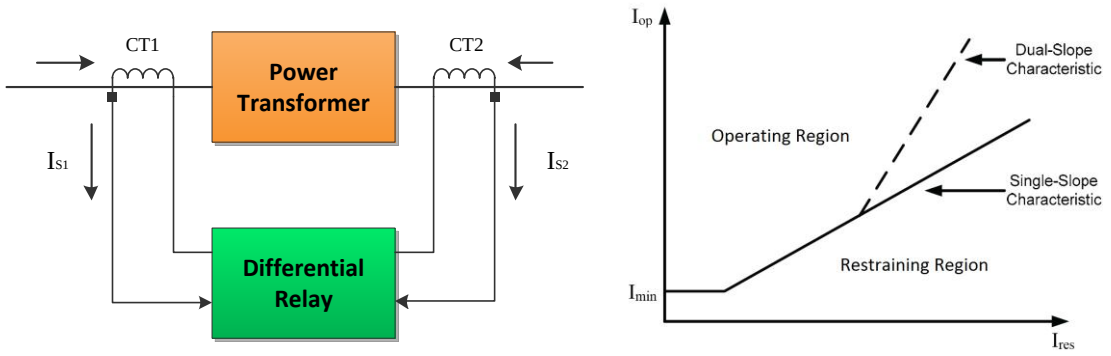

(a) (b)

Figure 2 - 1. Differential protection demonstration

Typically, the differential relay utilizes an increasing percentage as the fault-current level increases, shown as Figure 2-1 (b). The slope characteristic provides a lower sensitivity (desensitized) to avoid the risk of mal-operations when low levels of current are flowing into transformers [19]-[20]. However, if transformer energization happens, the generated inrush current resembles the condition of an internal fault, and differential relays cannot differentiate it from internal-fault current. As a consequence, differential relays tend to falsely trip the transformer and cause unnecessary system disturbances.

2.2.2 Harmonic-restraint differential protection

Harmonic-restraint differential relays are introduced to solve the problem caused by transformer energization [21]-[27]. The methods are based on an assumption that internal-fault currents and inrush currents contain different levels of second-harmonic components. Researchers claim that the second and fourth harmonic components of the inrush currents are typically above 15% of the fundamental currents, while the levels are very low for internal faults. Therefore, the harmonic-restraint differential relay monitors the second and fourth harmonic levels, and it will block any trip signal if the

levels are higher than the settings. However, technology has changed this situation. Today, the levels of second-harmonic components in inrush currents are substantially lower in transformers with improved core steels [28]-[29]. It is difficult to determine whether an internal fault exists based only on the level of second-harmonic components. Moreover, if a fault happens at the time a transformer is energized, harmonics in the magnetizing current could prevent the relay from tripping.

2.2.3 Negative-sequence differential protection

Traditional differential relays can detect most internal transformer faults, except for inter-turn faults and faults near the neutral, since transformer turn-turn faults do not generate differential currents. To solve the problem, a negative-sequence differential relay has been introduced [30]-[36]. When the inter-turn faults happen, the transformer terminal currents become asymmetrical. Therefore, negative-sequence currents at the primary and secondary sides are good indicators of inter-turn faults. The magnitudes and angles of terminal negative-sequence currents are compared, and the negative-sequence differential relay would trip the transformer if the angle or ratio of magnitudes exceeds certain thresholds. However, the negative-sequence differential relay cannot protect the transformer if turn-turn faults exist at the time transformer is energized or in case of CT saturation. Because when the transformer is energized, the relay has to be desensitized to avoid blocking possible trips from other protection functions [37]. In addition, if the CT is saturated the differential-restraining point may move to the operating boundary, causing unnecessary mis-operations. Furthermore, the negative-

sequence differential protection is not sensitive enough if the inter-turn fault is too small (less than 1%).

2.2.4 Overcurrent protection

The overcurrent relays are also widely used for transformer protection [38]-[44]. They would trip the transformer if the values of terminal currents exceed the pick-up settings. Overcurrent relays are able to detect some obvious faults of transformers, while they could not cover other internal faults. For example, if the turn-turn or turn-ground faults happen inside the transformer, depending on the location of the fault, the terminal currents may not change enough to alert the relay about the existence of faults. However, the currents in the fault loop can be extremely large and can cause significant damage if not detected and isolated in time. In addition, if energization happens, it tends to draw a high-magnitude inrush current from the supply that can be typically many times the normal full-load current. The inrush current could cause nuisance tripping of the overcurrent relay.

2.2.5 Volts-over-hertz protection

Volts-over-hertz schemes are implemented to protect transformers from harmful core saturation that can generate harmonics, increased heating and increased inter-lamination voltages causing iron damage [45]-[50]. To protect the transformer, the ratio of volts-over-hertz is continuously monitored. At normal operating conditions, the ratio of volts-over-hertz is constant and known. If the transformer is over-excited, the ratio

of volts-over-hertz will increase. In other words, the ratio “Volts-over-hertz” indicates the level of the magnetic flux linkage in the transformer. Transformers are designed in such a way to operate near the magnetization knee region under normal operation. If the magnetic flux linkage in the transformer increases, the iron core of the transformer will be driven into saturation. In this case, excessive losses in the iron core may increase the temperature of the transformer and damage the transformer. The relay will protect transformer according to a time characteristic related to the ratio of volts-over-hertz. The more that ratio exceeds normal operating settings, the faster that relay will trip the transformer. However, the volts-over-hertz relay is limited to protect the transformer from over- or under-excitations, thus additional functions are required to protect the transformer from damage caused by other internal faults.

2.2.6 Thermal protection

The transformer should also be protected against high temperatures as they will deteriorate insulation leading to electric faults. The maximum temperature anywhere in the transformer is referred to as the hot-spot temperature. In general the hot spot temperature should not exceed about 110^0C [51]-[56]. When the transformer is overloaded, overexcited or the cooling equipment is broken, relatively high temperatures can be developed inside the transformer, increasing the hot-spot temperature. A transformer thermal relay calculates the hot-spot temperature based on readings from thermocouples, the thermal model, terminal voltages and currents and ambient temperature. Thermal relays can protect transformers from overloads, short

circuits, cooling equipment failure and catastrophic failures by tripping the transformer when pre-set temperature thresholds are exceeded. However, when an inter-turn fault occurs inside the transformer, it will be too late to protect the transformer if waiting for the thermal relay to operate.

2.2.7 Gas-and-pressure protection

Gas-and-pressure relays are utilized as protective devices for oil-filled transformers. The accumulation of gas and pressure changes inside the transformer tank are good indicators of internal faults [57]-[62]. A combined gas-accumulator and pressure relay, called the “Buchholz” relay, has been in successful service for over 70 years [63]. However, gas-and-pressure relays can only detect the faults below the oil level inside transformer, while it could not trip the transformer if faults happen at the bushings or terminal connections. Furthermore, gas-and-pressure relays are relatively vulnerable to ambient disturbances. If vibration, leaking or corrosion happens, relays might mal-operate and cause severe damage.

2.3 Recently Proposed Alternative Protection Methods

The aforementioned protection schemes are presently provided with commercial numerical relays. Apart from these legacy protection functions, researchers have also proposed some new alternative schemes to protect transformers.

2.3.1 Frequency analysis, ANN, fuzzy logic, and wavelet-based protection

Frequency analysis-based protective relaying functions have been studied in [64]-[69]. In [64], the differential current was analyzed in terms of its Fourier series, the peaks of fundamental and second-harmonic contents were calculated, as well as the second-harmonic level in the differential current. The second-harmonic level is monitored to block mis-operations during transformer energization (second-harmonic level is high) Similar research has been proposed based on the frequency response analysis to achieve fast computations to detect winding deformation under the influence of short circuits [65]-[66]. The algorithm generates the Fourier coefficients by addition and subtraction routines only. The frequency responses were classified into high-, medium- and low-frequency responses and they corresponded to different fault situations. With different responses, researchers could figure out whether a fault happened inside the transformer. Unfortunately, these frequency analysis-based methods are not reliable enough. Fault conditions inside transformer could be complex so frequency responses are insufficient to make a convincing conclusion in some cases. Moreover, almost all these schemes are based on the conditions of periodicity and stationarity. While disturbances in power systems are of non-periodic, non-stationary, short duration [67].

Artificial neural network (ANN) and fuzzy logic-based protection schemes have been proposed [70]-[80]. ANN can be represented as a parallel multi-layer information processing structure that enables the inclusion of expert knowledge into the processing,

recognition and classification of signals. A feed forward ANN-based training method has been proposed to discriminate between power transformer inrush and fault currents [70]. The back-propagation method was used for the training. The transfer functions of units were changed to hard limiters with thresholds equal to the biases obtained from the sigmoid during training process to increase the computation speed of the network. Once the network was trained, the ANN-based method can quickly detect certain internal faults (if the faults have been included in the training sets) by checking the transformer terminal measurements. Fuzzy logic-based schemes have also been studied for transformer protection. In 1995, a multi-criterion differential relay based on fuzzy was introduced [77]. It. The consequences of wrong protection decisions are considered, and the relay “more inclined to trip” or “more inclined to block” depends on actual conditions. The use of the cost of wrong decision-making and the amount of information inflow improves the reliability of the protection scheme. Wavelet-based differential protection schemes for transformers have also been introduced [81]-[86]. These methods focus on detecting the difference between internal fault currents and inrush currents, with the fact that their energy distributions in time and frequency were very different. However, all the above methods introduce high computational burdens and may requires additional expensive apparatus. For example, the ANN and fuzzy logic-based methods require long training time and large training sets, which might even not be inclusive of all the events that may occur in the real world. In general, these methods have not been used in field conditions and they have not been accepted for

practice.

2.3.2 Adaptive differential protection

In the last few years, adaptive differential relays have been studied to detect the internal faults of transformers [87]-[93]. These relays are based on the percentage differential protection scheme, but they can adjust the characteristic automatically according to the differential currents and transformer status such as tap settings. A multi-region adaptive differential relay has been introduced in [93]. Based on the current trajectories and fault conditions, the operational zone of relay characteristic is divided into three operating regions. When the current trajectory enters the relay operational zone, a weighting factor is adopted based on its region. The relay will trip the transformer when the summation of the weighted-points exceeds a certain pre-specified value. Protection characteristics are self-regulated according to power system conditions so that the relay can achieve both security and sensitivity. However, adaptive differential protection relays cannot guarantee 100% protection of the transformer. The sensitivities of adaptive differential relays are not high enough to detect minor internal transformer faults such as inter-turn faults of a transformer.

2.4 Summary

Today, commercially available transformer relays have been implemented with multiple methods listed above, while the complicated coordination and settings of relays increase the risk of improper protection actions. It is feasible to substitute the

listed legacy methods from one to six as well as the aforementioned newly proposed schemes with only one approach: the proposed dynamic state estimation-based protection scheme. This method requires no coordination with other relays and has only very few and simple settings, while, as it will be shown, provides better security than legacy methods. The proposed method is not limited to detection of faults that are within the capabilities of legacy functions. It is sensitive enough to deal with the faults that are very difficult to detect by legacy methods, such as the inter-turn faults and faults near the neutral terminal.

CHAPTER 3 THE OVERALL APPROACH

3.1 Overview

In this chapter, a dynamic state estimation-based transformer protection scheme is proposed. This scheme requires no coordination with other functions and it has only very few simple settings. The DSE-based protection scheme is an extension of differential protection. It measures voltages, currents, temperatures, etc. and then fits the real time measurement data to the transformer mathematical model. This is achieved in a mathematical rigorous way by the use of dynamic state estimation. DSE calculates the degree of consistency between measurements and the transformer dynamic model. If there is a mismatch, something is wrong inside the transformer and protective actions should be taken.

The proposed scheme has been implemented in an object-oriented manner. The transformer model and measurements are expressed in an object with specific syntax referred to as the algebraic quadratic companion form (AQCF) [94]. The dynamic state estimation algorithm operates directly with the measurement models expressed in above objects. The laboratory hardware implemented with the proposed DSE-based protection algorithm is presented to mimic the actual field application.

3.2 The Proposed Approach

The proposed DSE-based protection scheme is shown in Figure 3-1. The procedure for DSE-based protection has been streamlined. Initially, the transformer device model

is written in algebraic quadratic companion form (AQCF) and proposed algorithm automatically formulates the measurement model in AQCF syntax, as illustrated in Figure 2.

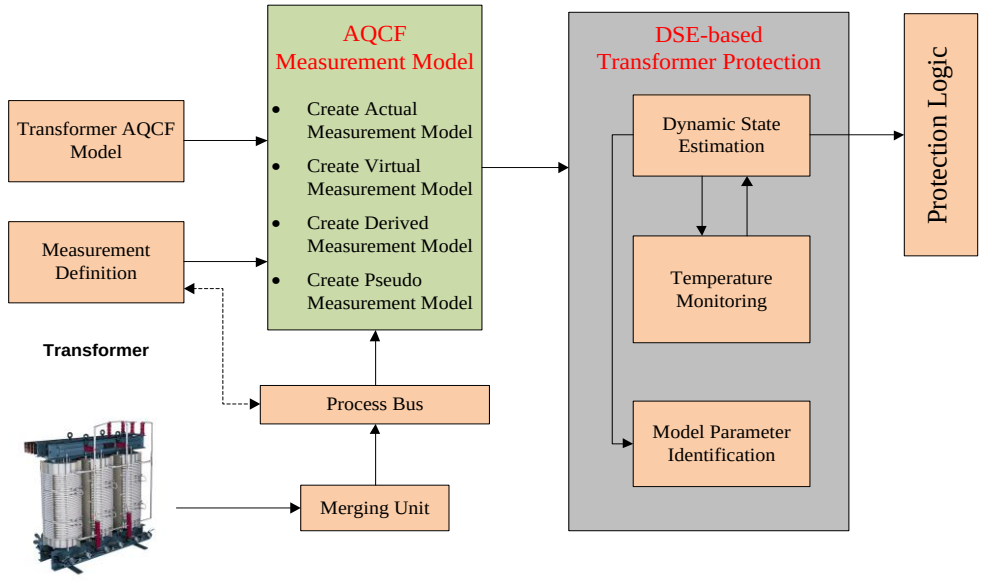

Figure 3 - 1. Overview of DSE-based transformer protection scheme

The only setting for the proposed scheme is the maximum permissible operating conditions such as maximum permissible temperature. The DSE-based protection approach has two types of input data. One is the measurement model of the transformer; the other is the real-time measurements data coming from merging units (process bus). The real-time measurements data are utilized in a dynamic state estimation by fitting the measurement data to the model equations of the transformer. The dynamic state estimation problem can be solved by three methods, namely the unconstrained weighted least square (UCWLS) method, the constrained weighted least square (CWLS) method and the extended Kalman filter (EKF) method. The dynamic state estimation gives the best estimates of all the states of the transformer including temperatures and, if needed, parameter identification. Following the estimation of the states, a Chi-square test is

applied to determine the probability that the measurements are consistent with the transformer dynamic model [95]. This probability (or confidence level) indicates whether there are internal abnormalities in the transformer, such as a ground fault, an inter-turn fault, etc. An integral function is applied to accumulate the confidence level values and diminishes the effect of unnecessary transients. The protection scheme will trip the transformer if any internal fault is detected.

To make sure that the proposed DSE-based scheme can be applied to any type of transformer, the transformer electro-thermal models are built in a standard manner, which is referred to as the algebraic quadratic companion form (AQCF). Details of the AQCF will be introduced in the next chapter. The measurements model is also expressed in an object with similar syntax as the AQCF. The proposed DSE-based protection algorithm directly works with the measurement models expressed in the above AQCF objects, thus the DSE-based scheme is object-oriented.

The proposed DSE-based scheme is a model-based scheme, therefore, it relies on high-fidelity transformer models. Modeling accuracy of the transformer is fundamental for the DSE-based approach. The actual transformer parameters used for state estimation are often quite different from the nameplate ratings, thus reliable transformer parameters calibration method is necessary to ensure the feasibility and correctness of the proposed method. To calibrate the transformer parameters, some independent parameters are included in the dynamic state estimation as state variables. With enough redundancy, both the transformer states and the key parameters can be estimated with

a high confidence. Therefore the proposed method can also provide better models with field-validated parameters compared with traditional approaches.

There are many transformer faults hard to be detected or correctly treated by the legacy protection functions, such as transformer faults near the neutral, internal faults during energization, inter-turn faults, etc. In this dissertation, the proposed DSE-based protection is compared against the legacy methods for these “hard-to-detect” faults.

Another advantage of the proposed DSE-based method is that the scheme does not require coordination with other relays. In addition it only requires very few and simple settings. In contrast to the numerical relays in which the trip decision is based on the settings or coordination logic, the proposed method accurately makes the protection decision only based on the operating condition of the transformer. In this way, some unnecessary relay failures due to improper coordination, or improper settings, or even human errors can be avoided.

3.3 Laboratory Hardware Implementation for DSE-Based Protection Scheme

Laboratory testing is the most effective way to test any innovative methodologies. The proposed DSE-based protection scheme is tested in the laboratory. The implementation uses merging units, GPS signals and IEC-61850 communications. The laboratory hardware implementation for proposed scheme is shown Figure 3-2.

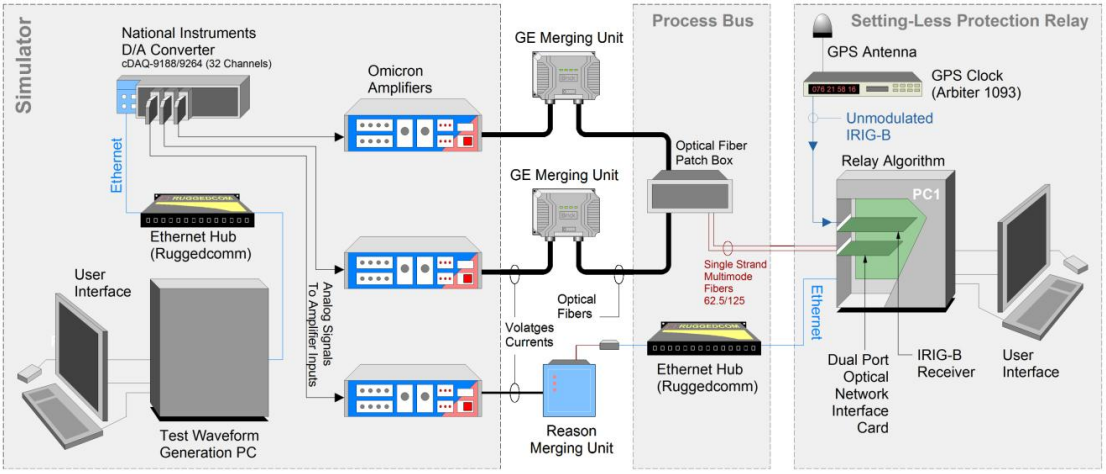

Figure 3 - 2. Laboratory hardware implementation for proposed scheme

The simulation platform (program WinXFM) generates and streams digital waveforms of transformer events to a National Instrument D/A converter. The National Instrument D/A converters send the analog signals to a bank of OMICRON amplifiers that amplify them to standard relay instrumentation voltages and currents. These signals are in the range of typical outputs from CT/VTs so that they are used to mimic the actual field signals. These signals are fed to the merging units. The merging unit acts as a bridge between primary equipment and protection devices that captures and transmits signals [96]. It converts the analog signals from analog CT/VT signals to digital signals, which are then transmitted to the process bus via standard protocol (IEC-61850) [97]-[99]. The process bus offers the obvious possibility of bringing many measurements (as a matter of fact all the measurements) to the process bus. Data are synchronized by the used of an Arbiter 1093 GPS clock. A personal computer is connected to the process bus and acts as a data concentrator that feeds the collected data to dynamic state estimator.

3.4 Summary

A DSE-based transformer protection scheme is proposed in this chapter. The overall structure of the proposed method has been introduced. In general, the proposed method monitors the health status of the transformer and it can identify any internal abnormality of the transformer within a few samples (a fraction of one ms). This method does not degrade the security because it does not trip in the event of normal behavior of the transformer, for example, the inrush currents or over excitation currents. Because in these cases, as long as the inrush currents are consistent with the transient behavior of the transformer as dictated by the dynamic model, the method will produce a high confidence level that the transients are consistent with the model of the component. The laboratory hardware implementation is also presented to mimic the actual field application in this chapter.

CHAPTER 4 TRANSFORMER ELECTRO-THERMAL MODEL

4.1 Overview

In this chapter, the transformer electro-thermal model is presented. First, the transformer physical model will be presented in the quadratized device model (QDM) with both electric and thermal part. Then the physical model will be cast into the standard algebraic quadratic companion form (AQCF) format using the quadratic integration method [100]-[101]. Finally, the measurement model is automatically generated in the AQCF syntax with the introduction of measurement definition. The DSE-based protection scheme directly works on the AQCF objects.

For simplicity, a single-phase saturable-core transformer and a single-phase auto-transformer with tertiary winding are taken as examples in this section. However, they can be easily generalized to three-phase multi-winding transformers or the three-phase auto-transformer bank. An example of constructing a three-phase transformer with three single-phase transformers is also provided in this chapter.

4.2 Transformer Physical Electro-Thermal Quadratized Model

The quadratized models of a single-phase saturable-core transformer and a single-phase auto-transformer with tertiary winding are introduced in this section. The saturable cores of both transformers are modeled by high-fidelity equations to represent the nonlinear magnetization characteristics. Extra states and equations are added to decrease the highest order of the models back to two.

4.2.1 Single-Phase Saturable-Core Transformer Physical Electro-Thermal Quadratized Model

The electro-thermal model of a single-phase saturable-core transformer is introduced in this part. The equivalent circuit of a single-phase saturable-core transformer with both electric part and thermal part is shown in Figure 4-1.

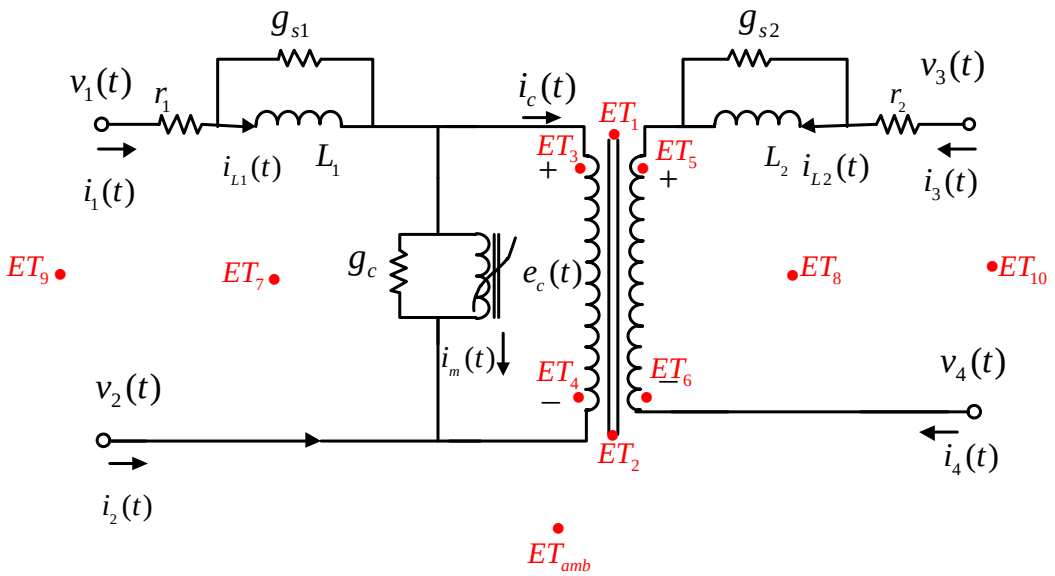

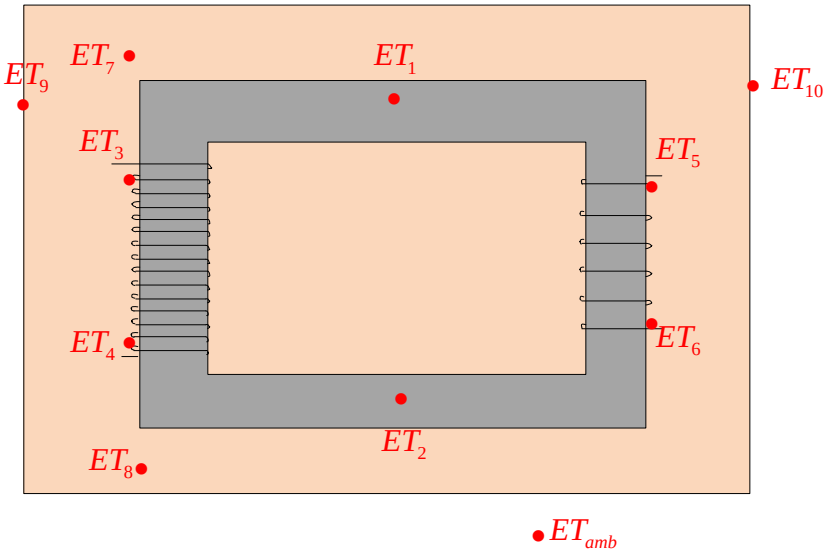

Figure 4 - 1. Equivalent electro-thermal circuit of a single-phase transformer

The "numerical stabilizers" $g_{s1} \sim g_{s4}$ are introduced to eliminate possible numerical problems. The numerical stabilizers introduce errors orders of magnitude below the measurement errors and therefore do not affect the overall accuracy of the proposed protection method. For the thermal part, the 11 red spots (ET_X) are the thermal temperature points. ET_1 and ET_2 are the thermal temperature points at the core (top and bottom), ET_3 to ET_4 are the thermal temperature points at the primary coil (top and bottom), ET_5 to ET_6 are the thermal temperature points at the secondary coils (top and bottom), ET_7 and ET_8 are the thermal temperature points at the oil (top and bottom), ET_9 and ET_{10} are the thermal temperature points at the tank (front and rear), ET_{amb} is the ambient temperature point. The transformer losses are computed from the measured voltage and current waveforms at the transformer terminals. Computed losses include winding coil losses (Ohmic losses) as well as magnetic core losses. [102].

At first, the transformer compact model of the single-phase saturable-core transformer is introduced in the following differential algebraic equations:

$$i_1(t) = i_{L1}(t) + g_{s1} L_1 \frac{di_{L1}(t)}{dt}$$

$$i_2(t) = -i_{L1}(t) - g_{s1} L_1 \frac{di_{L1}(t)}{dt}$$

$$i_3(t) = i_{L2}(t) + g_{s2} L_2 \frac{di_{L2}(t)}{dt}$$

$$i_4(t) = -i_{L2}(t) - g_{s2} L_2 \frac{di_{L2}(t)}{dt}$$

$$0 = v_1(t) - v_2(t) - r_1 \left(i_{L1}(t) + g_{s1} L_1 \frac{di_{L1}(t)}{dt} \right) - L_1 \frac{di_{L1}(t)}{dt} - e_c(t)$$

$$0 = v_3(t) - v_4(t) - r_2 \left(i_{L2}(t) + g_{s2} L_2 \frac{di_{L2}(t)}{dt} \right) - L_2 \frac{di_{L2}(t)}{dt} - \frac{N_2}{N_1} e_c(t)$$

$$0 = N_1 i_c(t) + N_2 \left(i_{L2}(t) + g_{s2} L_2 \frac{di_{L2}(t)}{dt} \right)$$

$$0 = e_c(t) - \frac{d\lambda(t)}{dt}$$

$$0 = -i_{L1}(t) - g_{s1} L_1 \frac{di_{L1}(t)}{dt} + i_c(t) + i_m(t) + g_c e_c(t)$$

$$0 = i_m(t) - i_0 \left| \frac{\lambda(t)}{\lambda_0} \right|^n sign(\lambda(t))$$

$$0 = C_1 \frac{dET_1(t)}{dt} + \sum_{i \neq 1}^{n=10} \left(g_{1,i} \right) ET_1(t) - \sum_{j \neq 1}^{n=10} \left(g_{1,j} ET_j(t) \right) - Q_{core,1}(t)$$

$$0 = C_2 \frac{dET_2(t)}{dt} + \sum_{i \neq 2}^{n=10} \left(g_{2,i} \right) ET_2(t) - \sum_{j \neq 2}^{n=10} \left(g_{2,j} ET_j(t) \right) - Q_{core,2}(t)$$

$$0 = C_3 \frac{dET_3(t)}{dt} + \sum_{i \neq 3}^{n=10} \left(g_{3,i} \right) ET_3(t) - \sum_{j \neq 3}^{n=10} \left(g_{3,j} ET_j(t) \right) - Q_{coil\_pri,1}(t)$$

$$0 = C_4 \frac{dET_4(t)}{dt} + \sum_{i \neq 4}^{n=10} \left(g_{4,i} \right) ET_4(t) - \sum_{j \neq 4}^{n=10} \left(g_{4,j} ET_j(t) \right) - Q_{coil\_pri,2}(t)$$

$$0 = C_5 \frac{dET_5(t)}{dt} + \sum_{i \neq 5}^{n=10} \left(g_{5,i} \right) ET_6(t) - \sum_{j \neq 5}^{n=10} \left(g_{5,j} ET_j(t) \right) - Q_{coil\_sec,1}(t)$$

$$0 = C_6 \frac{dET_6(t)}{dt} + \sum_{i \neq 6}^{n=10} \left(g_{6,i} \right) ET_7(t) - \sum_{j \neq 6}^{n=10} \left(g_{6,j} ET_j(t) \right) - Q_{coil\_sec,2}(t)$$

$$0 = C_7 \frac{dET_7(t)}{dt} + \sum_{i\neq 7}^{n=10} \left(g_{7,i} \right) ET_7(t) - \sum_{j\neq 7}^{n=10} \left(g_{7,j} ET_j(t) \right)$$

$$0 = C_8 \frac{dET_8(t)}{dt} + \sum_{i\neq 8}^{n=10} \left(g_{8,i} \right) ET_8(t) - \sum_{j\neq 8}^{n=10} \left(g_{8,j} ET_j(t) \right)$$

$$0 = C_9 \frac{dET_9(t)}{dt} + \sum_{i\neq 9}^{n=9+T_{amb}} \left(g_{9,i} \right) ET_9(t) - \sum_{j\neq 9}^{n=9+T_{amb}} \left(g_{9,j} ET_j(t) \right) - g_{9,T} ET_{amb}$$

$$0 = C_{10} \frac{dET_{10}(t)}{dt} + \sum_{i\neq 1}^{n=10+T_{amb}} \left(g_{10,i} \right) ET_{10}(t) - \sum_{j\neq 10}^{n=10+T_{amb}} \left(g_{10,j} ET_j(t) \right) - g_{10,T} ET_{ambient}$$

$$0 = Q_{core,1}(t) - \frac{1}{2} \alpha_{e+h} \lambda(t)^2$$

$$0 = Q_{core,2}(t) - \frac{1}{2} \alpha_{e+h} \lambda(t)^2$$

$$0 = Q_{coil\_pri,1}(t) - \frac{1}{2} r_1 i_{L1}(t)^2$$

$$0 = Q_{coil\_pri,2}(t) - \frac{1}{2} r_1 i_{L1}(t)^2$$

$$0 = Q_{coil\_sec,1}(t) - \frac{1}{2} r_2 i_{L2}(t)^2$$

$$0 = Q_{coil\_sec,2}(t) - \frac{1}{2} r_2 i_{L2}(t)^2$$

where $v_{1\sim4}(t)$ and $i_{1\sim4}(t)$ are the terminal voltages and currents, $ET_{1\sim10}(t)$ are the temperature points, r_1, r_2, L_1, L_2 are the corresponding resistances and inductances, $C_1 \sim C_{10}, g_{i,j}$ $(where\, i, j = 1\sim10, i \neq j)$ are the corresponding thermal capacitance and conductance, N_1 and N_2 are the number of turns at the primary and secondary windings, gc is the excitation conductance, $i_m(t)$ is the magnetizing current and $\lambda(t)$ is the flux linkage through the iron core, $Q_{core,1}(t), Q_{core,2}(t)$ are the heat generated at the core, $Q_{core\_pri,1}(t), Q_{core\_pri,2}(t)$ are the heat generated at the primary winding, $Q_{core\_sec,1}(t), Q_{core\_sec,2}(t)$ are the heat generated at the secondary winding.

There are 26 state variables and 26 equations in the compact model. The model is

quadratized by introducing additional internal state variables so that the n^{th} exponent is replaced by equations of at most quadratic degree. Since the exact degree of nonlinearity is not known until the user specifies it, the model performs automatic quadratization of the equations. A special procedure is used, so that the model is quadratized using the minimum number of additional internal states, which also minimizes the additional equations. The methodology is based on expressing the exponent in binary form. The binary representation provides all the information about the number of new variables and equations that need to be introduced and added to the model. Specifically, the equation:

$$0 = i_m(t) - i_0 \left| \frac{\lambda(t)}{\lambda_0} \right|^n sign(\lambda(t))$$

is quadratized with the newly introduced states as:

$$0 = i_m(t) - i_0 y_m(t) \left[sign(\lambda(t)) \right]^{n+1}$$

$$0 = y_1(t) - \frac{\lambda(t)^2}{\lambda_0^2}$$

$$0 = y_2(t) - y_1(t)^2$$

… …

$$0 = y_{m1}(t) - y_{m1-1}(t)^2$$

$$0 = y_{m1+1}(t) - y_{i1}(t) y_{j1}(t)$$

$$0 = y_{m1+2}(t) - y_{m1+1}(t) y_{j2}(t)$$

… …

$$\begin{cases} 0 = y_m(t) - y_{m-1}(t) y_{jm2}(t), \ \textit{if } n \textit{ even} \\ 0 = y_m(t) - y_{m-1}(t) \dfrac{\lambda(t)}{\lambda_0}, \ \textit{if } n \textit{ odd} \end{cases}$$

where the states $y_1(t) \sim y_m(t)$ are introduced to ensure that transformer mathematical model consists of equations of at most quadratic degree, and $m = m_1 + m_2$, $m_1 = \text{int}\left(\log_2(n)\right)$ and $m_2 = \#\ \textit{of ones in binary form of}\ n\ -1$.

The quadratized device model (QDM) of the single-phase saturable-core transformer is expressed as:

$$i_1(t) = i_{L1}(t) + g_{s1} L_1 \frac{di_{L1}(t)}{dt}$$

$$i_2(t) = -i_{L1}(t) - g_{s1} L_1 \frac{di_{L1}(t)}{dt}$$

$$i_3(t) = i_{L2}(t) + g_{s2} L_2 \frac{di_{L2}(t)}{dt}$$

$$i_4(t) = -i_{L2}(t) - g_{s2} L_2 \frac{di_{L2}(t)}{dt}$$

$$0 = v_1(t) - v_2(t) - r_1\left(i_{L1}(t) + g_{s1} L_1 \frac{di_{L1}(t)}{dt}\right) - L_1 \frac{di_{L1}(t)}{dt} - e_c(t)$$

$$0 = v_3(t) - v_4(t) - r_2\left(i_{L2}(t) + g_{s2} L_2 \frac{di_{L2}(t)}{dt}\right) - L_2 \frac{di_{L2}(t)}{dt} - \frac{N_2}{N_1} e_c(t)$$

$$0 = N_1 i_c(t) + N_2\left(i_{L2}(t) + g_{s2} L_2 \frac{di_{L2}(t)}{dt}\right)$$

$$0 = e_c(t) - \frac{d\lambda(t)}{dt}$$

$$0 = -i_{L1}(t) - g_{s1} L_1 \frac{di_{L1}(t)}{dt} + i_c(t) + i_m(t) + g_c e_c(t)$$

$$0 = i_m(t) - i_0 y_m(t)\left[sign(\lambda(t))\right]^{n+1}$$

$$0 = C_1 \frac{dET_1(t)}{dt} + \sum_{i\neq 1}^{n=10}\left(g_{1,i}\right) ET_1(t) - \sum_{j\neq 1}^{n=10}\left(g_{1,j} ET_j(t)\right) - Q_{core,1}(t)$$

$$0 = C_2 \frac{dET_2(t)}{dt} + \sum_{i\neq 2}^{n=10}\left(g_{2,i}\right) ET_2(t) - \sum_{j\neq 2}^{n=10}\left(g_{2,j} ET_j(t)\right) - Q_{core,2}(t)$$

$$0 = C_3 \frac{dET_3(t)}{dt} + \sum_{i\neq 3}^{n=10}\left(g_{3,i}\right)ET_3(t) - \sum_{j\neq 3}^{n=10}\left(g_{3,j}ET_j(t)\right) - Q_{coil\_pri,1}(t)$$

$$0 = C_4 \frac{dET_4(t)}{dt} + \sum_{i\neq 4}^{n=10}\left(g_{4,i}\right)ET_4(t) - \sum_{j\neq 4}^{n=10}\left(g_{4,j}ET_j(t)\right) - Q_{coil\_pri,2}(t)$$

$$0 = C_5 \frac{dET_5(t)}{dt} + \sum_{i\neq 5}^{n=10}\left(g_{5,i}\right)ET_6(t) - \sum_{j\neq 5}^{n=10}\left(g_{5,j}ET_j(t)\right) - Q_{coil\_sec,1}(t)$$

$$0 = C_6 \frac{dET_6(t)}{dt} + \sum_{i\neq 6}^{n=10}\left(g_{6,i}\right)ET_7(t) - \sum_{j\neq 6}^{n=10}\left(g_{6,j}ET_j(t)\right) - Q_{coil\_sec,2}(t)$$

$$0 = C_7 \frac{dET_7(t)}{dt} + \sum_{i\neq 7}^{n=10}\left(g_{7,i}\right)ET_7(t) - \sum_{j\neq 7}^{n=10}\left(g_{7,j}ET_j(t)\right)$$

$$0 = C_8 \frac{dET_8(t)}{dt} + \sum_{i\neq 8}^{n=10}\left(g_{8,i}\right)ET_8(t) - \sum_{j\neq 8}^{n=10}\left(g_{8,j}ET_j(t)\right)$$

$$0 = C_9 \frac{dET_9(t)}{dt} + \sum_{i\neq 9}^{n=9+T_{amb}}\left(g_{9,i}\right)ET_9(t) - \sum_{j\neq 9}^{n=9+T_{amb}}\left(g_{9,j}ET_j(t)\right) - g_{9,T}ET_{amb}$$

$$0 = C_{10} \frac{dET_{10}(t)}{dt} + \sum_{i\neq 1}^{n=10+T_{amb}}\left(g_{10,i}\right)ET_{10}(t) - \sum_{j\neq 10}^{n=10+T_{amb}}\left(g_{10,j}ET_j(t)\right) - g_{10,T}ET_{ambient}$$

$$0 = y_1(t) - \frac{\lambda(t)^2}{\lambda_0^2}$$

$$0 = y_2(t) - y_1(t)^2$$

… …

$$0 = y_{m1}(t) - y_{m1-1}(t)^2$$

$$0 = y_{m1+1}(t) - y_{i1}(t)y_{j1}(t)$$

$$0 = y_{m1+2}(t) - y_{m1+1}(t)y_{j2}(t)$$

… …

$$\begin{cases} 0 = y_m(t) - y_{m-1}(t) y_{jm2}(t), \ \textit{if n even} \\ 0 = y_m(t) - y_{m-1}(t) \dfrac{\lambda(t)}{\lambda_0}, \ \textit{if n odd} \end{cases}$$

$$0 = Q_{core,1}(t) - \frac{1}{2}\alpha_{e+h}\lambda(t)^2$$

$$0 = Q_{core,2}(t) - \frac{1}{2}\alpha_{e+h}\lambda(t)^2$$

$$0 = Q_{coil\_pri,1}(t) - \frac{1}{2} r_1 i_{L1}(t)^2$$

$$0 = Q_{coil\_pri,2}(t) - \frac{1}{2} r_1 i_{L1}(t)^2$$

$$0 = Q_{coil\_sec,1}(t) - \frac{1}{2} r_2 i_{L2}(t)^2$$

$$0 = Q_{coil\_sec,2}(t) - \frac{1}{2} r_2 i_{L2}(t)^2$$

A standard format is introduced here to represent the above QDM of the transformer as follows:

$$i(t) = Y_{eqx1}\mathbf{x}(t) + D_{eqxd1}\frac{d\mathbf{x}(t)}{dt} + C_{eqc1}$$

$$0 = Y_{eqx2}\mathbf{x}(t) + D_{eqxd2}\frac{d\mathbf{x}(t)}{dt} + C_{eqc2}$$

$$0 = Y_{eqx3}\mathbf{x}(t) + \left\{ \begin{array}{c} \vdots \\ \mathbf{x}(t)^T \left\langle F^i_{eqxx3} \right\rangle \mathbf{x}(t) \\ \vdots \end{array} \right\} + C_{eqc3}$$

$$\mathbf{h}(\mathbf{x},\mathbf{u}) = Y_{feqx}\mathbf{x} + \left\{ \begin{array}{c} \vdots \\ \mathbf{x}^T \left\langle F^i_{feqxxx} \right\rangle \mathbf{x} \\ \vdots \end{array} \right\} + C_{feqc}$$

Connectivity: *TerminalNodeName*

$$\textit{subject to}: \ \mathbf{h}_{\min} \le \mathbf{h}(\mathbf{x},\mathbf{u}) \le \mathbf{h}_{\max}, \ \mathbf{x}_{\min} \le \mathbf{x} \le \mathbf{x}_{\max}$$

where

$i(t)$ is the through variables of the device model;

$\mathbf{x}(t)$ is the external and internal state variables of the device model;

Y_{eqx1} is the matrix defining the linear part of state variables in linear through variable

equations;

D_{eqxd1} is the matrix defining the differential part of state variables in linear through variable equations;

C_{eqc1} is the constant vector of the device model in linear through variable equations;

Y_{eqx2} is the matrix defining the linear part of state variables in linear virtual equations;

D_{eqxd2} is the matrix defining the differential part for state variables in linear virtual equations

C_{eqc2} is the constant vector of the device model in linear virtual equations;

Y_{eqx3} is the matrix defining the linear part of state variables in the remaining quadratic equations,

C_{eqc3} is the constant vector of the device model in the remaining quadratic equations;

F_{eqxx} is the matrix defining the quadratic part of state variables in the remaining quadratic equations;

TerminalNodeName is the terminal names defining the connectivity of the device model;

Y_{feqx} is the constraint matrix defining the linear part of state variables;

F_{feqx} is the constraint matrix defining the quadratic part of state variables;

C_{feqc} is the constraint history dependent vector of the device model;

$\mathbf{h}_{\min} \le \mathbf{h}(\mathbf{x},\mathbf{u}) \le \mathbf{h}_{\max}$ is the functional constraint;

$\mathbf{x}_{\min}, \mathbf{x}_{\max}$ are the lower and upper bounds of the state variables.

The transformer QDM has three sets of equations. The first set of equations are external equations and the left sides are terminal currents. The second and third sets of

equations are both internal equations of the transformer. The second set of equations is linear while the third set is nonlinear. The matrices coefficients of the QDM are (assume the exponent n equals 11):

$$Y_{eqx1} = \begin{bmatrix} 0 & 0 & 0 & 0 & 1 & 0 & 0 & 0 & 0 & 0 & 0 & 0 & 0 & 0 & 0 & 0 & 0 & 0 & 0 & 0 & 0 & 0 \\ 0 & 0 & 0 & 0 & -1 & 0 & 0 & 0 & 0 & 0 & 0 & 0 & 0 & 0 & 0 & 0 & 0 & 0 & 0 & 0 & 0 & 0 \\ 0 & 0 & 0 & 0 & 0 & 1 & 0 & 0 & 0 & 0 & 0 & 0 & 0 & 0 & 0 & 0 & 0 & 0 & 0 & 0 & 0 & 0 \\ 0 & 0 & 0 & 0 & 0 & -1 & 0 & 0 & 0 & 0 & 0 & 0 & 0 & 0 & 0 & 0 & 0 & 0 & 0 & 0 & 0 & 0 \end{bmatrix}$$

$$D_{eqx1} = \begin{bmatrix} 0 & 0 & 0 & 0 & g_{s1}L_1 & 0 & 0 & 0 & 0 & 0 & 0 & 0 & 0 & 0 & 0 & 0 & 0 & 0 & 0 & 0 & 0 & 0 \\ 0 & 0 & 0 & 0 & -g_{s1}L_1 & 0 & 0 & 0 & 0 & 0 & 0 & 0 & 0 & 0 & 0 & 0 & 0 & 0 & 0 & 0 & 0 & 0 \\ 0 & 0 & 0 & 0 & 0 & g_{s2}L_2 & 0 & 0 & 0 & 0 & 0 & 0 & 0 & 0 & 0 & 0 & 0 & 0 & 0 & 0 & 0 & 0 \\ 0 & 0 & 0 & 0 & 0 & -g_{s2}L_2 & 0 & 0 & 0 & 0 & 0 & 0 & 0 & 0 & 0 & 0 & 0 & 0 & 0 & 0 & 0 & 0 \end{bmatrix}$$

$$C_{eqc1} = 0$$

$$Y_{eqx2} = \begin{bmatrix} 1 & -1 & 0 & 0 & -r_1 & 0 & 0 & -1 & 0 & 0 & 0 & 0 & 0 & 0 & 0 & 0 & 0 & 0 & 0 & 0 & 0 & 0 \\ 0 & 0 & 1 & -1 & 0 & -r_2 & 0 & \frac{N_2}{N_1} & 0 & 0 & 0 & 0 & 0 & 0 & 0 & 0 & 0 & 0 & 0 & 0 & 0 & 0 \\ 0 & 0 & 0 & 0 & 0 & N_2 & 0 & 0 & N_1 & 0 & 0 & 0 & 0 & 0 & 0 & 0 & 0 & 0 & 0 & 0 & 0 & 0 \\ 0 & 0 & 0 & 0 & 0 & 0 & 1 & 0 & 0 & 0 & 0 & 0 & 0 & 0 & 0 & 0 & 0 & 0 & 0 & 0 & 0 & 0 \\ 0 & 0 & 0 & 0 & -1 & 0 & g_c & 0 & 1 & 1 & 0 & 0 & 0 & 0 & 0 & 0 & 0 & 0 & 0 & 0 & 0 & 0 \\ 0 & 0 & 0 & 0 & 0 & 0 & 0 & 0 & 0 & 1 & 0 & 0 & 0 & 0 & -i_0 & 0 & 0 & 0 & 0 & 0 & 0 & 0 \\ 0 & 0 & 0 & 0 & 0 & 0 & 0 & 0 & 0 & 0 & 0 & 0 & 0 & 0 & 0 & g_1+g_2+g_3+g_4 & -g_1 & -g_2 & -g_3 & -g_4 & 0 & 0 & 0 \\ 0 & 0 & 0 & 0 & 0 & 0 & 0 & 0 & 0 & 0 & 0 & 0 & 0 & 0 & 0 & -g_1 & g_1+g_5+g_6+g_7 & -g_5 & -g_6 & -g_7 & 0 & 0 & 0 \\ 0 & 0 & 0 & 0 & 0 & 0 & 0 & 0 & 0 & 0 & 0 & 0 & 0 & 0 & 0 & -g_2 & -g_5 & g_2+g_5+g_8+g_9 & -g_8 & -g_9 & 0 & 0 & 0 \\ 0 & 0 & 0 & 0 & 0 & 0 & 0 & 0 & 0 & 0 & 0 & 0 & 0 & 0 & 0 & -g_3 & -g_6 & -g_8 & g_3+g_6+g_8+g_{10} & -g_{10} & 0 & 0 & 0 \\ 0 & 0 & 0 & 0 & 0 & 0 & 0 & 0 & 0 & 0 & 0 & 0 & 0 & 0 & 0 & -g_4 & -g_7 & -g_9 & -g_{10} & g_4+g_7+g_9+g_{10}+g_{11} & 0 & 0 & 0 \end{bmatrix}$$

$$D_{eqx2} = \begin{bmatrix} 0 & 0 & 0 & 0 & -r_1 g_{s1} L_1 - L_1 & 0 & 0 & 0 & 0 & 0 & 0 & 0 & 0 & 0 & 0 & 0 & 0 & 0 & 0 & 0 & 0 \\ 0 & 0 & 0 & 0 & 0 & -r_2 g_{22} L_2 - L_2 & 0 & 0 & 0 & 0 & 0 & 0 & 0 & 0 & 0 & 0 & 0 & 0 & 0 & 0 & 0 \\ 0 & 0 & 0 & 0 & 0 & N_2 g_{s2} L_2 & 0 & 0 & 0 & 0 & 0 & 0 & 0 & 0 & 0 & 0 & 0 & 0 & 0 & 0 & 0 \\ 0 & 0 & 0 & 0 & 0 & 0 & -1 & 0 & 0 & 0 & 0 & 0 & 0 & 0 & 0 & 0 & 0 & 0 & 0 & 0 & 0 \\ 0 & 0 & 0 & 0 & -g_{s1} L_1 & 0 & 0 & 0 & 0 & 0 & 0 & 0 & 0 & 0 & 0 & 0 & 0 & 0 & 0 & 0 & 0 \\ 0 & 0 & 0 & 0 & 0 & 0 & 0 & 0 & 0 & 0 & 0 & 0 & 0 & 0 & 0 & 0 & 0 & 0 & 0 & 0 & 0 \\ 0 & 0 & 0 & 0 & 0 & 0 & 0 & 0 & 0 & 0 & 0 & 0 & 0 & 0 & C_1 & 0 & 0 & 0 & 0 & 0 & 0 \\ 0 & 0 & 0 & 0 & 0 & 0 & 0 & 0 & 0 & 0 & 0 & 0 & 0 & 0 & 0 & C_2 & 0 & 0 & 0 & 0 & 0 \\ 0 & 0 & 0 & 0 & 0 & 0 & 0 & 0 & 0 & 0 & 0 & 0 & 0 & 0 & 0 & 0 & \ddots & 0 & 0 & 0 & 0 \\ 0 & 0 & 0 & 0 & 0 & 0 & 0 & 0 & 0 & 0 & 0 & 0 & 0 & 0 & 0 & 0 & 0 & \ddots & 0 & 0 & 0 \\ 0 & 0 & 0 & 0 & 0 & 0 & 0 & 0 & 0 & 0 & 0 & 0 & 0 & 0 & 0 & 0 & 0 & 0 & C_{10} & 0 & 0 \end{bmatrix}$$

$$C_{eqc2} = \begin{bmatrix} 0 & 0 & 0 & 0 & 0 & 0 & 0 & 0 & \cdots & \cdots & -g_{10,T} T_{ambient} \end{bmatrix}^T$$

$$Y_{eqx3} = \begin{bmatrix} 0 & 0 & 0 & 0 & 0 & 0 & 0 & 0 & 0 & 0 & 1 & 0 & 0 & 0 & 0 & 0 & 0 & 0 & 0 & 0 & 0 & 0 \\ 0 & 0 & 0 & 0 & 0 & 0 & 0 & 0 & 0 & 0 & 0 & 1 & 0 & 0 & 0 & 0 & 0 & 0 & 0 & 0 & 0 & 0 \\ 0 & 0 & 0 & 0 & 0 & 0 & 0 & 0 & 0 & 0 & 0 & 0 & 1 & 0 & 0 & 0 & 0 & 0 & 0 & 0 & 0 & 0 \\ 0 & 0 & 0 & 0 & 0 & 0 & 0 & 0 & 0 & 0 & 0 & 0 & 0 & 1 & 0 & 0 & 0 & 0 & 0 & 0 & 0 & 0 \\ 0 & 0 & 0 & 0 & 0 & 0 & 0 & 0 & 0 & 0 & 0 & 0 & 0 & 0 & 1 & 0 & 0 & 0 & 0 & 0 & 0 & 0 \\ 0 & 0 & 0 & 0 & 0 & 0 & 0 & 0 & 0 & 0 & 0 & 0 & 0 & 0 & 0 & 0 & 0 & 0 & 0 & 1 & 0 & 0 \\ 0 & 0 & 0 & 0 & 0 & 0 & 0 & 0 & 0 & 0 & 0 & 0 & 0 & 0 & 0 & 0 & 0 & 0 & 0 & 0 & 1 & 0 \\ 0 & 0 & 0 & 0 & 0 & 0 & 0 & 0 & 0 & 0 & 0 & 0 & 0 & 0 & 0 & 0 & 0 & 0 & 0 & 0 & 0 & 1 \end{bmatrix}$$

$$F_{eqxx3}\langle 0, (6,6) \rangle = -\frac{1}{\lambda_0^2}$$

$$F_{eqxx3}\langle 1, (10,10) \rangle = -1$$

$$F_{eqxx3}\langle 2, (11,11) \rangle = -1$$

$$F_{eqxx3}\langle 3, (10,12) \rangle = -1$$

$$F_{eqxx3}\langle 4, (6,13) \rangle = -\frac{1}{\lambda_0}$$

$$F_{eqxx3}\langle 5, (6,6) \rangle = -\frac{1}{2}\alpha_{e+h}$$

$$F_{eqxx3}\langle 6,(6,6)\rangle = -\frac{1}{2}\alpha_{e+h}$$

$$F_{eqxx3}\langle 7,(4,4)\rangle = -\frac{1}{2}r_1$$

$$F_{eqxx3}\langle 8,(4,4)\rangle = -\frac{1}{2}r_1$$

$$F_{eqxx3}\langle 9,(5,5)\rangle = -\frac{1}{2}r_2$$

$$F_{eqxx3}\langle 10,(5,5)\rangle = -\frac{1}{2}r_2$$

$$C_{eqc3} = 0$$

There are 31 state variables and 31 equations in the model. The definition of the external state, internal state, and through variables are listed in Table 4-1 to Table 4-3, respectively.

Table 4 - 1. External states of the transformer.

Index	Variable	Description
0	$v_1(t)$	terminal voltage of transformer high side (V)
1	$v_2(t)$	terminal voltage of transformer high neutral (V)
2	$v_3(t)$	terminal voltage of transformer low side (V)
3	$v_4(t)$	terminal voltage of transformer low neutral (V)

Table 4 - 2. Internal states of the transformer.

Index	Variable	Description
4	$i_{L1}(t)$	current through the high side inductance (A)
5	$i_{L2}(t)$	current through the low side inductance (A)
6	$\lambda(t)$	flux linkage (Web)

Table 4 - 2 continued

Index	Variable	Description
7	$e_c(t)$	voltage generated by the flux (A)
8	$i_c(t)$	current through high side windings (A)
9	$i_m(t)$	magnetizing current (A)
10	$y_1(t)$	introduced state (p.u.)
11	$y_2(t)$	introduced state (p.u.)
12	$y_3(t)$	introduced state (p.u.)
13	$y_4(t)$	introduced state (p.u.)
14	$y_5(t)$	introduced state (p.u.)
15	$ET_1(t)$	temperature at core up point (Celsius)
16	$ET_2(t)$	temperature at core down point (Celsius)
17	$ET_3(t)$	temperature at primary coil up point (Celsius)
18	$ET_4(t)$	temperature at primary coil down point (Celsius)
19	$ET_5(t)$	temperature at secondary coil up point (Celsius)
20	$ET_6(t)$	temperature at secondary coil down point (Celsius)
21	$ET_7(t)$	temperature at internal oil up point (Celsius)
22	$ET_8(t)$	temperature at internal oil down point (Celsius)
23	$ET_9(t)$	temperature at transformer tank front point (Celsius)
24	$ET_{10}(t)$	temperature at transformer tank rear point (Celsius)
25	$Q_{core,1}(t)$	heat generated at core up point (W)

Table 4 - 2 continued

Index	Variable	Description
26	$Q_{core,2}(t)$	heat generated at core down point (W)
27	$Q_{coil\_pri,1}(t)$	heat generated at primary coil up point (W)
28	$Q_{coil\_pri,2}(t)$	heat generated at primary coil down point (W)
29	$Q_{coil\_sec,1}(t)$	heat generated at secondary coil up point (W)
30	$Q_{coil\_sec,2}(t)$	heat generated at secondary coil down point (W)

Table 4 - 3. Through variables of the transformer.

Index	Variable	Description
0	$i_1(t)$	current through transformer high side
1	$i_2(t)$	current through transformer high side neutral
2	$i_3(t)$	current through transformer low side
3	$i_4(t)$	current through transformer low side neutral

4.2.2 Single-Phase Auto-Transformer Physical Electro-Thermal Quadratized Model

The electro-thermal model of a single-phase auto-transformer is introduced in this part. The equivalent circuit of a single-phase auto-transformer with both electric part and thermal part is shown in Figure 4-2.

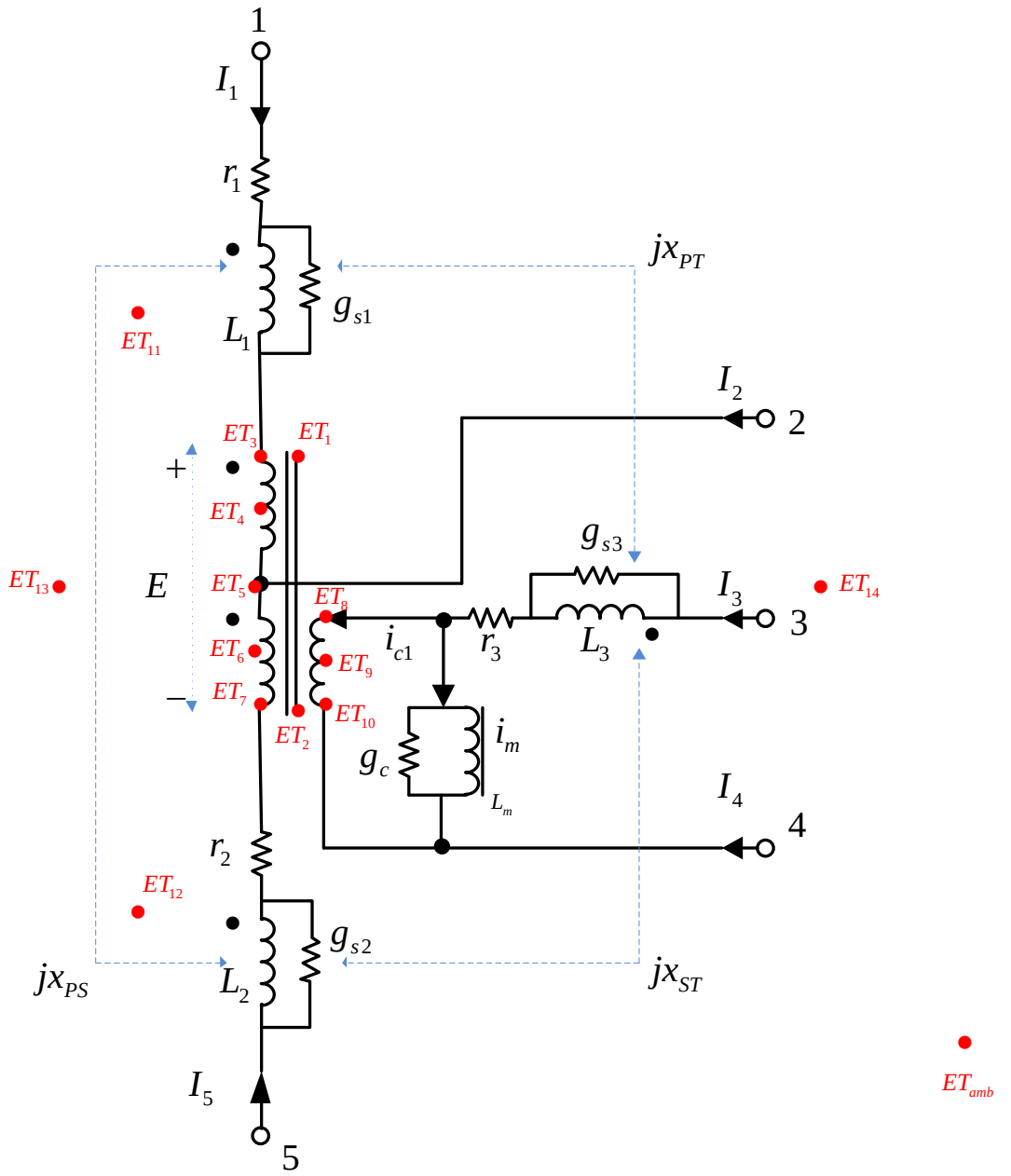

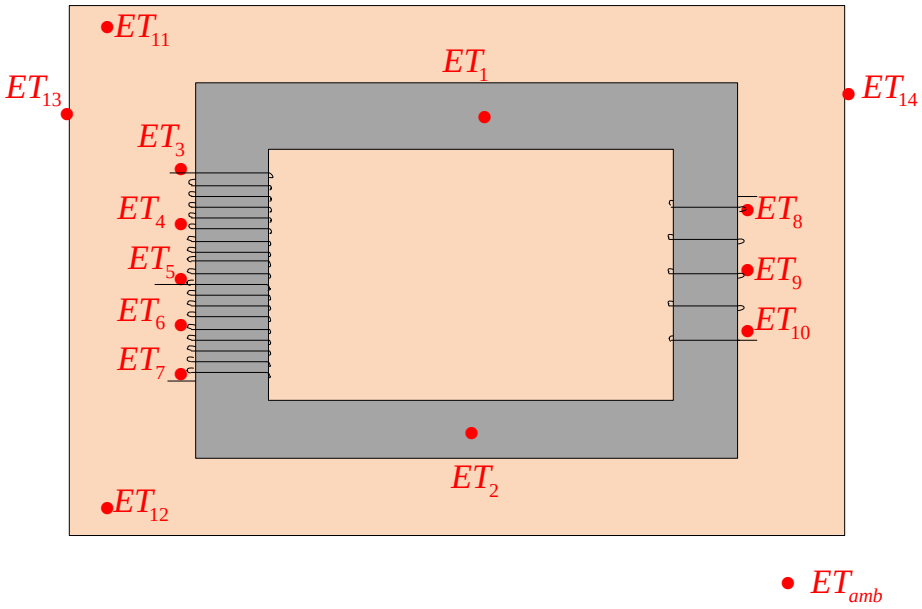

Figure 4 - 2. Equivalent electro-thermal circuit of a single-phase autotransformer with tertiary winding

The "numerical stabilizers" $g_{s1} \sim g_{s3}$ are introduced to eliminate possible numerical problems. The numerical stabilizers introduce errors orders of magnitude below the measurement errors and therefore do not affect the overall accuracy of the proposed protection method. The red spots (ET_x) are the thermocouple points. ET_1 and ET_2 are the thermal temperature points at the core (top and bottom), ET_3 to ET_7 are the thermal temperature points at the primary and secondary coils (top, middle, and bottom), ET_8 to ET_{10} are the thermal temperature points at the tertiary coils (top, middle, and bottom), ET_{11} and ET_{12} are the thermal temperature points at the oil (top and bottom), ET_{13} and ET_{14} are the thermal temperature points at the tank (front and rear), ET_{amb} is the ambient temperature point. The transformer losses are computed from the measured voltage and current waveforms at the transformer terminals. Computed losses include winding coil losses (Ohmic losses) as well as magnetic core losses.

At first, the transformer compact model of the single phase autotransformer with

tertiary winding is introduced in the following differential algebraic equations:

$$i_1(t) = i_{L1}(t) + i_{gs1}(t)$$

$$i_2(t) = -i_{L1}(t) - i_{gs1}(t) - i_{L2}(t) - i_{gs2}(t)$$

$$i_3(t) = i_{L3}(t) + i_{gs3}(t)$$

$$i_4(t) = -i_{L3}(t) - i_{gs3}(t)$$

$$i_5(t) = i_{L2}(t) + i_{gs2}(t)$$

$$0 = v_1(t) - v_2(t) - r_1\left(i_{L1}(t) + i_{gs1}(t)\right) - i_{gs1}(t) / g_{s1} - \frac{N_1}{N_1 + N_2}\frac{d\lambda(t)}{dt}$$

$$0 = v_5(t) - v_2(t) - r_2\left(i_{L2}(t) + i_{gs2}(t)\right) - i_{gs2}(t) / g_{s2} + \frac{N_2}{N_1 + N_2}\frac{d\lambda(t)}{dt}$$

$$0 = v_3(t) - v_4(t) - r_3\left(i_{L3}(t) + i_{gs3}(t)\right) - i_{gs3}(t) / g_{s3} - \frac{N_3}{N_1 + N_2}\frac{d\lambda(t)}{dt}$$

$$0 = i_{gs1}(t) / g_{s1} - L_1\frac{di_{L1}(t)}{dt} + L_{PS}\frac{di_{L2}(t)}{dt} - L_{PT}\frac{di_{L3}(t)}{dt}$$

$$0 = i_{gs2}(t) / g_{s2} - L_2\frac{di_{L2}(t)}{dt} + L_{PS}\frac{di_{L1}(t)}{dt} + L_{ST}\frac{di_{L3}(t)}{dt}$$

$$0 = i_{gs3}(t) / g_{s3} - L_3\frac{di_{L3}(t)}{dt} + L_{ST}\frac{di_{L2}(t)}{dt} - L_{PT}\frac{di_{L1}(t)}{dt}$$

$$0 = -i_{L3}(t) - i_{gs3}(t) + i_{c1}(t) + i_m(t) + g_c\frac{N_3}{N_1 + N_2}e_c(t)$$

$$0 = N_1\left(i_{L1}(t) + i_{gs1}(t)\right) - N_2\left(i_{L2}(t) + i_{gs2}(t)\right) + N_3 i_{c1}(t)$$

$$0 = i_m(t) - i_0\left|\frac{\lambda(t)}{\lambda_0}\right|^n sign\left(\lambda(t)\right)$$

$$0 = C_1\frac{dET_1(t)}{dt} + \sum_{i\neq 1}^{n=14}\left(g_{1,i}\right)ET_1(t) - \sum_{j\neq 1}^{n=14}\left(g_{1,j}ET_j(t)\right) - Q_{core,1}(t)$$

$$0 = C_2\frac{dET_2(t)}{dt} + \sum_{i\neq 2}^{n=14}\left(g_{2,i}\right)ET_2(t) - \sum_{j\neq 2}^{n=14}\left(g_{2,j}ET_j(t)\right) - Q_{core,2}(t)$$

$$0 = C_3 \frac{dET_3(t)}{dt} + \sum_{i\neq 3}^{n=14}\left(g_{3,i}\right)ET_3(t) - \sum_{j\neq 3}^{n=14}\left(g_{3,j}ET_j(t)\right) - Q_{coil\_pri,1}(t)$$

$$0 = C_4 \frac{dET_4(t)}{dt} + \sum_{i\neq 4}^{n=14}\left(g_{4,i}\right)ET_4(t) - \sum_{j\neq 4}^{n=14}\left(g_{4,j}ET_j(t)\right) - Q_{coil\_pri,2}(t)$$

$$0 = C_5 \frac{dET_5(t)}{dt} + \sum_{i\neq 5}^{n=14}\left(g_{5,i}\right)ET_5(t) - \sum_{j\neq 5}^{n=14}\left(g_{5,j}ET_j(t)\right) - \frac{1}{2}\left(Q_{coil\_pri,2}(t) + Q_{coil\_sec,1}(t)\right)$$

$$0 = C_6 \frac{dET_6(t)}{dt} + \sum_{i\neq 6}^{n=14}\left(g_{6,i}\right)ET_6(t) - \sum_{j\neq 6}^{n=14}\left(g_{6,j}ET_j(t)\right) - Q_{coil\_sec,1}(t)$$

$$0 = C_7 \frac{dET_7(t)}{dt} + \sum_{i\neq 7}^{n=14}\left(g_{7,i}\right)ET_7(t) - \sum_{j\neq 7}^{n=14}\left(g_{7,j}ET_j(t)\right) - Q_{coil\_sec,2}(t)$$

$$0 = C_8 \frac{dET_8(t)}{dt} + \sum_{i\neq 8}^{n=14}\left(g_{8,i}\right)ET_8(t) - \sum_{j\neq 8}^{n=14}\left(g_{8,j}ET_j(t)\right) - Q_{coil\_ter,1}(t)$$

$$0 = C_9 \frac{dET_9(t)}{dt} + \sum_{i\neq 9}^{n=14}\left(g_{9,i}\right)ET_9(t) - \sum_{j\neq 9}^{n=14}\left(g_{9,j}ET_j(t)\right) - \frac{1}{2}\left(Q_{coil\_ter,1}(t) + Q_{coil\_ter,2}(t)\right)$$

$$0 = C_{10} \frac{dET_{10}(t)}{dt} + \sum_{i\neq 10}^{n=14}\left(g_{10,i}\right)ET_{10}(t) - \sum_{j\neq 10}^{n=14}\left(g_{10,j}ET_j(t)\right) - Q_{coil\_ter,2}(t)$$

$$0 = C_{11} \frac{dET_{11}(t)}{dt} + \sum_{i\neq 11}^{n=14}\left(g_{11,i}\right)ET_{11}(t) - \sum_{j\neq 11}^{n=14}\left(g_{11,j}ET_j(t)\right)$$

$$0 = C_{12} \frac{dET_{12}(t)}{dt} + \sum_{i\neq 12}^{n=14}\left(g_{12,i}\right)ET_{12}(t) - \sum_{j\neq 12}^{n=14}\left(g_{12,j}ET_j(t)\right)$$

$$0 = C_{13} \frac{dET_{13}(t)}{dt} + \sum_{i\neq 13}^{n=14+T_{amb}}\left(g_{13,i}\right)ET_{13}(t) - \sum_{j\neq 13}^{n=14+T_{amb}}\left(g_{13,j}ET_j(t)\right) - g_{13,T}ET_{amb}$$

$$0 = C_{14} \frac{dET_{14}(t)}{dt} + \sum_{i\neq 1}^{n=14+T_{amb}}\left(g_{14,i}\right)ET_{14}(t) - \sum_{j\neq 14}^{n=14+T_{amb}}\left(g_{14,j}ET_j(t)\right) - g_{14,T}ET_{amb}$$

$$0 = Q_{core,1}(t) - \frac{1}{2}\alpha_{e+h}\lambda(t)^2$$

$$0 = Q_{core,2}(t) - \frac{1}{2}\alpha_{e+h}\lambda(t)^2$$

$$0 = Q_{coil\_pri,1}(t) - \frac{1}{2} r_1 i_{L1}(t)^2$$

$$0 = Q_{coil\_pri,2}(t) - \frac{1}{2} r_1 i_{L1}(t)^2$$

$$0 = Q_{coil\_sec,1}(t) - \frac{1}{2} r_2 i_{L2}(t)^2$$

$$0 = Q_{coil\_sec,2}(t) - \frac{1}{2} r_2 i_{L2}(t)^2$$

$$0 = Q_{coil\_ter,1}(t) - \frac{1}{2} r_3 i_{L3}(t)^2$$

$$0 = Q_{coil\_ter,2}(t) - \frac{1}{2} r_3 i_{L3}(t)^2$$

where $v_{1\sim5}(t)$ and $i_{1\sim5}(t)$ are the terminal voltages and currents, $ET_{1\sim14}(t)$ are the temperature at the hotspots, $r_1, r_2, r_3, L_1, L_2, L_3$ are the corresponding resistances and inductances, L_{PS}, L_{PT}, L_{ST} are the corresponding mutual inductances, $C_1 \sim C_{14}, g_{i,j} (where\, i, j = 1 \sim 14, i \neq j)$ are the corresponding thermal capacitance and conductance, N_1 , N_2 and N_3 are the number of turns at the primary, secondary and tertiary windings, g_c is the excitation conductance, $i_m(t)$ is the magnetizing current and $\lambda(t)$ is the flux linkage through the iron core, $Q_{core,1}(t), Q_{core,2}(t)$ are the heat generated at the core, $Q_{coil\_pri,1}(t), Q_{coil\_pri,2}(t)$ are the heat generated at the primary winding, $Q_{coil\_sec,1}(t), Q_{coil\_sec,2}(t)$ are the heat generated at the secondary winding and $Q_{coil\_ter,1}(t), Q_{coil\_ter,2}(t)$ are the heat generated at the tertiary winding.

There are 36 state variables and 36 equations in the compact model. Similar to the single-phase saturable-core transformer presented in last section, the auto-transformer model is also quadratized by introducing additional state variables and equations. Specifically, the equation:

$$0 = i_m(t) - i_0 \left| \frac{\lambda(t)}{\lambda_0} \right|^n sign(\lambda(t))$$

is also quadratized with the newly introduced states as:

$$0 = i_m(t) - i_0 y_m(t) \left[sign(\lambda(t)) \right]^{n+1}$$

$$0 = y_1(t) - \frac{\lambda(t)^2}{\lambda_0^2}$$

$$0 = y_2(t) - y_1(t)^2$$

… …

$$0 = y_{m1}(t) - y_{m1-1}(t)^2$$

$$0 = y_{m1+1}(t) - y_{i1}(t) y_{j1}(t)$$

$$0 = y_{m1+2}(t) - y_{m1+1}(t) y_{j2}(t)$$

… …

$$\begin{cases} 0 = y_m(t) - y_{m-1}(t) y_{jm2}(t), \ if \ n \ even \\ 0 = y_m(t) - y_{m-1}(t) \dfrac{\lambda(t)}{\lambda_0}, \ if \ n \ odd \end{cases}$$

where the states $y_1(t) \sim y_m(t)$ are introduced to ensure that transformer mathematical model consists of equations of at most quadratic degree, and $m = m_1 + m_2$, $m_1 = \text{int}\left(\log_2(n)\right)$ and $m_2 = \#\ of\ ones\ in\ binary\ form\ of\ n\ -1.$

The quadratized device model (QDM) of the single-phase auto-transformer is expressed as:

$$i_1(t) = i_{L1}(t) + i_{gs1}(t)$$

$$i_2(t) = -i_{L1}(t) - i_{gs1}(t) - i_{L2}(t) - i_{gs2}(t)$$

$$i_3(t) = i_{L3}(t) + i_{gs3}(t)$$

$$i_4(t) = -i_{L3}(t) - i_{gs3}(t)$$

$$i_5(t) = i_{L2}(t) + i_{gs2}(t)$$

$$0 = z_1(t) - \frac{di_{L1}(t)}{dt}$$

$$0 = z_2(t) - \frac{di_{L2}(t)}{dt}$$

$$0 = z_3(t) - \frac{di_{L3}(t)}{dt}$$

$$0 = e_c(t) - \frac{d\lambda(t)}{dt}$$

$$0 = v_1(t) - v_2(t) - r_1\left(i_{L1}(t) + i_{gs1}(t)\right) - i_{gs1}(t) / g_{s1} - \frac{N_1}{N_1 + N_2} e_c(t)$$

$$0 = v_5(t) - v_2(t) - r_2\left(i_{L2}(t) + i_{gs2}(t)\right) - i_{gs2}(t) / g_{s2} + \frac{N_2}{N_1 + N_2} e_c(t)$$

$$0 = v_3(t) - v_4(t) - r_3\left(i_{L3}(t) + i_{gs3}(t)\right) - i_{gs3}(t) / g_{s3} - \frac{N_3}{N_1 + N_2} e_c(t)$$

$$0 = i_{gs1}(t) / g_{s1} - L_1 z_1(t) + L_{PS} z_2(t) - L_{PT} z_3(t)$$

$$0 = i_{gs2}(t) / g_{s2} - L_2 z_2(t) + L_{PS} z_1(t) + L_{ST} z_3(t)$$

$$0 = i_{gs3}(t) / g_{s3} - L_3 z_3(t) + L_{ST} z_2(t) - L_{PT} z_1(t)$$

$$0 = -i_{L3}(t) - i_{gs3}(t) + i_{c1}(t) + i_m(t) + g_c \frac{N_3}{N_1 + N_2} e_c(t)$$

$$0 = N_1\left(i_{L1}(t) + i_{gs1}(t)\right) - N_2\left(i_{L2}(t) + i_{gs2}(t)\right) + N_3 i_{c1}(t)$$

$$0 = i_{m1}(t) - i_0 y_m(t) sign\left(\lambda(t)\right)^{n+1}$$

$$0 = C_1 \frac{dET_1(t)}{dt} + \sum_{i \neq 1}^{n=14}\left(g_{1,i}\right) ET_1(t) - \sum_{j \neq 1}^{n=14}\left(g_{1,j} ET_j(t)\right) - Q_{core,1}(t)$$

$$0 = C_2 \frac{dET_2(t)}{dt} + \sum_{i \neq 2}^{n=14}\left(g_{2,i}\right) ET_2(t) - \sum_{j \neq 2}^{n=14}\left(g_{2,j} ET_j(t)\right) - Q_{core,2}(t)$$

$$0 = C_3 \frac{dET_3(t)}{dt} + \sum_{i \neq 3}^{n=14}\left(g_{3,i}\right) ET_3(t) - \sum_{j \neq 3}^{n=14}\left(g_{3,j} ET_j(t)\right) - Q_{coil\_pri,1}(t)$$

$$0 = C_4 \frac{dET_4(t)}{dt} + \sum_{i \neq 4}^{n=14}\left(g_{4,i}\right) ET_4(t) - \sum_{j \neq 4}^{n=14}\left(g_{4,j} ET_j(t)\right) - Q_{coil\_pri,2}(t)$$

$$0 = C_5 \frac{dET_5(t)}{dt} + \sum_{i\neq 5}^{n=14}\left(g_{5,i}\right)ET_5(t) - \sum_{j\neq 5}^{n=14}\left(g_{5,j}ET_j(t)\right) - \frac{1}{2}\left(Q_{coil\_pri,2}(t) + Q_{coil\_sec,1}(t)\right)$$

$$0 = C_6 \frac{dET_6(t)}{dt} + \sum_{i\neq 6}^{n=14}\left(g_{6,i}\right)ET_6(t) - \sum_{j\neq 6}^{n=14}\left(g_{6,j}ET_j(t)\right) - Q_{coil\_sec,1}(t)$$

$$0 = C_7 \frac{dET_7(t)}{dt} + \sum_{i\neq 7}^{n=14}\left(g_{7,i}\right)ET_7(t) - \sum_{j\neq 7}^{n=14}\left(g_{7,j}ET_j(t)\right) - Q_{coil\_sec,2}(t)$$

$$0 = C_8 \frac{dET_8(t)}{dt} + \sum_{i\neq 8}^{n=14}\left(g_{8,i}\right)ET_8(t) - \sum_{j\neq 8}^{n=14}\left(g_{8,j}ET_j(t)\right) - Q_{coil\_ter,1}(t)$$

$$0 = C_9 \frac{dET_9(t)}{dt} + \sum_{i\neq 9}^{n=14}\left(g_{9,i}\right)ET_9(t) - \sum_{j\neq 9}^{n=14}\left(g_{9,j}ET_j(t)\right) - \frac{1}{2}\left(Q_{coil\_ter,1}(t) + Q_{coil\_ter,2}(t)\right)$$

$$0 = C_{10} \frac{dET_{10}(t)}{dt} + \sum_{i\neq 10}^{n=14}\left(g_{10,i}\right)ET_{10}(t) - \sum_{j\neq 10}^{n=14}\left(g_{10,j}ET_j(t)\right) - Q_{coil\_ter,2}(t)$$

$$0 = C_{11} \frac{dET_{11}(t)}{dt} + \sum_{i\neq 11}^{n=14}\left(g_{11,i}\right)ET_{11}(t) - \sum_{j\neq 11}^{n=14}\left(g_{11,j}ET_j(t)\right)$$

$$0 = C_{12} \frac{dET_{12}(t)}{dt} + \sum_{i\neq 12}^{n=14}\left(g_{12,i}\right)ET_{12}(t) - \sum_{j\neq 12}^{n=14}\left(g_{12,j}ET_j(t)\right)$$

$$0 = C_{13} \frac{dET_{13}(t)}{dt} + \sum_{i\neq 13}^{n=14+T_{amb}}\left(g_{13,i}\right)ET_{13}(t) - \sum_{j\neq 13}^{n=14+T_{amb}}\left(g_{13,j}ET_j(t)\right) - g_{13,T}ET_{amb}$$

$$0 = C_{14} \frac{dET_{14}(t)}{dt} + \sum_{i\neq 1}^{n=14+T_{amb}}\left(g_{14,i}\right)ET_{14}(t) - \sum_{j\neq 14}^{n=14+T_{amb}}\left(g_{14,j}ET_j(t)\right) - g_{14,T}ET_{amb}$$

$$0 = y_1(t) - \frac{\lambda(t)^2}{\lambda_0^2}$$

$$0 = y_2(t) - y_1(t)^2$$

.....

$$0 = y_{m1}(t) - y_{m1-1}(t)^2$$

$$0 = y_{m1+1}(t) - y_{i1}(t)y_{j1}(t)$$

$$0 = y_{m1+2}(t) - y_{m1+1}(t) y_{j2}(t)$$

.....

$$\begin{cases} 0 = y_m(t) - y_{m-1}(t) y_{jm2}(t), & if\ n\ even \\ 0 = y_m(t) - y_{m-1}(t) \dfrac{\lambda(t)}{\lambda_0}, & if\ n\ odd \end{cases}$$

$$0 = Q_{core,1}(t) - \frac{1}{2}\alpha_{e+h}\lambda(t)^2$$

$$0 = Q_{core,2}(t) - \frac{1}{2}\alpha_{e+h}\lambda(t)^2$$

$$0 = Q_{coil\_pri,1}(t) - \frac{1}{2} r_1 i_{L1}(t)^2$$

$$0 = Q_{coil\_pri,2}(t) - \frac{1}{2} r_1 i_{L1}(t)^2$$

$$0 = Q_{coil\_sec,1}(t) - \frac{1}{2} r_2 i_{L2}(t)^2$$

$$0 = Q_{coil\_sec,2}(t) - \frac{1}{2} r_2 i_{L2}(t)^2$$

$$0 = Q_{coil\_ter,1}(t) - \frac{1}{2} r_3 i_{L3}(t)^2$$

$$0 = Q_{coil\_ter,2}(t) - \frac{1}{2} r_3 i_{L3}(t)^2$$

Similar to the single-phase saturable-core transformer, a standard format is also introduced here to represent the above QDM of the single-phase auto-transformer as follows:

$$i(t) = Y_{eqx1}\mathbf{x}(t) + D_{eqxd1}\frac{d\mathbf{x}(t)}{dt} + C_{eqc1}$$

$$0 = Y_{eqx2}\mathbf{x}(t) + D_{eqxd2}\frac{d\mathbf{x}(t)}{dt} + C_{eqc2}$$

$$0 = Y_{eqx3}\mathbf{x}(t) + \left\{ \begin{array}{c} \vdots \\ \mathbf{x}(t)^T \left\langle F^i_{eqxx3} \right\rangle \mathbf{x}(t) \\ \vdots \end{array} \right\} + C_{eqc3}$$

$$\mathbf{h}(\mathbf{x},\mathbf{u}) = Y_{feqx}\mathbf{x} + \left\{ \begin{array}{c} \vdots \\ \mathbf{x}^T \left\langle F^i_{feqxxx} \right\rangle \mathbf{x} \\ \vdots \end{array} \right\} + C_{feqc}$$

Connectivity: *TerminalNodeName*

$$\textit{subject to}: \ \mathbf{h}_{\min} \le \mathbf{h}(\mathbf{x},\mathbf{u}) \le \mathbf{h}_{\max}, \ \mathbf{x}_{\min} \le \mathbf{x} \le \mathbf{x}_{\max}$$

where the matrices coefficients of the QDM are (assume the exponent n equals 11):

$$Y_{eqx1} = \begin{bmatrix} 0 & 0 & 0 & 0 & 0 & 1 & 0 & 0 & 1 & 0 & 0 & 0 & 0 & 0 & 0 & 0 & \cdots & 0 & 0 & 0 \\ 0 & 0 & 0 & 0 & 0 & -1 & -1 & 0 & -1 & -1 & 0 & 0 & 0 & 0 & 0 & 0 & \cdots & 0 & 0 & 0 \\ 0 & 0 & 0 & 0 & 0 & 0 & 0 & 1 & 0 & 0 & 1 & 0 & 0 & 0 & 0 & 0 & \cdots & 0 & 0 & 0 \\ 0 & 0 & 0 & 0 & 0 & 0 & 0 & -1 & 0 & 0 & 0 & -1 & 0 & 0 & 0 & 0 & \cdots & 0 & 0 & 0 \\ 0 & 0 & 0 & 0 & 0 & 0 & 1 & 0 & 0 & 1 & 0 & 0 & 0 & 0 & 0 & 0 & \cdots & 0 & 0 & 0 \end{bmatrix}$$

$$D_{eqx1} = 0$$

$$C_{eqc1} = 0$$

$$Y_{eqx2} = \begin{bmatrix} Y_{A11}(13 \times 23) & Y_{A12}(13 \times 20) \\ Y_{A21}(12 \times 23) & Y_{A22}(12 \times 20) \end{bmatrix}$$

$$Y_{A11} = \begin{bmatrix} 0 & 0 & 0 & 0 & 0 & 0 & 0 & 0 & 0 & 0 & 0 & 1 & 0 & 0 & 0 & 0 & 0 & 0 & 0 & 0 & 0 & 0 & 0 \\ 0 & 0 & 0 & 0 & 0 & 0 & 0 & 0 & 0 & 0 & 0 & 0 & 1 & 0 & 0 & 0 & 0 & 0 & 0 & 0 & 0 & 0 & 0 \\ 0 & 0 & 0 & 0 & 0 & 0 & 0 & 0 & 0 & 0 & 0 & 0 & 0 & 1 & 0 & 0 & 0 & 0 & 0 & 0 & 0 & 0 & 0 \\ 0 & 0 & 0 & 0 & 0 & 0 & 0 & 0 & 0 & 0 & 0 & 0 & 0 & 0 & 1 & 0 & 0 & 0 & 0 & 0 & 0 & 0 & 0 \\ 1 & -1 & 0 & 0 & 0 & -r_1 & 0 & 0 & -r_1 - \frac{1}{g_{s1}} & 0 & 0 & 0 & 0 & 0 & \frac{-N_1}{N_1+N_2} & 0 & 0 & 0 & 0 & 0 & 0 & 0 & 0 \\ 0 & -1 & 0 & 0 & 1 & 0 & -r_2 & 0 & 0 & -r_2 - \frac{1}{g_{s2}} & 0 & 0 & 0 & 0 & \frac{N_2}{N_1+N_2} & 0 & 0 & 0 & 0 & 0 & 0 & 0 & 0 \\ 0 & 0 & 1 & -1 & 0 & 0 & 0 & -r_3 & 0 & 0 & -r_3 - \frac{1}{g_{s3}} & 0 & 0 & 0 & \frac{-N_3}{N_1+N_2} & 0 & 0 & 0 & 0 & 0 & 0 & 0 & 0 \\ 0 & 0 & 0 & 0 & 0 & 0 & 0 & 0 & \frac{1}{g_{s1}} & 0 & 0 & -L_1 & L_{PS} & -L_{PT} & 0 & 0 & 0 & 0 & 0 & 0 & 0 & 0 & 0 \\ 0 & 0 & 0 & 0 & 0 & 0 & 0 & 0 & 0 & \frac{1}{g_{s2}} & 0 & L_{PS} & -L_2 & L_{ST} & 0 & 0 & 0 & 0 & 0 & 0 & 0 & 0 & 0 \\ 0 & 0 & 0 & 0 & 0 & 0 & 0 & 0 & 0 & 0 & \frac{1}{g_{s3}} & -L_{PT} & L_{ST} & -L_3 & 0 & 0 & 0 & 0 & 0 & 0 & 0 & 0 & 0 \\ 0 & 0 & 0 & 0 & 0 & 0 & 0 & -1 & 0 & 0 & -1 & 0 & 0 & 0 & \frac{g_c N_3}{N_1+N_2} & 1 & 0 & 1 & 0 & 0 & 0 & 0 & 0 \\ 0 & 0 & 0 & 0 & 0 & N_1 & -N_2 & 0 & N_1 & -N_2 & 0 & 0 & 0 & 0 & 0 & N_3 & 0 & 0 & 0 & 0 & 0 & 0 & 0 \\ 0 & 0 & 0 & 0 & 0 & 0 & 0 & 0 & 0 & 0 & 0 & 0 & 0 & 0 & 0 & 0 & 0 & 1 & 0 & 0 & 0 & 0 & -i_0 \end{bmatrix}$$

$$Y_{A22} = \begin{bmatrix}
\sum_{i\neq 1}^{n=14} g_{1,i} & -g_{1,2} & -g_{1,3} & -g_{1,4} & -g_{1,5} & -g_{1,6} & -g_{1,7} & -g_{1,8} & -g_{1,9} & -g_{1,10} & -g_{1,11} & -g_{1,12} & -g_{1,13} & -g_{1,14} & -1 & 0 & 0 & 0 & 0 & 0 & 0 & 0 \\
-g_{2,1} & \sum_{i\neq 2}^{n=14} g_{2,i} & -g_{2,3} & -g_{2,4} & -g_{2,5} & -g_{2,6} & -g_{2,7} & -g_{2,8} & -g_{2,9} & -g_{2,10} & -g_{2,11} & -g_{2,12} & -g_{2,13} & -g_{2,14} & 0 & -1 & 0 & 0 & 0 & 0 & 0 & 0 \\
-g_{3,1} & -g_{3,2} & \sum_{i\neq 3}^{n=14} g_{3,i} & -g_{3,4} & -g_{3,5} & -g_{3,6} & -g_{3,7} & -g_{3,8} & -g_{3,9} & -g_{3,10} & -g_{3,11} & -g_{3,12} & -g_{3,13} & -g_{3,14} & 0 & 0 & -1 & 0 & 0 & 0 & 0 & 0 \\
-g_{4,1} & -g_{4,2} & -g_{4,3} & \sum_{i\neq 4}^{n=14} g_{4,i} & -g_{4,5} & -g_{4,6} & -g_{4,7} & -g_{4,8} & -g_{4,9} & -g_{4,10} & -g_{4,11} & -g_{4,12} & -g_{4,13} & -g_{4,14} & 0 & 0 & 0 & -1 & 0 & 0 & 0 & 0 \\
-g_{5,1} & -g_{5,2} & -g_{5,3} & -g_{5,4} & \sum_{i\neq 5}^{n=14} g_{5,i} & -g_{5,6} & -g_{5,7} & -g_{5,8} & -g_{5,9} & -g_{5,10} & -g_{5,11} & -g_{5,12} & -g_{5,13} & -g_{5,14} & 0 & 0 & 0 & -0.5 & -0.5 & 0 & 0 & 0 \\
-g_{6,1} & -g_{6,2} & -g_{6,3} & -g_{6,4} & -g_{6,5} & \sum_{i\neq 6}^{n=14} g_{6,i} & -g_{6,7} & -g_{6,8} & -g_{6,9} & -g_{6,10} & -g_{6,11} & -g_{6,12} & -g_{6,13} & -g_{6,14} & 0 & 0 & 0 & 0 & -1 & 0 & 0 & 0 \\
-g_{7,1} & -g_{7,2} & -g_{7,3} & -g_{7,4} & -g_{7,5} & -g_{7,6} & \sum_{i\neq 7}^{n=14} g_{7,i} & -g_{7,8} & -g_{7,9} & -g_{7,10} & -g_{7,11} & -g_{7,12} & -g_{7,13} & -g_{7,14} & 0 & 0 & 0 & 0 & -0.5 & -0.5 & 0 & 0 \\
-g_{8,1} & -g_{8,2} & -g_{8,3} & -g_{8,4} & -g_{8,5} & -g_{8,6} & -g_{8,7} & \sum_{i\neq 8}^{n=14} g_{8,i} & -g_{8,9} & -g_{8,10} & -g_{8,11} & -g_{8,12} & -g_{8,13} & -g_{8,14} & 0 & 0 & 0 & 0 & 0 & -1 & 0 & 0 \\
-g_{9,1} & -g_{9,2} & -g_{9,3} & -g_{9,4} & -g_{9,5} & -g_{9,6} & -g_{9,7} & -g_{9,8} & \sum_{i\neq 9}^{n=14} g_{9,i} & -g_{9,10} & -g_{9,11} & -g_{9,12} & -g_{9,13} & -g_{9,14} & 0 & 0 & 0 & 0 & 0 & 0 & -1 & 0 \\
-g_{10,1} & -g_{10,2} & -g_{10,3} & -g_{10,4} & -g_{10,5} & -g_{10,6} & -g_{10,7} & -g_{10,8} & -g_{10,9} & \sum_{i\neq 10}^{n=14} g_{10,i} & -g_{10,11} & -g_{10,12} & -g_{10,13} & -g_{10,14} & 0 & 0 & 0 & 0 & 0 & 0 & 0 & -1 \\
-g_{11,1} & -g_{11,2} & -g_{11,3} & -g_{11,4} & -g_{11,5} & -g_{11,6} & -g_{11,7} & -g_{11,8} & -g_{11,9} & -g_{11,10} & \sum_{i\neq 11}^{n=14} g_{11,i} & -g_{11,12} & -g_{11,13} & -g_{11,14} & 0 & 0 & 0 & 0 & 0 & 0 & 0 & 0 \\
-g_{12,1} & -g_{12,2} & -g_{12,3} & -g_{12,4} & -g_{12,5} & -g_{12,6} & -g_{12,7} & -g_{12,8} & -g_{12,9} & -g_{12,10} & -g_{12,11} & \sum_{i\neq 11}^{n=14} g_{11,i} & -g_{12,13} & -g_{12,14} & 0 & 0 & 0 & 0 & 0 & 0 & 0 & 0 \\
-g_{13,1} & -g_{13,2} & -g_{13,3} & -g_{13,4} & -g_{13,5} & -g_{13,6} & -g_{13,7} & -g_{13,8} & -g_{13,9} & -g_{13,10} & -g_{13,11} & -g_{13,12} & \sum_{i\neq 11}^{n=14} g_{11,i} & -g_{13,14} & 0 & 0 & 0 & 0 & 0 & 0 & 0 & 0 \\
-g_{14,1} & -g_{14,2} & -g_{14,3} & -g_{14,4} & -g_{14,5} & -g_{14,6} & -g_{14,7} & -g_{14,8} & -g_{14,9} & -g_{14,10} & -g_{14,11} & -g_{14,12} & -g_{14,13} & \sum_{i\neq 11}^{n=14} g_{11,i} & 0 & 0 & 0 & 0 & 0 & 0 & 0 & 0
\end{bmatrix}$$

$$Y_{A12} = 0$$

$$Y_{A12} = 0$$

$$D_{eqx2} = \begin{bmatrix} D_{A11}(13\times 23) & D_{A12}(13\times 22) \\ D_{A21}(14\times 23) & D_{A22}(14\times 22) \end{bmatrix}$$

$$D_{A11} = \begin{bmatrix}
0 & 0 & 0 & 0 & 0 & -1 & 0 & 0 & 0 & 0 & 0 & 0 & 0 & 0 & 0 & 0 & 0 & 0 & 0 & 0 & 0 & 0 \\
0 & 0 & 0 & 0 & 0 & 0 & -1 & 0 & 0 & 0 & 0 & 0 & 0 & 0 & 0 & 0 & 0 & 0 & 0 & 0 & 0 & 0 \\
0 & 0 & 0 & 0 & 0 & 0 & 0 & -1 & 0 & 0 & 0 & 0 & 0 & 0 & 0 & 0 & 0 & 0 & 0 & 0 & 0 & 0 \\
0 & 0 & 0 & 0 & 0 & 0 & 0 & 0 & 0 & 0 & 0 & 0 & 0 & 0 & 0 & 0 & -1 & 0 & 0 & 0 & 0 & 0 & 0 \\
0 & 0 & 0 & 0 & 0 & 0 & 0 & 0 & 0 & 0 & 0 & 0 & 0 & 0 & 0 & 0 & 0 & 0 & 0 & 0 & 0 & 0 & 0 \\
0 & 0 & 0 & 0 & 0 & 0 & 0 & 0 & 0 & 0 & 0 & 0 & 0 & 0 & 0 & 0 & 0 & 0 & 0 & 0 & 0 & 0 & 0 \\
0 & 0 & 0 & 0 & 0 & 0 & 0 & 0 & 0 & 0 & 0 & 0 & 0 & 0 & 0 & 0 & 0 & 0 & 0 & 0 & 0 & 0 & 0 \\
0 & 0 & 0 & 0 & 0 & 0 & 0 & 0 & 0 & 0 & 0 & 0 & 0 & 0 & 0 & 0 & 0 & 0 & 0 & 0 & 0 & 0 & 0 \\
0 & 0 & 0 & 0 & 0 & 0 & 0 & 0 & 0 & 0 & 0 & 0 & 0 & 0 & 0 & 0 & 0 & 0 & 0 & 0 & 0 & 0 & 0 \\
0 & 0 & 0 & 0 & 0 & 0 & 0 & 0 & 0 & 0 & 0 & 0 & 0 & 0 & 0 & 0 & 0 & 0 & 0 & 0 & 0 & 0 & 0 \\
0 & 0 & 0 & 0 & 0 & 0 & 0 & 0 & 0 & 0 & 0 & 0 & 0 & 0 & 0 & 0 & 0 & 0 & 0 & 0 & 0 & 0 & 0 \\
0 & 0 & 0 & 0 & 0 & 0 & 0 & 0 & 0 & 0 & 0 & 0 & 0 & 0 & 0 & 0 & 0 & 0 & 0 & 0 & 0 & 0 & 0 \\
0 & 0 & 0 & 0 & 0 & 0 & 0 & 0 & 0 & 0 & 0 & 0 & 0 & 0 & 0 & 0 & 0 & 0 & 0 & 0 & 0 & 0 & 0 \\
0 & 0 & 0 & 0 & 0 & 0 & 0 & 0 & 0 & 0 & 0 & 0 & 0 & 0 & 0 & 0 & 0 & 0 & 0 & 0 & 0 & 0 & 0 \\
0 & 0 & 0 & 0 & 0 & 0 & 0 & 0 & 0 & 0 & 0 & 0 & 0 & 0 & 0 & 0 & 0 & 0 & 0 & 0 & 0 & 0 & 0
\end{bmatrix}$$

$$D_{A12} = 0$$

$$D_{A12} = 0$$

$$D_{A22}=\begin{bmatrix}
C_1 & 0 & 0 & 0 & 0 & 0 & 0 & 0 & 0 & 0 & 0 & 0 & 0 & 0 & 0 & 0 & 0 & 0 & 0 \\
0 & C_2 & 0 & 0 & 0 & 0 & 0 & 0 & 0 & 0 & 0 & 0 & 0 & 0 & 0 & 0 & 0 & 0 & 0 \\
0 & 0 & C_3 & 0 & 0 & 0 & 0 & 0 & 0 & 0 & 0 & 0 & 0 & 0 & 0 & 0 & 0 & 0 & 0 \\
0 & 0 & 0 & C_4 & 0 & 0 & 0 & 0 & 0 & 0 & 0 & 0 & 0 & 0 & 0 & 0 & 0 & 0 & 0 \\
0 & 0 & 0 & 0 & C_5 & 0 & 0 & 0 & 0 & 0 & 0 & 0 & 0 & 0 & 0 & 0 & 0 & 0 & 0 \\
0 & 0 & 0 & 0 & 0 & C_6 & 0 & 0 & 0 & 0 & 0 & 0 & 0 & 0 & 0 & 0 & 0 & 0 & 0 \\
0 & 0 & 0 & 0 & 0 & 0 & C_7 & 0 & 0 & 0 & 0 & 0 & 0 & 0 & 0 & 0 & 0 & 0 & 0 \\
0 & 0 & 0 & 0 & 0 & 0 & 0 & C_8 & 0 & 0 & 0 & 0 & 0 & 0 & 0 & 0 & 0 & 0 & 0 \\
0 & 0 & 0 & 0 & 0 & 0 & 0 & 0 & C_9 & 0 & 0 & 0 & 0 & 0 & 0 & 0 & 0 & 0 & 0 \\
0 & 0 & 0 & 0 & 0 & 0 & 0 & 0 & 0 & C_{10} & 0 & 0 & 0 & 0 & 0 & 0 & 0 & 0 & 0 \\
0 & 0 & 0 & 0 & 0 & 0 & 0 & 0 & 0 & 0 & C_{11} & 0 & 0 & 0 & 0 & 0 & 0 & 0 & 0 \\
0 & 0 & 0 & 0 & 0 & 0 & 0 & 0 & 0 & 0 & 0 & C_{12} & 0 & 0 & 0 & 0 & 0 & 0 & 0 \\
0 & 0 & 0 & 0 & 0 & 0 & 0 & 0 & 0 & 0 & 0 & 0 & C_{13} & 0 & 0 & 0 & 0 & 0 & 0 \\
0 & 0 & 0 & 0 & 0 & 0 & 0 & 0 & 0 & 0 & 0 & 0 & 0 & C_{14} & 0 & 0 & 0 & 0 & 0
\end{bmatrix}$$

$$C_{eqc2}=\begin{bmatrix}0 & 0 & 0 & 0 & 0 & \cdots & \cdots & 0 & 0 & -g_{11}T_{ambient} & -g_{12}T_{ambient}\end{bmatrix}^T$$

$$Y_{eqx3}=\begin{bmatrix}Y_{B1}(13\times 23) & Y_{B2}(13\times 20)\end{bmatrix}$$

$$Y_{B1}=\begin{bmatrix}
0 & 0 & 0 & 0 & 0 & 0 & 0 & 0 & 0 & 0 & 0 & 0 & 0 & 0 & 0 & 0 & 0 & 0 & 1 & 0 & 0 & 0 & 0 \\
0 & 0 & 0 & 0 & 0 & 0 & 0 & 0 & 0 & 0 & 0 & 0 & 0 & 0 & 0 & 0 & 0 & 0 & 0 & 1 & 0 & 0 & 0 \\
0 & 0 & 0 & 0 & 0 & 0 & 0 & 0 & 0 & 0 & 0 & 0 & 0 & 0 & 0 & 0 & 0 & 0 & 0 & 0 & 1 & 0 & 0 \\
0 & 0 & 0 & 0 & 0 & 0 & 0 & 0 & 0 & 0 & 0 & 0 & 0 & 0 & 0 & 0 & 0 & 0 & 0 & 0 & 0 & 1 & 0 \\
0 & 0 & 0 & 0 & 0 & 0 & 0 & 0 & 0 & 0 & 0 & 0 & 0 & 0 & 0 & 0 & 0 & 0 & 0 & 0 & 0 & 0 & 1 \\
0 & 0 & 0 & 0 & 0 & 0 & 0 & 0 & 0 & 0 & 0 & 0 & 0 & 0 & 0 & 0 & 0 & 0 & 0 & 0 & 0 & 0 & 0 \\
0 & 0 & 0 & 0 & 0 & 0 & 0 & 0 & 0 & 0 & 0 & 0 & 0 & 0 & 0 & 0 & 0 & 0 & 0 & 0 & 0 & 0 & 0 \\
0 & 0 & 0 & 0 & 0 & 0 & 0 & 0 & 0 & 0 & 0 & 0 & 0 & 0 & 0 & 0 & 0 & 0 & 0 & 0 & 0 & 0 & 0 \\
0 & 0 & 0 & 0 & 0 & 0 & 0 & 0 & 0 & 0 & 0 & 0 & 0 & 0 & 0 & 0 & 0 & 0 & 0 & 0 & 0 & 0 & 0 \\
0 & 0 & 0 & 0 & 0 & 0 & 0 & 0 & 0 & 0 & 0 & 0 & 0 & 0 & 0 & 0 & 0 & 0 & 0 & 0 & 0 & 0 & 0 \\
0 & 0 & 0 & 0 & 0 & 0 & 0 & 0 & 0 & 0 & 0 & 0 & 0 & 0 & 0 & 0 & 0 & 0 & 0 & 0 & 0 & 0 & 0 \\
0 & 0 & 0 & 0 & 0 & 0 & 0 & 0 & 0 & 0 & 0 & 0 & 0 & 0 & 0 & 0 & 0 & 0 & 0 & 0 & 0 & 0 & 0 \\
0 & 0 & 0 & 0 & 0 & 0 & 0 & 0 & 0 & 0 & 0 & 0 & 0 & 0 & 0 & 0 & 0 & 0 & 0 & 0 & 0 & 0 & 0
\end{bmatrix}$$

$$Y_{B2}=\begin{bmatrix}0&0&0&0&0&0&0&0&0&0&0&0&0&0&0&0&0&0&0&0\\0&0&0&0&0&0&0&0&0&0&0&0&0&0&0&0&0&0&0&0\\0&0&0&0&0&0&0&0&0&0&0&0&0&0&0&0&0&0&0&0\\0&0&0&0&0&0&0&0&0&0&0&0&0&0&0&0&0&0&0&0\\0&0&0&0&0&0&0&0&0&0&0&0&0&0&0&0&0&0&0&0\\0&0&0&0&0&0&0&0&0&0&0&0&1&0&0&0&0&0&0&0\\0&0&0&0&0&0&0&0&0&0&0&0&0&1&0&0&0&0&0&0\\0&0&0&0&0&0&0&0&0&0&0&0&0&0&1&0&0&0&0&0\\0&0&0&0&0&0&0&0&0&0&0&0&0&0&0&1&0&0&0&0\\0&0&0&0&0&0&0&0&0&0&0&0&0&0&0&0&1&0&0&0\\0&0&0&0&0&0&0&0&0&0&0&0&0&0&0&0&0&1&0&0\\0&0&0&0&0&0&0&0&0&0&0&0&0&0&0&0&0&0&1&0\\0&0&0&0&0&0&0&0&0&0&0&0&0&0&0&0&0&0&0&1\end{bmatrix}$$

$$F_{eqxx3}\left\langle 0,(16,16)\right\rangle=-\frac{1}{\lambda_0^2}$$

$$F_{eqxx3}\left\langle 1,(18,18)\right\rangle=-1$$

$$F_{eqxx3}\left\langle 2,(19,19)\right\rangle=-1$$

$$F_{eqxx3}\left\langle 3,(18,20)\right\rangle=-1$$

$$F_{eqxx3}\left\langle 4,(16,21)\right\rangle=-\frac{1}{\lambda_0}$$

$$F_{eqxx3}\left\langle 5,(16,16)\right\rangle=-\frac{1}{2}\alpha_{e+h}$$

$$F_{eqxx3}\left\langle 6,(16,16)\right\rangle=-\frac{1}{2}\alpha_{e+h}$$

$$F_{eqxx3}\left\langle 7,(5,5)\right\rangle=-\frac{1}{2}r_1$$

$$F_{eqxx3}\left\langle 8,(5,5)\right\rangle=-\frac{1}{2}r_1$$

$$F_{eqxx3}\left\langle 9,(5,5)\right\rangle=-\frac{1}{4}r_1$$

$$F_{eqxx3}\left\langle 9,(6,6)\right\rangle=-\frac{1}{4}r_2$$

$$F_{eqxx3}\left\langle 10,(6,6)\right\rangle=-\frac{1}{2}r_2$$

$$F_{eqxx3}\langle 11,(6,6)\rangle = -\frac{1}{2}r_2$$

$$F_{eqxx3}\langle 12,(7,7)\rangle = -\frac{1}{2}r_3$$

$$F_{eqxx3}\langle 13,(7,7)\rangle = -\frac{1}{2}r_3$$

$$F_{eqxx3}\langle 14,(7,7)\rangle = -\frac{1}{2}r_3$$

$$C_{eqc3} = 0$$

There are 45 state variables and 45 equation in the model. The definition of the external state, internal state, and through variables of the auto-transformer are listed in Table 4-4 to Table 4-6, respectively.

Table 4 - 4. External states of the auto-transformer.

Index	Variable	Description
0	$v_1(t)$	terminal voltage of transformer primary side (V)
1	$v_2(t)$	terminal voltage of transformer secondary side (V)
2	$v_3(t)$	terminal voltage of transformer tertiary side (V)
3	$v_4(t)$	terminal voltage of transformer tertiary neutral (V)
4	$v_5(t)$	terminal voltage of transformer primary neutral (V)

Table 4 - 5. Internal states of the auto-transformer.

Index	Variable	Description
5	$i_{L1}(t)$	current through the primary side inductance (A)
6	$i_{L2}(t)$	current through the secondary side inductance (A)
7	$i_{L3}(t)$	current through the tertiary side inductance (A)
8	$i_{gs1}(t)$	current through the primary side stabilizer (A)

Table 4 – 5 continued

Index	Variable	Description
9	$i_{gs2}(t)$	current through the secondary side stabilizer (A)
10	$i_{gs3}(t)$	current through the tertiary side stabilizer (A)
11	$z_1(t)$	introduced state
12	$z_2(t)$	introduced state
13	$z_3(t)$	introduced state
14	$e_c(t)$	voltage generated by the flux (A)
15	$i_c(t)$	current through tertiary side windings (A)
16	$\lambda(t)$	flux linkage (Web)
17	$i_m(t)$	magnetizing current (A)
18	$y_1(t)$	introduced state (p.u.)
19	$y_2(t)$	introduced state (p.u.)
20	$y_3(t)$	introduced state (p.u.)
21	$y_4(t)$	introduced state (p.u.)
22	$y_5(t)$	introduced state (p.u.)
23	$ET_1(t)$	temperature at core up point (Celsius)
24	$ET_2(t)$	temperature at core down point (Celsius)
25	$ET_3(t)$	temperature at primary coil up point (Celsius)
26	$ET_4(t)$	temperature at primary coil mid point (Celsius)
27	$ET_5(t)$	temperature at primary/secondary coil connection

Table 4 – 5 continued

Index	Variable	Description
28	$ET_6(t)$	temperature at secondary coil mid point (Celsius)
29	$ET_7(t)$	temperature at secondary coil down point (Celsius)
30	$ET_8(t)$	temperature at tertiary coil up point (Celsius)
31	$ET_9(t)$	temperature at tertiary coil midpoint (Celsius)
32	$ET_{10}(t)$	temperature at tertiary coil down point (Celsius)
33	$ET_{11}(t)$	temperature at internal oil up point (Celsius)
34	$ET_{12}(t)$	temperature at internal oil down point (Celsius)
35	$ET_{13}(t)$	temperature at transformer tank front point (Celsius)
36	$ET_{14}(t)$	temperature at transformer tank rear point (Celsius)
37	$Q_{core,1}(t)$	heat generated at core up point (W)
38	$Q_{core,2}(t)$	heat generated at core down point (W)
39	$Q_{coil\_pri,1}(t)$	heat generated at primary coil up point (W)
40	$Q_{coil\_pri,2}(t)$	heat generated at primary coil down point (W)
41	$Q_{coil\_sec,1}(t)$	heat generated at secondary coil up point (W)
42	$Q_{coil\_sec,2}(t)$	heat generated at secondary coil down point (W)
43	$Q_{coil\_ter,1}(t)$	heat generated at tertiary coil up point (W)
44	$Q_{coil\_ter,2}(t)$	heat generated at tertiary coil down point (W)

Table 4 - 6. Through variables of the auto-transformer.

Index	Variable	Description
0	$i_1(t)$	current through transformer primary side (A)
1	$i_2(t)$	current through transformer secondary side (A)
2	$i_3(t)$	current through transformer tertiary side (A)
3	$i_4(t)$	current through transformer tertiary neutral (A)
4	$i_5(t)$	current through transformer primary neutral (A)

4.3 Transformer AQCF Device Model

In this section, the transformer AQCF device model is presented. The device AQCF model is a mathematical model derived from the physical electro-thermal circuit of the transformer directly, using the quadratic integration method, seen in Figure 4-3. Section. Details of the quadratic integration method is presented in Appendix A.

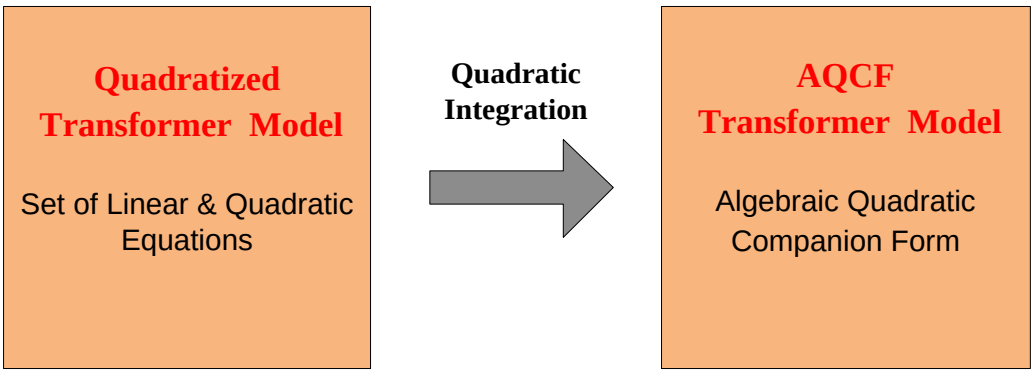

Figure 4 - 3. Derive the AQCF format with quadratic integration method

Because the AQCF format automatically derived in an object-oriented manner, there are a standard procedure and standard syntax for the transformer AQCF model,

no matter what kind of the transformer is. Therefore, with the quadratic device models in section 4.2, the AQCF models of the single-phase saturable transformer and the single-phase auto-transformer are automatically generated in the following format:

$$\begin{Bmatrix} i(t) \\ 0 \\ 0 \\ i(t_m) \\ 0 \\ 0 \end{Bmatrix} = Y_{eqx}\mathbf{x} + \begin{Bmatrix} \vdots \\ \mathbf{x}^T \left\langle F_{eqx}^i \right\rangle \mathbf{x} \\ \vdots \end{Bmatrix} - B_{eq}$$

$$B_{eq} = -N_{eqx}\mathbf{x}(t-h) - M_{eq}i(t-h) - K_{eq}$$

$$\mathbf{h}(\mathbf{x}) = Y_{feqx}\mathbf{x} + \begin{Bmatrix} \vdots \\ \mathbf{x}^T \left\langle F_{feqxxx}^i \right\rangle \mathbf{x} \\ \vdots \end{Bmatrix} + C_{feqc}$$

Connectivity: *TerminalNodeName*

$$subject\ to:\ \mathbf{h}_{\min} \le \mathbf{h}(\mathbf{x}) \le \mathbf{h}_{\max},\ \mathbf{x}_{\min} \le \mathbf{x} \le \mathbf{x}_{\max}$$

where

$i(t)$ *and* $i(t_m)$ are the through variables of the device model;

$\mathbf{x}$ is the external and internal state variables of the device model;

Y_{eqx} is the matrix defining the linear part of state variables, F_{eqx} is the matrix defining the quadratic part of state variables;

B_{eq} is the history dependent vector of the device model;

N_{eqx} is the matrix defining the last integration step state variables part;

M_{eq} is the matrix defining the last integration step through variables part;

K_{eq} is the constant vector of the device mode;

TerminalNodeName is the terminal names defining the connectivity of the device

model;

Y_{feqx} is the constraint matrix defining the linear part of state variables;

F_{feqx} is the constraint matrix defining the quadratic part of state variables;

C_{feqc} is the constraint history dependent vector of the device model

$\mathbf{h}_{\min} \le \mathbf{h}(\mathbf{x},\mathbf{u}) \le \mathbf{h}_{\max}$ is the functional constraint;

$\mathbf{x}_{\min}, \mathbf{x}_{\max}$ are the lower and upper bounds of the state variables.

The transformer AQCF model is automatically generated with the QDM model with the time step *h* as:

$$Y_{eqx} = \begin{bmatrix} \frac{4}{h} D_{eqxd1} + Y_{eqx1} & -\frac{8}{h} D_{eqxd1} \\ D_{eqxd2} + \frac{h}{6} Y_{eqx2} & \frac{2h}{3} Y_{eqx2} \\ Y_{eqx3} & 0 \\ \frac{1}{2h} D_{eqxd1} & \frac{2}{h} D_{eqxd1} + Y_{eqx1} \\ -\frac{h}{24} Y_{eqx2} & D_{eqxd2} + \frac{h}{3} Y_{eqx2} \\ 0 & Y_{eqx3} \end{bmatrix}$$

$$F_{eqx} = \begin{bmatrix} 0 & 0 \\ 0 & 0 \\ F_{eqxx3} & 0 \\ 0 & 0 \\ 0 & 0 \\ 0 & F_{eqxx3} \end{bmatrix}$$

$$N_{eqx}=\begin{bmatrix} -Y_{eqx1}+\frac{4}{h}D_{eqxd1} \\ \frac{h}{6}Y_{eqx2}-D_{eqxd2} \\ 0 \\ \frac{1}{2}Y_{eqx1}-\frac{5}{2h}D_{eqxd1} \\ \frac{5h}{24}Y_{eqx2}-D_{eqxd2} \\ 0 \end{bmatrix}$$

$$M_{eq}=\begin{bmatrix} I_{size(i(t))} \\ 0 \\ 0 \\ \frac{1}{2}I_{size(i(t))} \\ 0 \\ 0 \end{bmatrix}$$

$$K_{eq}=\begin{bmatrix} 0 \\ hC_{eqc2} \\ C_{eqc3} \\ \frac{3}{2}C_{eqc1} \\ \frac{1}{2}hC_{eqc2} \\ C_{eqc3} \end{bmatrix}$$

4.4 Transformer AQCF Measurement Model

The AQCF measurement model is obtained by expressing measurements using the

states or equations in the transformer model. The transformer AQCF measurements are classified into four types: (1) actual measurements; (2) virtual measurements; (3) derived measurements and (4) pseudo measurements.

Actual measurements are the real measurements obtained by typical measuring equipment. For example, the terminal voltages and currents of transformer are the actual measurements. The actual measurements contain noises due to the data acquisition system.

Virtual measurements present the zeros on the left sides of the internal equations. These measurements are physical laws that transformer must obey. These physical laws are expressed with specific equations, which must be exactly satisfied and therefore the virtual measurements are exact measurements. Since those internal equations are derived from the physical laws, the virtual measurements are noiseless.

Derived measurements are the measurements derived from the actual available measurements. For example, three terminals are connected together and two terminal currents of them are measured as actual measurements, so the third current can be derived based on the Kirchhoff's current law (KCL). The derived measurements have same noise (error) as the actual ones.

Pseudo measurements are the measurements normally not measured, like the voltage at the neutral terminal. It represents a quantity for which one can expect to be at a certain level but do not have an actual measurement. Since the value of the pseudo measurement is not precise, it is considered that pseudo measurements contain larger

error (noise) than those actual, derived and virtual measurements.

The measurement definition and device model is sufficient to automatically derive the measurement model. The AQCF measurement model can be written as

$$\mathbf{z} = Y_{m,x}\mathbf{x} + \left\{ \begin{array}{c} \vdots \\ \mathbf{x}^T F^i_{m,x}\mathbf{x} \\ \vdots \end{array} \right\} + N_{m,x}\mathbf{x}(t-h) + M_m i(t-h) + C_m$$

Measurement noise error: dMeterScale, dMeterSigmaPU

Note: All the above variables are in per unit system.

where:

$\mathbf{z}$: measurement variables at both time t and time t_m, $\mathbf{z} = [\mathbf{z}(t), \mathbf{z}(t_m)]$

$\mathbf{x}$: external and internal state variables of the measurement model, $\mathbf{x} = [\mathbf{x}(t), \mathbf{x}(t_m)]$

$Y_{m,x}$: matrix defining the linear part for state variables,

$F_{m,x}$: matrices defining the quadratic part for state variables,

C_m : history dependent vector of the measurement model,

$N_{m,x}$: matrix defining the last integration step state variables part,

M_m : matrix defining the last integration step through variables part,

K_m : constant vector of the measurement model,

dMeterScale : the scale that meters use (in metric units),

dMeterSigmaPU : the standard deviation for the measurements (in per. unit),

Details of the creation of AQCF measurement model are described in [94].

4.5 Constructing a Three-Phase Transformer

In this section, the method of constructing a three-phase transformer is described.

No matter it is a regular saturable-core transformer or an auto-transformer, the AQCF model of a three-phase transformer can be constructed by connecting three single-phase models into one composite model. In this section, the regular saturable-core transformer is taken as an example.

To get the overall model, each phase are interconnected. The three-phase transformer AQCF model is shown below.

$$\begin{Bmatrix} i_{3\phi}(t) \\ 0 \\ 0 \\ i_{3\phi}(t_m) \\ 0 \\ 0 \end{Bmatrix} = Y_{eqx3\phi}\mathbf{x}_{3\phi} + \begin{Bmatrix} \vdots \\ \mathbf{x}_{3\phi}{}^{T}\left\langle F^{i}_{eqx3\phi}\right\rangle \mathbf{x}_{3\phi} \\ \vdots \end{Bmatrix} - B_{eq3\phi}$$

$$B_{eq3\phi} = -N_{eqx3\phi}\mathbf{x}_{3\phi}(t-h) - M_{eq3\phi}i_{3\phi}(t-h) - K_{eq3\phi}$$

$$\mathbf{h}_{3\phi}(\mathbf{x}) = Y_{feqx3\phi}\mathbf{x}_{3\phi} + \begin{Bmatrix} \vdots \\ \mathbf{x}_{3\phi}{}^{T}\left\langle F^{i}_{feqxxx3\phi}\right\rangle \mathbf{x}_{3\phi} \\ \vdots \end{Bmatrix} + C_{feqc3\phi}$$

Connectivity: $TerminalNodeName_{3\phi}$

$$subject\ to:\ \mathbf{h}_{\min 3\phi} \le \mathbf{h}_{3\phi}(\mathbf{x}) \le \mathbf{h}_{\max 3\phi},\ \mathbf{x}_{\min 3\phi} \le \mathbf{x}_{3\phi} \le \mathbf{x}_{\max 3\phi}$$

where $\mathbf{x}_{3\phi}$ are the states for three-phase transformer and the matrix $Y_{eqx3\phi}$, $F_{eqx3\phi}$, $N_{eqx3\phi}$, $M_{eq3\phi}$ and $K_{eq3\phi}$ are decided by the combinations of connecting the terminals in wye or delta configuration.

The total state vector of the three-phase transformer $\mathbf{x}_{3\phi}$ consists of $3n_{ph}^{\text{int}} + n^{ext}$ states. The number of external states is determined by the configuration that the phases of the transformer are connected. In general there are four configurations, namely the

wye-wye, wye-delta, delta-wye and delta-delta configurations. In subsequent paragraphs each one of these four cases are documented. The internal states are commonly defined for all these cases by directly appending to the state vector the internal states of each phase.

4.5.1 Wye-Wye Connected Transformer

The configuration of wye-wye connected transformer is illustrated in Figure 4-4. In this case, the number of external states is eight.

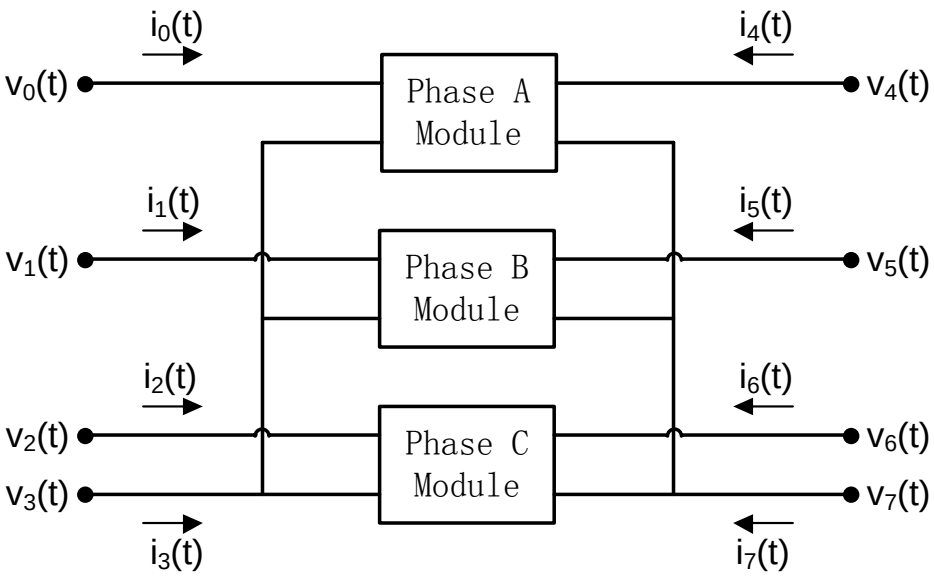

Figure 4 - 4. Three-phase wye-wye connected transformer

In order to integrate the three sets of the AQCF of the single-phase transformer, the state pointers of the AQCF of the single-phase transformer need to be re-assigned to those of the AQCF of the three-phase transformer. The indices relationship between the AQCFs of the single-phase transformer and the three-phase wye-wye connected transformer is shown in Figure 4-5. The total state number of this transformer configuration is $3n_{ph}^{\text{int}}+8$.

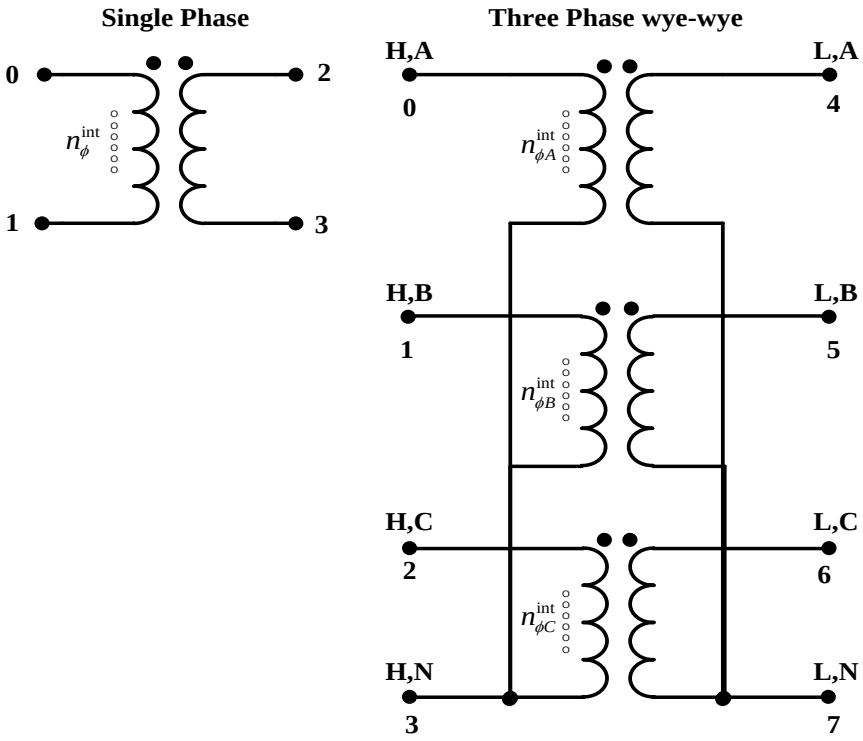

Figure 4 - 5. The indices relationship of the three-phase wye-wye connected transformer

The external states in this case are listed in Table 4-7:

Table 4 - 7. External States of wye-wye connected transformer

External States	
State Index	**State Name**
0	$v_{H,A}(t)$
1	$v_{H,B}(t)$
2	$v_{H,C}(t)$
3	$v_{H,N}(t)$
4	$v_{L,A}(t)$
5	$v_{L,B}(t)$
6	$v_{L,C}(t)$
7	$v_{L,N}(t)$

The correspondence between each external phase states (and equations) and the three phase transformer external states (and equations) for each phase is defined in Table 4-8.

Table 4 - 8. Correspondence between the external phase and bank states index

Phase A			
Phase State Index	**State Name**	**Bank State Index**	**Bank State Name**
0	$v_{0,A}(t)$	0	$v_{H,A}(t)$
1	$v_{1,A}(t)$	3	$v_{H,N}(t)$
2	$v_{2,A}(t)$	4	$v_{L,A}(t)$
3	$v_{3,A}(t)$	7	$v_{L,N}(t)$
Phase B			
0	$v_{0,B}(t)$	1	$v_{H,B}(t)$
1	$v_{1,B}(t)$	3	$v_{H,N}(t)$
2	$v_{2,B}(t)$	5	$v_{L,B}(t)$
3	$v_{3,B}(t)$	7	$v_{L,N}(t)$
Phase C			
0	$v_{0,C}(t)$	2	$v_{H,C}(t)$
1	$v_{1,C}(t)$	3	$v_{H,N}(t)$
2	$v_{2,C}(t)$	6	$v_{L,C}(t)$
3	$v_{3,C}(t)$	7	$v_{L,N}(t)$

Because each single-phase transformer is modeled in the standard AQCF syntax, it is

very easy to combine the three AQCF models into a (composite) three-phase transformer AQCF model. The terminals of three single-phase transformers are interconnected, by applying the Kirchhoff's Current Law (KCL) the terminal equations can be easily combined. The internal equations of each single-phase transformer will keep unchanged. The three-phase transformer AQCF model is shown below.

$$\begin{Bmatrix} i_{3\phi}(t) \\ 0 \\ 0 \\ i_{3\phi}(t_m) \\ 0 \\ 0 \end{Bmatrix} = Y_{eqx3\phi}\mathbf{x}_{3\phi} + \begin{Bmatrix} \vdots \\ \mathbf{x}_{3\phi}{}^{T}\left\langle F^{i}_{eqx3\phi}\right\rangle \mathbf{x}_{3\phi} \\ \vdots \end{Bmatrix} - B_{eq3\phi}$$

$$B_{eq3\phi} = -N_{eqx3\phi}\mathbf{x}_{3\phi}(t-h) - M_{eq3\phi}i_{3\phi}(t-h) - K_{eq3\phi}$$

$$\mathbf{h}_{3\phi}(\mathbf{x}) = Y_{feqx3\phi}\mathbf{x}_{3\phi} + \begin{Bmatrix} \vdots \\ \mathbf{x}_{3\phi}{}^{T}\left\langle F^{i}_{feqxxx3\phi}\right\rangle \mathbf{x}_{3\phi} \\ \vdots \end{Bmatrix} + C_{feqc3\phi}$$

Connectivity: $TerminalNodeName_{3\phi}$

$$subject\ to:\ \mathbf{h}_{\min 3\phi} \le \mathbf{h}_{3\phi}(\mathbf{x}) \le \mathbf{h}_{\max 3\phi},\ \mathbf{x}_{\min 3\phi} \le \mathbf{x}_{3\phi} \le \mathbf{x}_{\max 3\phi}$$

where $\mathbf{x}_{3\phi}$ are the states for three-phase transformer and the matrix $Y_{eqx3\phi}$, $F_{eqx3\phi}$, $N_{eqx3\phi}$, $M_{eq3\phi}$ and $K_{eq3\phi}$ are decided by the combinations of connecting the terminals in wye or delta configuration.

4.5.2 Wye-Delta Connected Transformer

The configuration of wye-delta connected transformer is illustrated in Figure 4-6. In this case, the number of external states is seven.

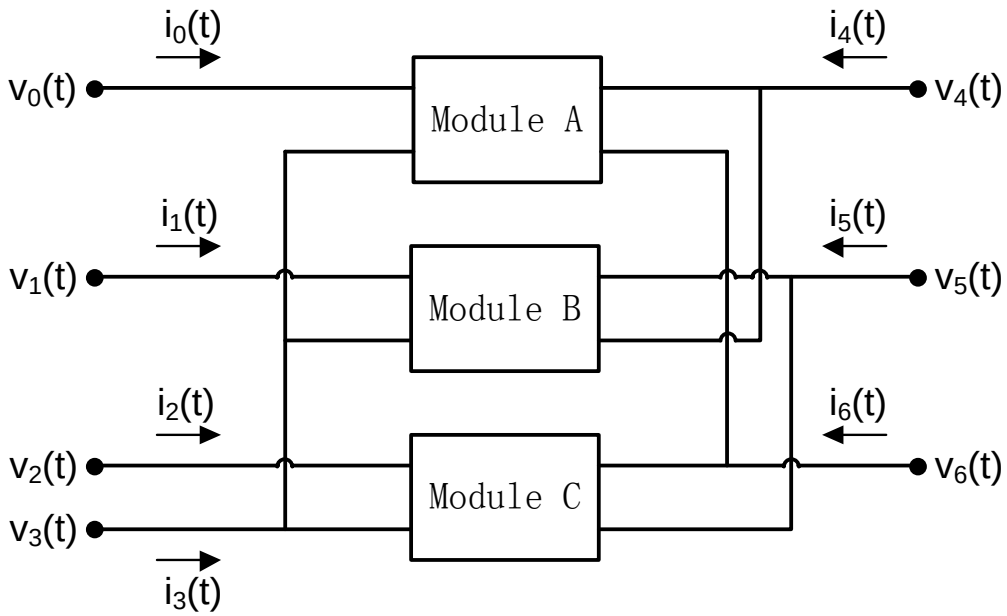

Figure 4 - 6. Three-phase wye-delta connected transformer

In order to integrate the three sets of the AQCF of the single-phase transformer, the state pointers of the AQCF of the single-phase transformer need to be re-assigned to those of the AQCF of the three-phase transformer. The indices relationship between the AQCFs of the single-phase transformer and the three-phase wye-delta connected transformer is shown in Figure 4-7. The total state number of this transformer configuration is $3n_{ph}^{\text{int}}+7$.

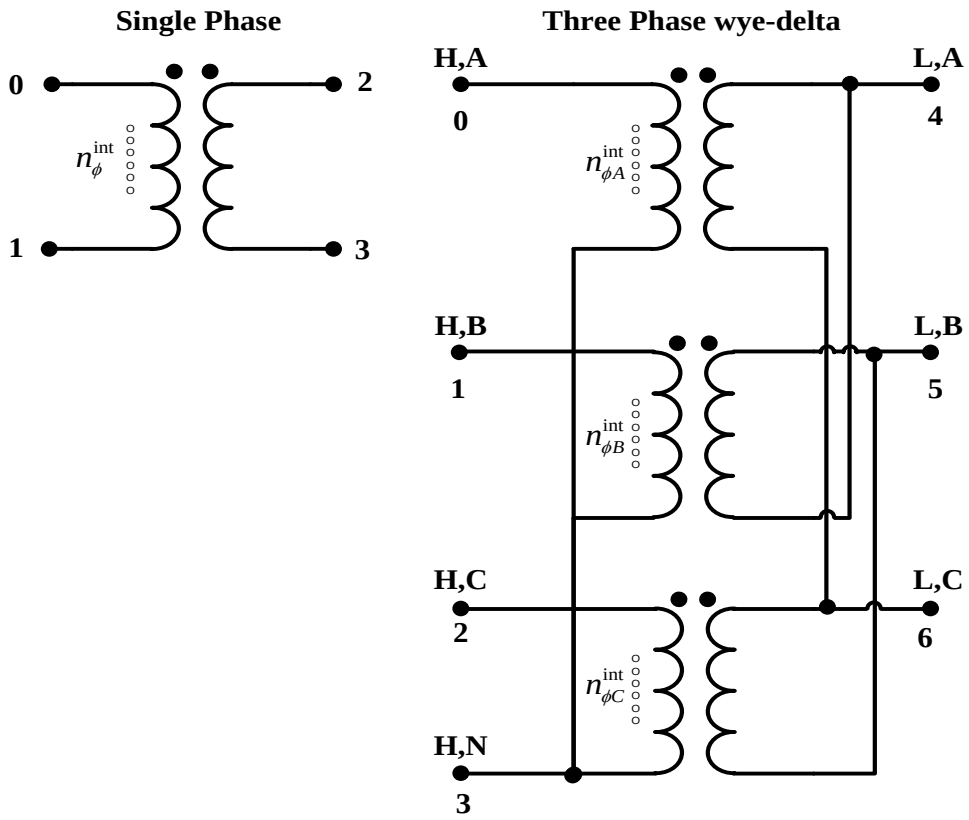

Figure 4 - 7. The indices relationship of the three-phase wye-delta connected transformer

The external states in this case are listed in Table 4-9:

Table 4 - 9. External States of wye-delta connected transformer

External States	
State Index	**State Name**
0	$v_{H,A}(t)$
1	$v_{H,B}(t)$
2	$v_{H,C}(t)$
3	$v_{H,N}(t)$
4	$v_{L,A}(t)$
5	$v_{L,B}(t)$
6	$v_{L,C}(t)$

The correspondence between the external phase states (and equations) and the three phase transformer external states (and equations) for each phase is defined as:

Table 4 - 10. Correspondence between the external phase and bank states index

Phase A			
Phase State Index	**State Name**	**Bank State Index**	**Bank State Name**
0	$v_{0,A}(t)$	0	$v_{H,A}(t)$
1	$v_{1,A}(t)$	3	$v_{H,N}(t)$
2	$v_{2,A}(t)$	4	$v_{L,A}(t)$
3	$v_{3,A}(t)$	6	$v_{L,C}(t)$
Phase B			
Phase State Index	**State Name**	**Bank State Index**	**Bank State Name**
0	$v_{0,B}(t)$	1	$v_{H,B}(t)$
1	$v_{1,B}(t)$	3	$v_{H,N}(t)$
2	$v_{2,B}(t)$	5	$v_{L,B}(t)$
3	$v_{3,B}(t)$	4	$v_{L,A}(t)$
Phase C			
Phase State Index	**State Name**	**Bank State Index**	**Bank State Name**
0	$v_{0,C}(t)$	2	$v_{H,C}(t)$
1	$v_{1,C}(t)$	3	$v_{H,N}(t)$
2	$v_{2,C}(t)$	6	$v_{L,C}(t)$
3	$v_{3,C}(t)$	5	$v_{L,B}(t)$

Because each single-phase transformer is modeled in the standard AQCF syntax, it is very easy to combine the three AQCF models into a (composite) three-phase transformer AQCF model. The terminals of three single-phase transformers are interconnected, by applying the Kirchhoff's Current Law (KCL) the terminal equations can be easily combined. The internal equations of each single-phase transformer will keep unchanged. The three-phase transformer AQCF model is shown below.

$$\begin{Bmatrix} i_{3\phi}(t) \\ 0 \\ 0 \\ i_{3\phi}(t_m) \\ 0 \\ 0 \end{Bmatrix} = Y_{eqx3\phi}\mathbf{x}_{3\phi} + \begin{Bmatrix} \vdots \\ \mathbf{x}_{3\phi}{}^{T}\left\langle F^{i}_{eqx3\phi}\right\rangle \mathbf{x}_{3\phi} \\ \vdots \end{Bmatrix} - B_{eq3\phi}$$

$$B_{eq3\phi} = -N_{eqx3\phi}\mathbf{x}_{3\phi}(t-h) - M_{eq3\phi}i_{3\phi}(t-h) - K_{eq3\phi}$$

$$\mathbf{h}_{3\phi}(\mathbf{x}) = Y_{feqx3\phi}\mathbf{x}_{3\phi} + \begin{Bmatrix} \vdots \\ \mathbf{x}_{3\phi}{}^{T}\left\langle F^{i}_{feqxxx3\phi}\right\rangle \mathbf{x}_{3\phi} \\ \vdots \end{Bmatrix} + C_{feqc3\phi}$$

Connectivity: $TerminalNodeName_{3\phi}$

$$subject\ to:\ \mathbf{h}_{\min 3\phi} \le \mathbf{h}_{3\phi}(\mathbf{x}) \le \mathbf{h}_{\max 3\phi},\ \mathbf{x}_{\min 3\phi} \le \mathbf{x}_{3\phi} \le \mathbf{x}_{\max 3\phi}$$

where $\mathbf{x}_{3\phi}$ are the states for three-phase transformer and the matrix $Y_{eqx3\phi}$, $F_{eqx3\phi}$, $N_{eqx3\phi}$, $M_{eq3\phi}$ and $K_{eq3\phi}$ are decided by the combinations of connecting the terminals in wye or delta configuration.

4.5.3 Delta-Wye Connected Transformer

The configuration of delta-wye connected transformer is illustrated in Figure 4-8.

In this case, the number of external states is seven.

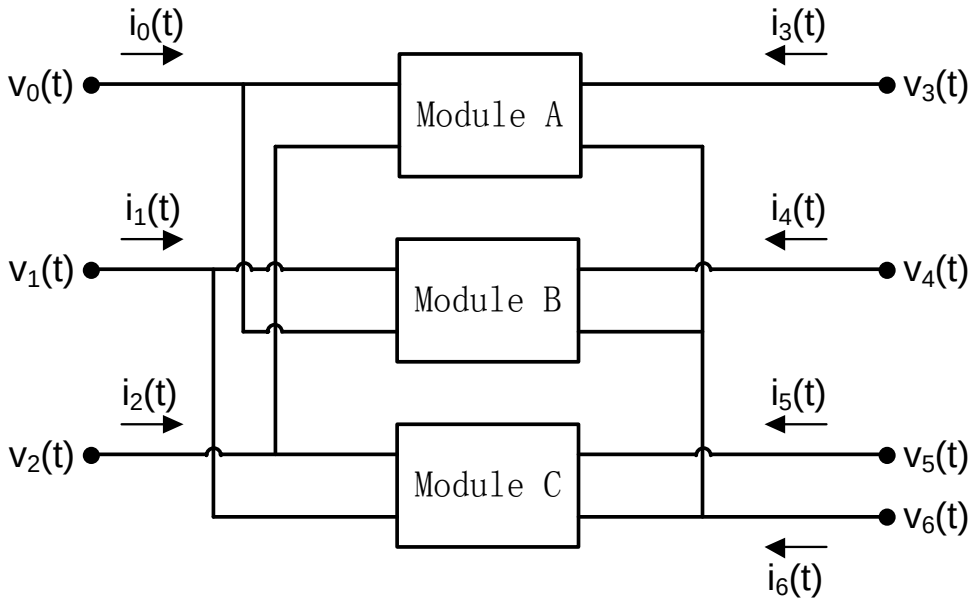

Figure 4 - 8. Three-phase delta-wye connected transformer

In order to integrate the three sets of the AQCF of the single-phase transformer, the state pointers of the AQCF of the single-phase transformer need to be re-assigned to those of the AQCF of the three-phase transformer. The indices relationship between the AQCFs of the single-phase transformer and the three-phase delta-wye connected transformer is shown in Figure 4-9. The total state number of this transformer configuration is $3n_{ph}^{\text{int}}+7$.

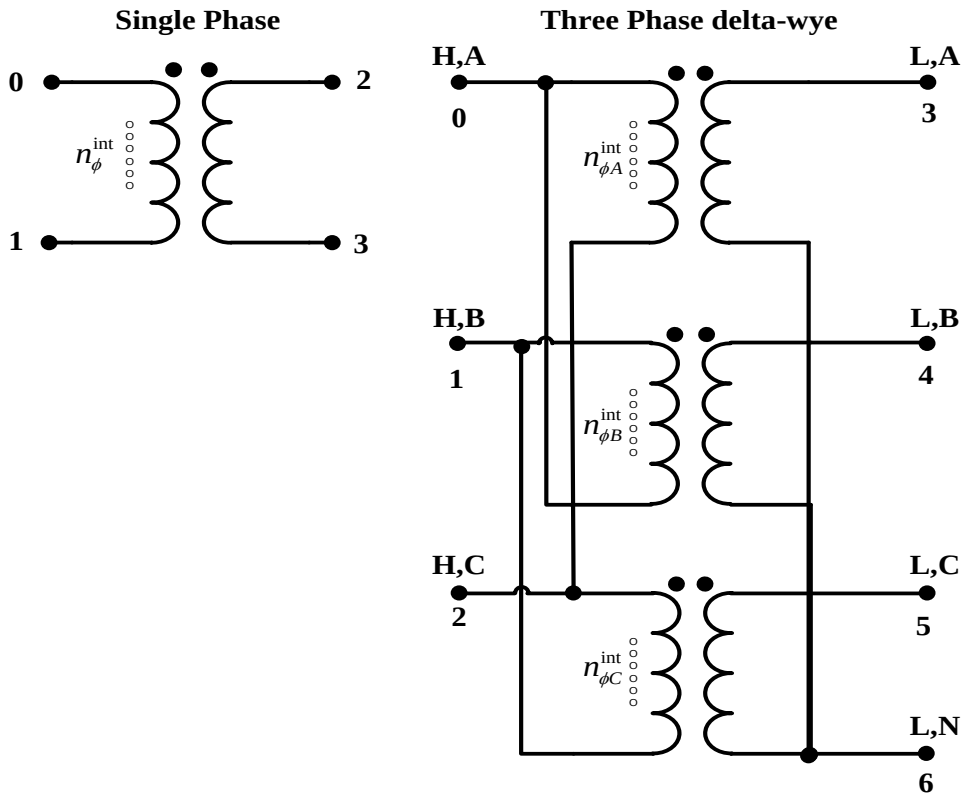

Figure 4 - 9. The indices relationship of the three-phase delta-wye connected transformer

The external states in this case are listed in Table 4-11:

Table 4 - 11. External States of delta-wye connected transformer

External States	
State Index	**State Name**
0	$v_{H,A}(t)$
1	$v_{H,B}(t)$
2	$v_{H,C}(t)$
3	$v_{L,A}(t)$
4	$v_{L,B}(t)$
5	$v_{L,C}(t)$
6	$v_{L,N}(t)$

The correspondence between the external phase states (and equations) and the three

phase transformer external states (and equations) for each phase is defined as:

Table 4 - 12. Correspondence between the external phase and bank states Index

Phase A			
Phase State Index	**State Name**	**Bank State Index**	**Bank State Name**
0	$v_{0,A}(t)$	0	$v_{H,A}(t)$
1	$v_{1,A}(t)$	2	$v_{H,C}(t)$
2	$v_{2,A}(t)$	3	$v_{L,A}(t)$
3	$v_{3,A}(t)$	6	$v_{L,N}(t)$
Phase B			
Phase State Index	**State Name**	**Bank State Index**	**Bank State Name**
0	$v_{0,B}(t)$	1	$v_{H,B}(t)$
1	$v_{1,B}(t)$	0	$v_{H,A}(t)$
2	$v_{2,B}(t)$	4	$v_{L,B}(t)$
3	$v_{3,B}(t)$	6	$v_{L,N}(t)$
Phase C			
Phase State Index	**State Name**	**Bank State Index**	**Bank State Name**
0	$v_{0,C}(t)$	2	$v_{H,C}(t)$
1	$v_{1,C}(t)$	1	$v_{H,B}(t)$
2	$v_{2,C}(t)$	5	$v_{L,C}(t)$
3	$v_{3,C}(t)$	6	$v_{L,N}(t)$

Because each single-phase transformer is modeled in the standard AQCF syntax, it is

very easy to combine the three AQCF models into a (composite) three-phase transformer AQCF model. The terminals of three single-phase transformers are interconnected, by applying the Kirchhoff's Current Law (KCL) the terminal equations can be easily combined. The internal equations of each single-phase transformer will keep unchanged. The three-phase transformer AQCF model is shown below.

$$\begin{Bmatrix} i_{3\phi}(t) \\ 0 \\ 0 \\ i_{3\phi}(t_m) \\ 0 \\ 0 \end{Bmatrix} = Y_{eqx3\phi}\mathbf{x}_{3\phi} + \begin{Bmatrix} \vdots \\ \mathbf{x}_{3\phi}{}^{T}\left\langle F^{i}_{eqx3\phi}\right\rangle \mathbf{x}_{3\phi} \\ \vdots \end{Bmatrix} - B_{eq3\phi}$$

$$B_{eq3\phi} = -N_{eqx3\phi}\mathbf{x}_{3\phi}(t-h) - M_{eq3\phi}i_{3\phi}(t-h) - K_{eq3\phi}$$

$$\mathbf{h}_{3\phi}(\mathbf{x}) = Y_{feqx3\phi}\mathbf{x}_{3\phi} + \begin{Bmatrix} \vdots \\ \mathbf{x}_{3\phi}{}^{T}\left\langle F^{i}_{feqxxx3\phi}\right\rangle \mathbf{x}_{3\phi} \\ \vdots \end{Bmatrix} + C_{feqc3\phi}$$

Connectivity: $TerminalNodeName_{3\phi}$

$$subject\ to:\ \mathbf{h}_{\min 3\phi} \le \mathbf{h}_{3\phi}(\mathbf{x}) \le \mathbf{h}_{\max 3\phi},\ \mathbf{x}_{\min 3\phi} \le \mathbf{x}_{3\phi} \le \mathbf{x}_{\max 3\phi}$$

where $\mathbf{x}_{3\phi}$ are the states for three-phase transformer and the matrix $Y_{eqx3\phi}$, $F_{eqx3\phi}$, $N_{eqx3\phi}$, $M_{eq3\phi}$ and $K_{eq3\phi}$ are decided by the combinations of connecting the terminals in wye or delta configuration.

4.3.4 Delta-Delta Connected Transformer

The configuration of delta-delta connected transformer is illustrated in Figure 4-10. In this case, the number of external states is six.

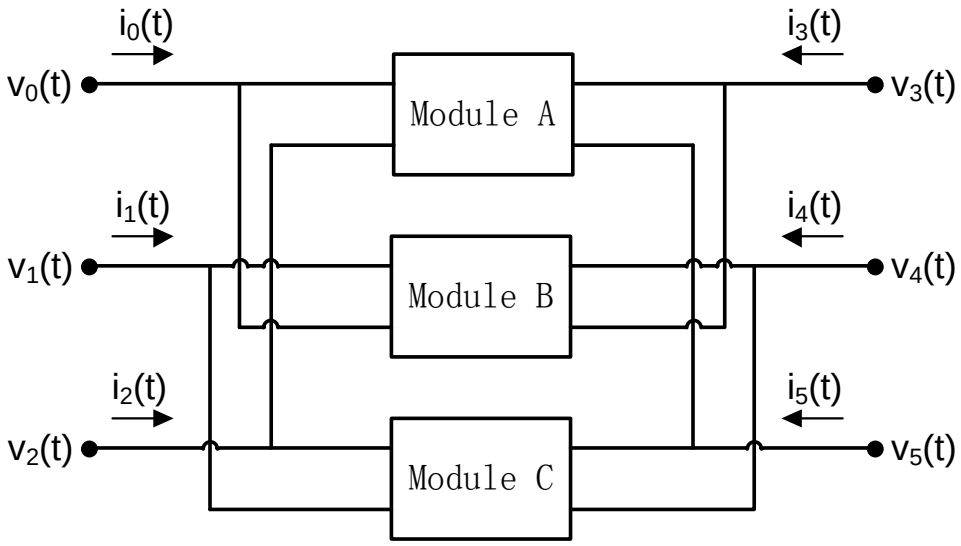

Figure 4 - 10. Three-phase delta-delta connected transformer

In order to integrate the three sets of the AQCF of the single-phase transformer, the state pointers of the AQCF of the single-phase transformer need to be re-assigned to those of the AQCF of the three-phase transformer. The indices relationship between the AQCFs of the single-phase transformer and the three-phase delta-delta connected transformer is shown in Figure 4-11. The total state number of this transformer configuration is $3n_{ph}^{\text{int}}+6$.

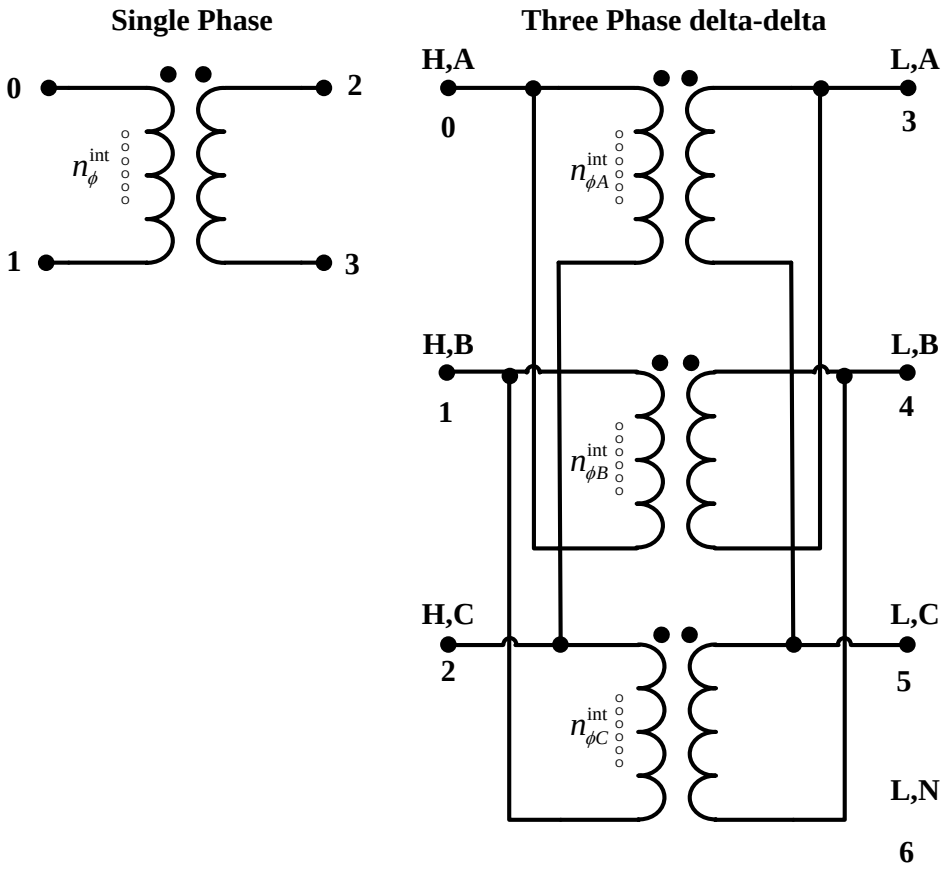

Figure 4 - 11. The indices relationship of the three-phase delta-wye connected transformer

The external states in this case are listed in Table 4-13:

Table 4 - 13. External States of delta-delta connected transformer

External States	
State Index	**State Name**
0	$v_{H,A}(t)$
1	$v_{H,B}(t)$
2	$v_{H,C}(t)$
3	$v_{L,A}(t)$
4	$v_{L,B}(t)$
5	$v_{L,C}(t)$

The correspondence between the external phase states (and equations) and the three

phase transformer external states (and equations) for each phase is defined as:

Table 4 - 14. Correspondence between the external phase and bank states Index

Phase A			
Phase State Index	**State Name**	**Bank State Index**	**Bank State Name**
0	$v_{0,A}(t)$	0	$v_{H,A}(t)$
1	$v_{1,A}(t)$	2	$v_{H,C}(t)$
2	$v_{2,A}(t)$	3	$v_{L,A}(t)$
3	$v_{3,A}(t)$	5	$v_{L,C}(t)$
Phase B			
Phase State Index	**State Name**	**Bank State Index**	**Bank State Name**
0	$v_{0,B}(t)$	1	$v_{H,B}(t)$
1	$v_{1,B}(t)$	0	$v_{H,A}(t)$
2	$v_{2,B}(t)$	4	$v_{L,B}(t)$
3	$v_{3,B}(t)$	3	$v_{L,A}(t)$
Phase C			
Phase State Index	**State Name**	**Bank State Index**	**Bank State Name**
0	$v_{0,C}(t)$	2	$v_{H,C}(t)$
1	$v_{1,C}(t)$	1	$v_{H,B}(t)$
2	$v_{2,C}(t)$	5	$v_{L,C}(t)$
3	$v_{3,C}(t)$	4	$v_{L,B}(t)$

Because each single-phase transformer is modeled in the standard AQCF syntax, it is

very easy to combine the three AQCF models into a (composite) three-phase transformer AQCF model. The terminals of three single-phase transformers are interconnected, by applying the Kirchhoff's Current Law (KCL) the terminal equations can be easily combined. The internal equations of each single-phase transformer will keep unchanged. The three-phase transformer AQCF model is shown below.

$$\begin{Bmatrix} i_{3\phi}(t) \\ 0 \\ 0 \\ i_{3\phi}(t_m) \\ 0 \\ 0 \end{Bmatrix} = Y_{eqx3\phi}\mathbf{x}_{3\phi} + \begin{Bmatrix} \vdots \\ \mathbf{x}_{3\phi}{}^{T}\left\langle F^{i}_{eqx3\phi}\right\rangle \mathbf{x}_{3\phi} \\ \vdots \end{Bmatrix} - B_{eq3\phi}$$

$$B_{eq3\phi} = -N_{eqx3\phi}\mathbf{x}_{3\phi}(t-h) - M_{eq3\phi}i_{3\phi}(t-h) - K_{eq3\phi}$$

$$\mathbf{h}_{3\phi}(\mathbf{x}) = Y_{feqx3\phi}\mathbf{x}_{3\phi} + \begin{Bmatrix} \vdots \\ \mathbf{x}_{3\phi}{}^{T}\left\langle F^{i}_{feqxxx3\phi}\right\rangle \mathbf{x}_{3\phi} \\ \vdots \end{Bmatrix} + C_{feqc3\phi}$$

Connectivity: $TerminalNodeName_{3\phi}$

$$subject\ to:\ \mathbf{h}_{\min 3\phi} \le \mathbf{h}_{3\phi}(\mathbf{x}) \le \mathbf{h}_{\max 3\phi},\ \mathbf{x}_{\min 3\phi} \le \mathbf{x}_{3\phi} \le \mathbf{x}_{\max 3\phi}$$

where $\mathbf{x}_{3\phi}$ are the states for three-phase transformer and the matrix $Y_{eqx3\phi}$, $F_{eqx3\phi}$, $N_{eqx3\phi}$, $M_{eq3\phi}$ and $K_{eq3\phi}$ are decided by the combinations of connecting the terminals in wye or delta configuration.

4.5 Summary

This chapter has presented the electro-thermal model of transformers. At first the quadratized device model (QDM) is presented, then it is integrated into the AQCF

device model by the quadratic integration method, and then next is the AQCF measurement model. Finally, the way of constructing a three-phase transformer with three single-phase transformers is presented along with the wye-wye, wye-delta, delta-wye and delta-delta four configurations. The DSE-based protection scheme directly works on the transformer AQCF objects so that this method is object-oriented. This method can be applied to other protection zone with the device and measurement models also in AQCF syntax.

CHAPTER 5 TRANSFORMER PROTECTION BASED ON DYNAMIC STATE ESTIMATION

5.1 Overview

Dynamic state estimation has been widely studied in power system analysis. With redundancy in measurements, dynamic state estimator can provide more accurate estimated states and measurements based on mathematic models. In this chapter, the dynamic state estimation method is applied to compute the best estimates of the operating states of transformers based on the transformer electro-thermal model in Chapter 4. Three approaches have been developed to solve the dynamic state estimation problem, namely the unconstrained weighted least square (UCWLS) method, the constrained weighted least square (CWLS) method and the extended Kalman filter (EKF) method. The three methods are discussed in this chapter.

With the solution of dynamic state estimation, a Chi-square test is performed to calculate the probability that the transformer measurements are consistent with its dynamic model. Based on this probability, appropriate protection decision can be made. The DSE-based protection method algorithm is also introduced in this chapter.

5.2 Three Methods for the DSE Problem

5.2.1 Approach One: UCWLS Method

Unconstrained Weighted Least Square (UCWLS) method has been widely used for state estimation [103]-[105]. WLS method provides a solution that minimizes the sum

of the squares of the errors (or residuals) of every single measurement equation. If the measurement model is linear, the WLS method provides a closed-form solution in a straightforward manner. Regarding the nonlinear measurement model, a local optimal solution can usually be reached using the Newton's method.

Specifically, in the UCWLS method for transformer dynamic state estimation, any measurement (actual, derived, pseudo and virtual measurement) can be expressed in terms of the transformer states with the aid of the transformer dynamic model in AQCF form:

$$z_k = h_k(x) + \eta_k = \sum_i a_{i,x}^k \cdot x_i + \sum_{i,j} b_{i,j,x}^k \cdot x_i \cdot x_j + c_k + \eta_k$$

where $\boldsymbol{z}$ is the combination of the actual measured measurement, derived measurement, pseudo measurement and virtual measurement, x is the state variables, a is the coefficient of linear terms, b is the coefficients of nonlinear terms, c is the constant term [102].

The object of UCWLS method is to minimize the weighted square of the measurement residuals, mathematically,

$$Minimize \quad J = \sum_{i=1}^{n} \left(\frac{h_i(x) - z_i}{\sigma_i} \right)^2 = \sum_{i=1}^{n} s_i^2 = \eta^T W \eta$$

where $\eta = h(x) - z,\ s_i = \frac{\eta_i}{\sigma_i}$ and $W = diag\left\{ \cdots, \frac{1}{\sigma_i^2}, \cdots \right\}$ and σ_i is the standard deviation of the meter by which the corresponding measurement z is measured; W is the diagonal weight matrix whose non-zero entries are the inverse of the variance of the measurement errors.

The best estimate of the system state is obtained from the Gauss-Newton iterative algorithm:

$$\hat{x}^{\nu+1} = \hat{x}^{\nu} - (H^T W H)^{-1} H^T W (h(\hat{x}^{\nu}) - z)$$

where $\hat{x}$ refers to the best estimate of the state vector x, and ***H*** is the Jacobian matrix of the measurement equations.

$$H = \frac{\partial h(\mathbf{x})}{\partial \mathbf{x}}$$

The covariance matrix of the state is defined as

$$C_x = E\left[(\hat{x} - \bar{x})(\hat{x} - \bar{x})^T\right]$$

where $\bar{x}$ denotes the true state value, and the covariance matrix computed as

$$C_x = \left(H^T W H\right)^{-1}.$$

5.2.2 Approach Two: CWLS Method

The UCWLS method works well to estimate the transformer states with a measurement set that represents actual measurements with usual measurement errors. However, when it is used to handle virtual measurements with very small uncertainty, it may generate numerical instabilities due to the large separation between the variances of the actual measurements and the virtual measurements [106]. To avoid these numerical instabilities, the constrained weighted least square (CWLS) method has been used [107]-[109].

The CWLS method is very similar to the unconstrained one, except for the virtual measurements that are treated as constraints here. Note that if virtual measurements do

not exist, then the method reverts to an unconstrained optimal problem.

Given the standard measurements model in AQCF form, they are separated into actual, derived and pseudo measurements as:

$$z_k = h_k(x) + \eta_k = \sum_i a_{i,x}^k \cdot x_i + \sum_{i,j} b_{i,j,x}^k \cdot x_i \cdot x_j + c_k + \eta_k \ ,$$

and virtual measurements expressed as:

$$0 = g_k(x) = \sum_i Y_{eqx,i}^{\ k} \cdot x_i + \sum_{i,j} F_{eqx,ij}^{\ k} \cdot x_i \cdot x_j - \sum_i b_{eq,i}^{\ k}$$

It is noted that the actual, derived and pseudo measurements contain some errors, while the virtual measurements do not have any errors. That is because the virtual measurements stand for the physical laws that the transformer model must obey, they are noiseless.

The object of CWLS method is to minimize the weighted square of the residuals of actual, pseudo and derived measurements subject to the virtual measurement constraints. Mathematically,

$$Minimize \quad J = \sum_{i=1}^{m} \left(\frac{h_i(x) - z_i}{\sigma_i} \right)^2 = \sum_{i=1}^{m} s_i^2 = \eta^T W \eta$$

$$Subject \quad to: \quad 0 = g_k(x) \quad k = 1, 2...n$$

where $\eta = h(x) - z,\ s_i = \dfrac{\eta_i}{\sigma_i}$ and $W = diag\left\{ \cdots, \dfrac{1}{\sigma_i^2}, \cdots \right\}$ and σ_i is the standard deviation of the meter by which the corresponding measurement z is measured; W is the diagonal weight matrix whose non-zero entries are the inverse of the variance of the measurement errors.

The method of Lagrange multipliers is applied here. A new variable λ called a Lagrange multiplier is introduced and the Lagrange function is defined as follows:

$$L(\mathbf{x},\boldsymbol{\lambda}) = J + \boldsymbol{\lambda}^T \mathbf{g}(\mathbf{x})$$

The necessary conditions for the Lagrange function are:

$$\frac{\partial L(\mathbf{x},\boldsymbol{\lambda})}{\partial x} = \left(\mathbf{h}_{nonVirtual}(\mathbf{x}) - \mathbf{z}\right)^T W \frac{\partial \mathbf{h}_{nonVirtual}(\mathbf{x})}{\partial \mathbf{x}} + \boldsymbol{\lambda}^T \frac{\partial \mathbf{g}(\mathbf{x})}{\partial \mathbf{x}} = 0$$

$$\frac{\partial L(\mathbf{x},\boldsymbol{\lambda})}{\partial \boldsymbol{\lambda}} = \mathbf{g}(\mathbf{x}) = 0$$

The solution of above equations could be obtained iteratively by Newton's iterative method with an initial guess $\boldsymbol{x_0}$ and $\boldsymbol{\lambda_0}$**.** The update is given by:

$$\mathbf{x}^{\nu+1} = \mathbf{x}^{\nu} + \Delta\mathbf{x}$$

$$\boldsymbol{\lambda}^{\nu+1} = \boldsymbol{\lambda}^{\nu} + \Delta\boldsymbol{\lambda}$$

Use the Taylor expansion at ν+1 iteration and ignore the higher order terms.

$$\mathbf{h}_{nonVirtual}(\mathbf{x}^{\nu} + \Delta\mathbf{x}) \approx \mathbf{h}_{nonVirtual}(\mathbf{x}^{\nu}) + H\Delta\mathbf{x}$$

$$\mathbf{g}(\mathbf{x}^{\nu} + \Delta\mathbf{x}) \approx \mathbf{g}(\mathbf{x}^{\nu}) + G\Delta\mathbf{x}$$

where $\boldsymbol{H}$ and $\boldsymbol{G}$ are the Jacobian matrices

$$H = \frac{\partial h_{nonVirtual}(x)}{\partial x}, G = \frac{\partial g(x)}{\partial x}.$$

Therefore, the necessary conditions for method of Lagrange multipliers are:

$$\left(\mathbf{h}_{nonVirtual}(\mathbf{x}^{\nu}) + H\Delta\mathbf{x} - \mathbf{z}\right)^T WH + (\boldsymbol{\lambda}^{\nu} + \Delta\boldsymbol{\lambda})G = 0$$

$$\mathbf{g}(\mathbf{x}^{\nu}) + G\Delta\mathbf{x} = 0$$

The above equations give:

$$\begin{bmatrix} \Delta x \\ \Delta\lambda \end{bmatrix} = -\begin{bmatrix} H^T WH & G^T \\ G & 0 \end{bmatrix}^{-1} \begin{bmatrix} H^T W\left(h(x^{\nu}) - z\right) + G^T\lambda^{\nu} \\ g(x^{\nu}) \end{bmatrix}$$

The best estimate of the system state is also obtained from the Gauss-Newton iterative algorithm:

$$\begin{bmatrix}\mathbf{x}^{v+1}\\ \boldsymbol{\lambda}^{v+1}\end{bmatrix}=\begin{bmatrix}\mathbf{x}^{v}\\ \boldsymbol{\lambda}^{v}\end{bmatrix}-\begin{bmatrix}H^TWH & G^T\\ G & 0\end{bmatrix}\begin{bmatrix}H^TW\left(\mathbf{h}_{nonVirtual}(\mathbf{x}^v)-\mathbf{z}\right)+G^T\boldsymbol{\lambda}^v\\ g(\mathbf{x}^v)\end{bmatrix}$$

The covariance of the state for this CWLS method is:

$$Cov\left(\begin{bmatrix}x(t,t_m)\\ \lambda(t,t_m)\end{bmatrix}\right)=E\begin{bmatrix}H^TWH & G^T\\ G & 0\end{bmatrix}^{-1}\begin{bmatrix}H^TW\eta+G^T\lambda\\ 0\end{bmatrix}\begin{bmatrix}\eta^TW^TH+\lambda^TG & 0\end{bmatrix}\begin{bmatrix}H^TWH & G^T\\ G & 0\end{bmatrix}^{-T}$$

With some additional calculation, the covariance is:

$$C=\begin{bmatrix}\left(H^TWH\right)^{-1}-\left(H^TWH\right)^{-1}G^T\left(G\left(H^TWH\right)^{-1}G^T\right)^{-1}G\left(H^TWH\right)^{-1} & 0\\ 0 & \left(G\left(H^TWH\right)^{-1}G^T\right)^{-1}+\lambda\lambda^T\end{bmatrix}$$

5.2.3 Approach Three: Extended Kalman Filter Method

Another widely used estimator is the Extended Kalman Filter (EKF) [110]-[112]. The EKF linearizes the nonlinear system to its first-order so that the traditional Kalman filter equations can be applied.

Given device quadratized model quadratized model:

$$i(t)=Y_{eqx1}\mathbf{x}(t)+D_{eqxd1}\frac{d\mathbf{x}(t)}{dt}+C_{eqc1}$$

$$0=Y_{eqx2}\mathbf{x}(t)+D_{eqxd2}\frac{d\mathbf{x}(t)}{dt}+C_{eqc2}$$

$$0=Y_{eqx3}\mathbf{x}(t)+\begin{Bmatrix}\vdots\\ \mathbf{x}(t)^T\left\langle F^i_{eqxx3}\right\rangle\mathbf{x}(t)\\ \vdots\end{Bmatrix}+C_{eqc3}$$

The above equations are discretized with trapezoidal integration method:

$$\left(i_k+i_{k-1}\right)=Y_{eqx1}\left(x_k+x_{k-1}\right)+\frac{2}{h}D_{eqxd1}(x_k-x_{k-1})+2C_{eqc1}$$

$$0=Y_{eqx2}\left(x_k+x_{k-1}\right)+\frac{2}{h}D_{eqxd2}(x_k-x_{k-1})+2C_{eqc2}$$

$$0 = Y_{eqx3}x_k + \left\{ \begin{array}{c} \vdots \\ x_k{}^T \left\langle F^i_{eqxx3} \right\rangle x_k \\ \vdots \end{array} \right\} + C_{eqc3}$$

One further step, the above equations can be re-written as:

$$D_{eqxd1}(x_k - x_{k-1}) = \frac{h}{2}\left(\left[i_k + i_{k-1} \right] - Y_{eqx1}\left[x_k + x_{k-1} \right] - 2C_{eqc1} \right)$$

$$D_{eqxd2}(x_k - x_{k-1}) = \frac{h}{2}\left(-Y_{eqx2}\left[x_k + x_{k-1} \right] - 2C_{eqc2} \right)$$

$$0 = Y_{eqx3}x_k + \left\{ \begin{array}{c} \vdots \\ x_k{}^T \left\langle F^i_{eqxx3} \right\rangle x_k \\ \vdots \end{array} \right\} + C_{eqc3}$$

The above equations are finally converted into standard EKF format:

$$x_k = Ax_{k-1} + B(\tilde{i}_{mk}, \tilde{i}_{mk-1}) + C_{const}$$

$$\mathbf{z}_k = h(x_k) = E_m \mathbf{x}_k + F_m \mathbf{x}_{k-1} + \left\{ \begin{array}{c} \vdots \\ \mathbf{x}_k{}^T F^i_m \mathbf{x}_k \\ \vdots \end{array} \right\} + C_m$$

where

$$A = \begin{bmatrix} D_{eqxd1} + \frac{h}{2}Y_{eqx1} \\ D_{eqxd2} + \frac{h}{2}Y_{eqx2} \\ Y_{eqx3} + x^0_k F_{eqxx3} + F_{eqxx3}x^0_k \end{bmatrix}^{-1} \begin{bmatrix} D_{eqxd1} - \frac{h}{2}Y_{eqx1} \\ D_{eqxd2} - \frac{h}{2}Y_{eqx2} \\ 0 \end{bmatrix}$$

$$B = \begin{bmatrix} D_{eqxd1} + \frac{h}{2}Y_{eqx1} \\ D_{eqxd2} + \frac{h}{2}Y_{eqx2} \\ Y_{eqx3} + x^0_k F_{eqxx3} + F_{eqxx3}x^0_k \end{bmatrix}^{-1} \begin{bmatrix} \frac{h}{2} \\ 0 \\ 0 \end{bmatrix}$$

$$C_{const} = \begin{bmatrix} D_{eqxd1} + \frac{h}{2}Y_{eqx1} \\ D_{eqxd2} + \frac{h}{2}Y_{eqx2} \\ Y_{eqx3} + x^0_k F_{eqxx3} + F_{eqxx3}x^0_k \end{bmatrix}^{-1} \begin{bmatrix} -hC_{eqc1} \\ -hC_{eqc2} \\ -C_{eqc3} \end{bmatrix}$$

The EKF method is implemented as a two-step prediction-correction process. The equations are given below:

Prediction:

$$\begin{cases} x_k^- = Ax_{k-1} + B(\tilde{i}_{mk}, \tilde{i}_{mk-1}) + C_{const} \\ \\ P_k^- = A_k P_{k-1} A_k^T + Q_k \end{cases}$$

Correction:

$$\begin{cases} K_k = P_k^- H_k^T (H_k P_k^- H_k^T + R_k)^{-1} \\ x_k = x_k^- + K_k \left(z_k - h\left(x_k^- \right) \right) \\ P_k = \left(I - K_k H_k \right) P_k^- \end{cases}$$

where H_k is the Jacobian matrix:

$$H_k = \frac{\partial h(x_k)}{\partial x}$$

and Q_k and R_k are the process and measurement noises respectively.

The covariance matrix of EKF method is contributed by both the matrix P_k and Q_k .

5.3 Proposed DSE-Based Transformer Protection Logic

The logic of proposed DSE-based transformer protection scheme is illustrated in Figure 5-1. According to this figure, the first step is to perform the dynamic state estimation with the dynamic model and measurements of transformer. The dynamic state estimator gives the best estimates of transformer states with aforementioned three methods.

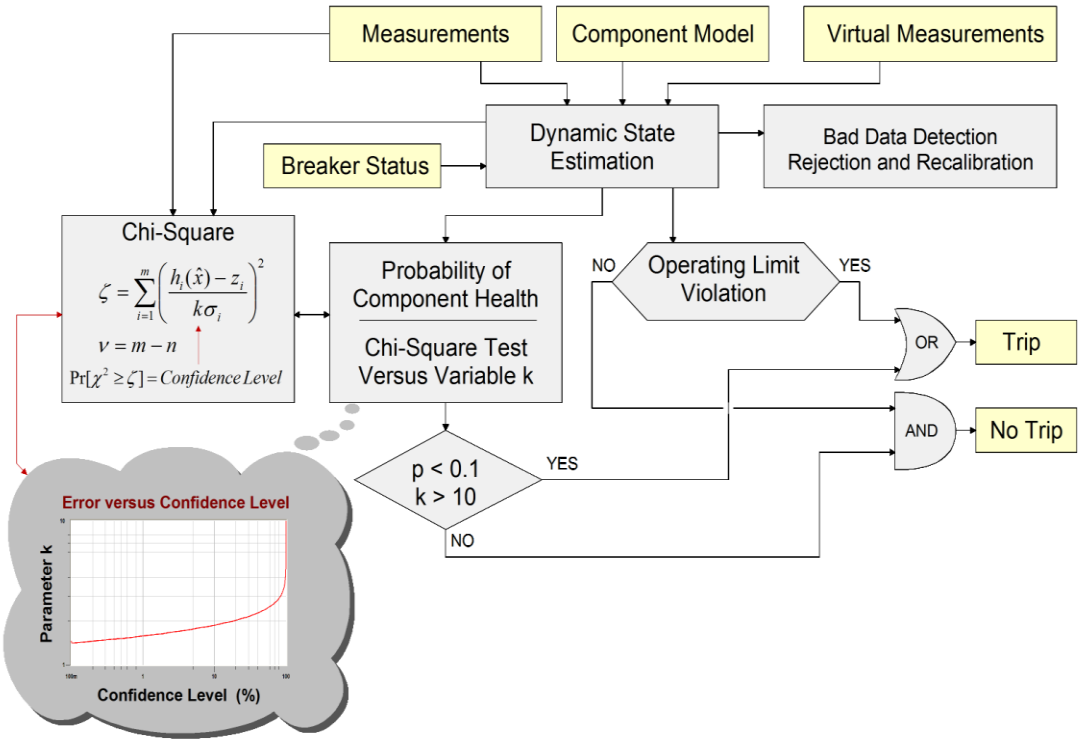

Figure 5 - 1. Proposed DSE-based protection logic

With the best estimates of transformer states from the DSE solutions, a Chi-square test is performed to calculate the probability that measurement data are consistent with the transformer model. The normalized residual (or error) for each measurement i is defined as:

$$s_i = \frac{\eta_i}{\sigma_i}$$

and thus the vector of normalized residuals is

$$s = \sqrt{W} \cdot \eta$$

The value of Chi-square test is defined as

$$\xi = \sum_{i=1}^{n} \left(\frac{h_i(\hat{\mathbf{x}}) - z_i}{\sigma_i} \right)^2$$

The Chi-square test quantifies the preciseness of fit between the model and measurements, i.e., the confidence level. The confidence level is expressed as the probability that the measurement errors are distributed within their expected range. Specifically, the preciseness of fit (confidence level) can be obtained as

$$Pr[\chi^2 \geq \xi] = 1 - Pr[\chi^2 \leq \xi] = 1 - Pr(\xi, v) \ .$$

where ζ is the Chi-square critical value, and $\boldsymbol{v}$ is the degree of freedom.

The degree of freedom is defined as difference between the number of measurements $\boldsymbol{m}$ and number of states $\boldsymbol{n}$. The degrees of freedom are always positive because that $\boldsymbol{m}$ is always greater than $\boldsymbol{n}$.

$$v = m - n$$

The chi-square test is utilized to provide the probability that the expected error of the estimated state values will be within a specific range. Because there are many data acquisition devices with different accuracy, a normalization constant k has been introduced. The variable k is defined as follows: if it is 1.0 then the standard deviation of each measurement is equal to the accuracy of the meter with which this measurement was obtained. If different than 1.0 then the standard deviation of the measurement error equal the accuracy of the meter times k. The introduction of the variable k allows us to

characterize the accuracy of the estimated state with only one variable. This is equivalent of providing the expected error (which equals the variable k times the standard deviation of the measurement error) versus probability (confidence level). Figure 5-2 illustrates the graph of the parameter k versus confidence level.

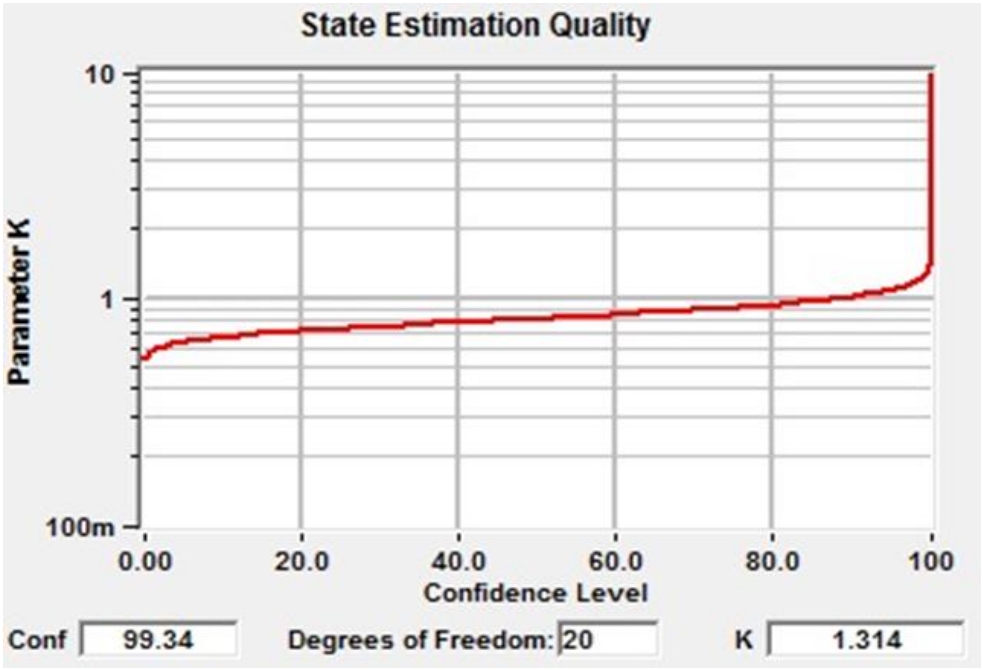

Figure 5 - 2. K-factor curve for chi-square test

The proposed method uses the confidence level as the health index of transformer. It is obvious that confidence level around 1.0 (small Chi-square value) infers the measurements are highly consistent with the transformer dynamic mode, which means there is no internal abnormality. On the other side, confidence level around 0.0 (large Chi-square value) infers the measurements do not fit with the transformer dynamic model. The proposed DSE-based scheme accurately makes the protection decision only based on the operating condition of the transformer.

It takes two consecutive samples to perform the dynamic state estimation. Theoretically, the proposed DSE-based method only requires two samples time (a

fraction of one ms) to determine whether an internal fault happens in the transformer. This means the proposed DSE-based scheme is faster than any existing transformer protection method for detecting the faults.

It is also noted that there is a possibility that the confidence level may drop (but return to 1.0) for a few samples when transients suddenly happen. To avoid false tripping caused by transients, the values of the chi-square test and confidence level are integrated over a user-selected interval (typically half or one cycles) before a trip command is issued.

5.3 Summary

This chapter has discussed the algorithm of protecting transformer using the dynamic state estimation method. Three approaches are used to solve the dynamic state estimation problem, namely the unconstrained weighted least square (UCWLS) method, the constrained weighted least square (CWLS) method and the extended Kalman filter (EKF) method. In the end of this chapter, the protection logic of the proposed DSE-based method is presented. A Chi-square test is performed to calculate the probability (confidence level) that measurement data are consistent with the transformer model. If the confidence level is around 1.0, the transformer is health; otherwise if the confidence level is around 0.0, something is wrong inside the transformer and the proposed method will send a signal to trip and protect the transformer.

CHAPTER 6 TRANSFORMER MODEL PARAMETER CALIBRATION

6.1 Overview

Dynamic state estimation-based transformer protection method is a model-based method. Modeling accuracy and fidelity are fundamental to guarantee the feasibility of the proposed method. The transformer parameters used for state estimation come from the nameplate provided by the manufacturers. However, the actual parameters are always quite different from the nameplate ratings because of the transformer ageing [113]-[114]. If the transformer parameters are not correct, the results of the proposed DSE-based protection method must include sizeable errors. To solve this problem, the proposed DSE-based protection method is also utilized to fine tune the transformer models and/or determine the parameters of the model with greater accuracy.

The basic approach of transformer parameters calibration is to expand the dynamic state estimation to include some independent parameters as state variables. Through this way the transformer model can be validated. Therefore, the proposed overall approach can also provide better models with validated parameters.

In this chapter, a demonstrating example of auto-transformer parameter calibration is presented.

6.2 Parameters Calibration

This section describes the parameter calibration of single-phase autotransformer with tertiary winding. The auto-transformer thermal conductance physical configuration is show in Figure 6-1.

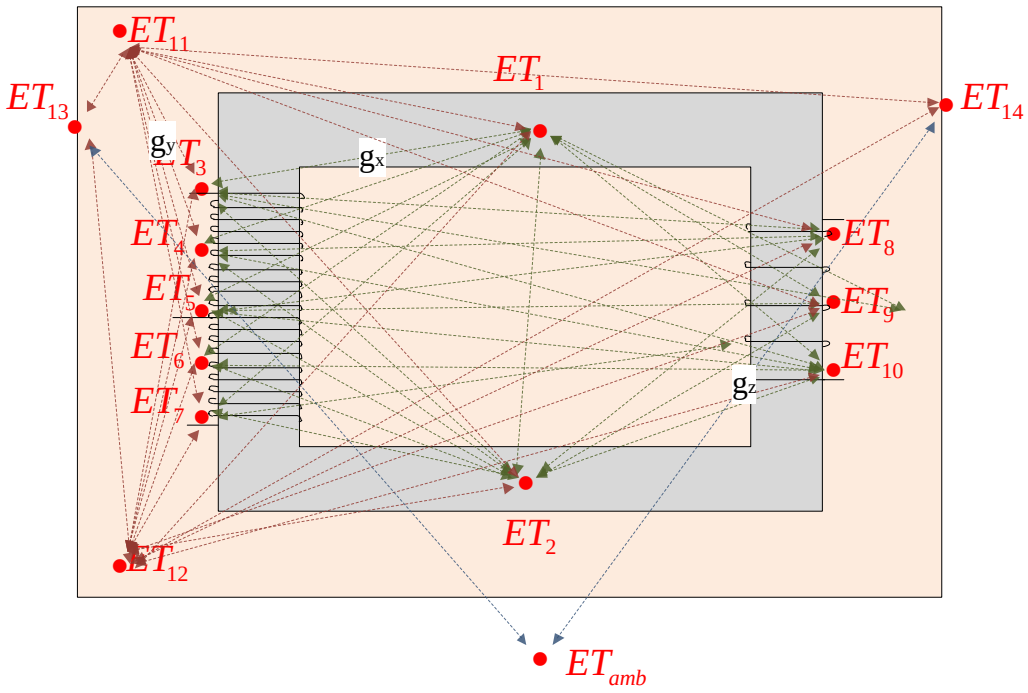

Figure 6 - 1. Auto-transformer physical parameter configuration

Because of the autotransformer physicals, the conductance parameters depend on few parameters, and they can be classified into three groups that are represented by green, brown and blue dash-lines respectively. In the first (green) group, all the thermal conductance can be represented by the value of core (ET_1) to coil (ET_3) conductance multiple certain coefficients; in the second (brown) group, all the thermal conductance can be represented by the value of coil (ET_3) to oil (ET_{11}) conductance multiple certain coefficients; in the third (blue) group, all the thermal conductance can be represented by the value of tank (ET_{13}) to ambient (ET_{amb}) conductance multiple certain coefficients.

The independent parameters of the auto-transformer as treated as states in the dynamic state estimation. These independent parameters that are summarized in Table 6-1.

Table 6 - 1. Parameters to be calibrated

No.	Variables	Description
1	g_x	Thermal conductance between $Core-Coil$ (ET_1-ET_3)
2	g_y	Thermal conductance between $Coil-Oil$ (ET_3-ET_{11})
3	g_z	Thermal conductance between $Tank-Amb$ $(ET_{13}-ET_{amb})$

The conductance between each temperature thermal point depends on the above three variables and the relationship is show in Table 6-2:

Table 6 - 2. Autotransformer thermal conductance

	ET1	ET2	ET3	ET4	ET5	ET6	ET7	ET8	ET9	ET10	ET11	ET12	ET13	ET14	ETamb
ET1	X	$0.6\,g_x$	g_x	$0.9\,g_x$	$0.8\,g_x$	$0.7\,g_x$	$0.6\,g_x$	$0.8\,g_x$	$0.7\,g_x$	$0.6\,g_x$	g_y	$0.6\,g_y$	X	X	X
ET2	$0.6\,g_x$	X	$0.6\,g_x$	$0.7\,g_x$	$0.8\,g_x$	$0.9\,g_x$	g_x	$0.8\,g_x$	$0.9\,g_x$	g_x	$0.6\,g_y$	g_y	X	X	X
ET3	g_x	$0.6\,g_x$	X	g_x	$0.9\,g_x$	$0.8\,g_x$	$0.7\,g_x$	$0.9\,g_x$	$0.8\,g_x$	$0.7\,g_x$	g_y	$0.6\,g_y$	X	X	X
ET4	$0.9\,g_x$	$0.7\,g_x$	g_x	X	g_x	$0.9\,g_x$	$0.8\,g_x$	g_x	$0.9\,g_x$	$0.8\,g_x$	$0.9\,g_y$	$0.7\,g_y$	X	X	X
ET5	$0.8\,g_x$	$0.8\,g_x$	$0.9\,g_x$	g_x	X	g_x	$0.9\,g_x$	g_x	$0.9\,g_x$	$0.8\,g_x$	$0.8\,g_y$	$0.8\,g_y$	X	X	X
ET6	$0.7\,g_x$	$0.9\,g_x$	$0.8\,g_x$	$0.9\,g_x$	g_x	X	g_x	$0.9\,g_x$	g_x	$0.9\,g_x$	$0.7\,g_y$	$0.9\,g_y$	X	X	X
ET7	$0.6\,g_x$	g_x	$0.7\,g_x$	$0.8\,g_x$	$0.9\,g_x$	g_x	X	$0.8\,g_x$	$0.9\,g_x$	g_x	$0.6\,g_y$	g_y	X	X	X
ET8	$0.8\,g_x$	$0.8\,g_x$	$0.9\,g_x$	g_x	g_x	$0.9\,g_x$	$0.8\,g_x$	X	g_x	$0.9\,g_x$	$0.8\,g_y$	$0.8\,g_y$	X	X	X
ET9	$0.7\,g_x$	$0.9\,g_x$	$0.8\,g_x$	$0.9\,g_x$	$0.9\,g_x$	g_x	$0.9\,g_x$	g_x	X	g_x	$0.7\,g_y$	$0.9\,g_y$	X	X	X
ET10	$0.6\,g_x$	g_x	$0.7\,g_x$	$0.8\,g_x$	$0.8\,g_x$	$0.9\,g_x$	g_x	$0.9\,g_x$	g_x	X	$0.6\,g_y$	g_y	X	X	X
ET11	g_y	$0.6\,g_y$	g_y	$0.9\,g_y$	$0.8\,g_y$	$0.7\,g_y$	$0.6\,g_y$	$0.8\,g_y$	$0.7\,g_y$	$0.6\,g_y$	X	$2\,g_y$	$0.5\,g_y$	$0.4\,g_y$	X
ET12	$0.6\,g_y$	g_y	$0.6\,g_y$	$0.7\,g_y$	$0.8\,g_y$	$0.9\,g_y$	g_y	$0.8\,g_y$	$0.9\,g_y$	g_y	$2\,g_y$	X	$0.4\,g_y$	$0.5\,g_y$	X
ET13	X	X	X	X	X	X	X	X	X	X	$0.5\,g_y$	$0.4\,g_y$	X	$2\,g_z$	g_z
ET14	X	X	X	X	X	X	X	X	X	X	$0.4\,g_y$	$0.5\,g_y$	$2\,g_z$	X	g_z
ETamb	X	X	X	X	X	X	X	X	X	X	X	X	g_z	g_z	X

The quadratized device model of single-phase autotransformer with tertiary winding for the purpose of parameter calibration is written as:

$$i_1(t) = i_{L1}(t) + i_{gs1}(t)$$

$$i_2(t) = -i_{L1}(t) - i_{gs1}(t) - i_{L2}(t) - i_{gs2}(t)$$

$$i_3(t) = i_{L3}(t) + i_{gs3}(t)$$

$$i_4(t) = -i_{L3}(t) - i_{gs3}(t)$$

$$i_5(t) = i_{L2}(t) + i_{gs2}(t)$$

$$0 = z_1(t) - \frac{di_{L1}(t)}{dt}$$

$$0 = z_2(t) - \frac{di_{L2}(t)}{dt}$$

$$0 = z_3(t) - \frac{di_{L3}(t)}{dt}$$

$$0 = e_c(t) - \frac{d\lambda(t)}{dt}$$

$$0 = v_1(t) - v_2(t) - r_1\left(i_{L1}(t) + i_{gs1}(t)\right) - i_{gs1}(t) / g_{s1} - \frac{N_1}{N_1 + N_2} e_c(t)$$

$$0 = v_5(t) - v_2(t) - r_2\left(i_{L2}(t) + i_{gs2}(t)\right) - i_{gs2}(t) / g_{s2} + \frac{N_2}{N_1 + N_2} e_c(t)$$

$$0 = v_3(t) - v_4(t) - r_3\left(i_{L3}(t) + i_{gs3}(t)\right) - i_{gs3}(t) / g_{s3} - \frac{N_3}{N_1 + N_2} e_c(t)$$

$$0 = i_{gs1}(t) / g_{s1} - L_1 z_1(t) + L_{PS} z_2(t) - L_{PT} z_3(t)$$

$$0 = i_{gs2}(t) / g_{s2} - L_2 z_2(t) + L_{PS} z_1(t) + L_{ST} z_3(t)$$

$$0 = i_{gs3}(t) / g_{s3} - L_3 z_3(t) + L_{ST} z_2(t) - L_{PT} z_1(t)$$

$$0 = -i_{L3}(t) - i_{gs3}(t) + i_{c1}(t) + i_m(t) + g_c \frac{N_3}{N_1 + N_2} e_c(t)$$

$$0 = N_1\left(i_{L1}(t) + i_{gs1}(t)\right) - N_2\left(i_{L2}(t) + i_{gs2}(t)\right) + N_3 i_{c1}(t)$$

$$0 = i_m(t) - i_0 y_m(t) sign\left(\lambda(t)\right)^{n+1}$$

$$0 = C_1 \frac{dET_1(t)}{dt} + \left(6.7 g_x(t) + 1.6 g_y(t)\right) ET_1(t) - \sum_{j \neq 1}^{n=14} \left(g_{1,j} ET_j(t)\right) - Q_{core,1}(t)$$

$$0 = C_2 \frac{dET_2(t)}{dt} + \left(7.3 g_x(t) + 1.6 g_y(t)\right) ET_2(t) - \sum_{j \neq 2}^{n=14} \left(g_{2,j} ET_j(t)\right) - Q_{core,2}(t)$$

$$0 = C_3 \frac{dET_3(t)}{dt} + \left(7.4g_x(t) + 1.6g_y(t)\right) ET_3(t) - \sum_{j\neq 3}^{n=14} \left(g_{3,j} ET_j(t)\right) - Q_{coil\_pri,1}(t)$$

$$0 = C_4 \frac{dET_4(t)}{dt} + \left(8g_x(t) + 1.6g_y(t)\right) ET_4(t) - \sum_{j\neq 4}^{n=14} \left(g_{4,j} ET_j(t)\right) - Q_{coil\_pri,2}(t)$$

$$0 = C_5 \frac{dET_5(t)}{dt} + \left(8.1g_x(t) + 1.6g_y(t)\right) ET_5(t) - \sum_{j\neq 5}^{n=14} \left(g_{5,j} ET_j(t)\right) - \frac{1}{2}\left(Q_{coil\_pri,2}(t) + Q_{coil\_sec,1}(t)\right)$$

$$0 = C_6 \frac{dET_6(t)}{dt} + \left(8.1g_x(t) + 1.6g_y(t)\right) ET_6(t) - \sum_{j\neq 6}^{n=14} \left(g_{6,j} ET_j(t)\right) - Q_{coil\_sec,1}(t)$$

$$0 = C_7 \frac{dET_7(t)}{dt} + \left(7.7g_x(t) + 1.6g_y(t)\right) ET_7(t) - \sum_{j\neq 7}^{n=14} \left(g_{7,j} ET_j(t)\right) - Q_{coil\_sec,2}(t)$$

$$0 = C_8 \frac{dET_8(t)}{dt} + \left(8.1g_x(t) + 1.6g_y(t)\right) ET_8(t) - \sum_{j\neq 8}^{n=14} \left(g_{8,j} ET_j(t)\right) - Q_{coil\_ter,1}(t)$$

$$0 = C_9 \frac{dET_9(t)}{dt} + \left(8.1g_x(t) + 1.6g_y(t)\right) ET_9(t) - \sum_{j\neq 9}^{n=14} \left(g_{9,j} ET_j(t)\right) - \frac{1}{2}\left(Q_{coil\_ter,1}(t) + Q_{coil\_ter,2}(t)\right)$$

$$0 = C_{10} \frac{dET_{10}(t)}{dt} + \left(7.7g_x(t) + 1.6g_y(t)\right) ET_{10}(t) - \sum_{j\neq 10}^{n=14} \left(g_{10,j} ET_j(t)\right) - Q_{coil\_ter,2}(t)$$

$$0 = C_{11} \frac{dET_{11}(t)}{dt} + 10.6g_y(t) ET_{11}(t) - \sum_{j\neq 11}^{n=14} \left(g_{11,j} ET_j(t)\right)$$

$$0 = C_{12} \frac{dET_{12}(t)}{dt} + 10.6g_y(t) ET_{12}(t) - \sum_{j\neq 12}^{n=14} \left(g_{12,j} ET_j(t)\right)$$

$$0 = C_{13} \frac{dET_{13}(t)}{dt} + \left(0.9g_y(t) + 3g_z(t)\right) ET_{13}(t) - \sum_{j\neq 13}^{n=14+ET_{amb}} \left(g_{13,j} ET_j(t)\right) - g_{13,T} ET_{amb}$$

$$0 = C_{14} \frac{dET_{14}(t)}{dt} + \left(0.9g_y(t) + 3g_z(t)\right) ET_{14}(t) - \sum_{j\neq 14}^{n=14+ET_{amb}} \left(g_{14,j} ET_j(t)\right) - g_{14,T} ET_{amb}$$

$$0 = y_1(t) - \frac{\lambda(t)^2}{\lambda_0^2}$$

$$0 = y_2(t) - y_1(t)^2$$

.....

$$0 = y_{m1}(t) - y_{m1-1}(t)^2$$

$$0 = y_{m1+1}(t) - y_{i1}(t)y_{j1}(t)$$

$$0 = y_{m1+2}(t) - y_{m1+1}(t)y_{j2}(t)$$

.....

$$\begin{cases} 0 = y_m(t) - y_{m-1}(t)y_{jm2}(t), & if\ n\ even \\ 0 = y_m(t) - y_{m-1}(t)\dfrac{\lambda(t)}{\lambda_0}, & if\ n\ odd \end{cases}$$

$$0 = Q_{core,1}(t) - \frac{1}{2}\alpha_{e+h}\lambda(t)^2$$

$$0 = Q_{core,2}(t) - \frac{1}{2}\alpha_{e+h}\lambda(t)^2$$

$$0 = Q_{coil\_pri,1}(t) - \frac{1}{2}r_1 i_{L1}(t)^2$$

$$0 = Q_{coil\_pri,2}(t) - \frac{1}{2}r_1 i_{L1}(t)^2$$

$$0 = Q_{coil\_sec,1}(t) - \frac{1}{2}r_2 i_{L2}(t)^2$$

$$0 = Q_{coil\_sec,2}(t) - \frac{1}{2}r_2 i_{L2}(t)^2$$

$$0 = Q_{coil\_ter,1}(t) - \frac{1}{2}r_3 i_{L3}(t)^2$$

$$0 = Q_{coil\_ter,2}(t) - \frac{1}{2}r_3 i_{L3}(t)^2$$

After the quadratization, the quadratic integration method is applied to above the auto-transformer quadratized model to convert the model to the standard AQCF syntax. This procedure is the same as the procedure discussed in Chapter 4, and the details are not listed here.

The external states, internal states and the actual measurements of the auto-transformer physical parameters identification problem are listed by Table 6-3 to Table 6-5, respectively.

Table 6 - 3. External state variables of auto-transformer

Index	Variable	Description
0	$v_1(t)$	terminal voltage of transformer primary side (V)
1	$v_2(t)$	terminal voltage of transformer secondary side (V)
2	$v_3(t)$	terminal voltage of transformer tertiary side (V)
3	$v_4(t)$	terminal voltage of transformer tertiary neutral (V)
4	$v_5(t)$	terminal voltage of transformer primary neutral (V)

Table 6 - 4. Internal state variables of auto-transformer

Index	Variable	Description
5	$i_{L1}(t)$	current through the primary side inductance (A)
6	$i_{L2}(t)$	current through the secondary side inductance (A)
7	$i_{L3}(t)$	current through the tertiary side inductance (A)
8	$i_{gs1}(t)$	current through the primary side stabilizer (A)
9	$i_{gs2}(t)$	current through the secondary side stabilizer (A)
10	$i_{gs3}(t)$	current through the tertiary side stabilizer (A)
11	$z_1(t)$	introduced state
12	$z_2(t)$	introduced state
13	$z_3(t)$	introduced state
14	$e_c(t)$	voltage generated by the flux (A)
15	$i_c(t)$	current through tertiary side windings (A)
16	$\lambda(t)$	flux linkage (Web)

Table 6 – 4 continued

Index	Variable	Description
17	$i_m(t)$	magnetizing current (A)
18	$y_1(t)$	introduced state (p.u.)
19	$y_2(t)$	introduced state (p.u.)
	…	introduced state (p.u.)
	…	introduced state (p.u.)
17+m	$y_m(t)$	introduced state (p.u.)
18+m	$ET_1(t)$	temperature at core up point (Celsius)
19+m	$ET_2(t)$	temperature at core down point (Celsius)
20+m	$ET_3(t)$	temperature at primary coil up point (Celsius)
21+m	$ET_4(t)$	temperature at primary coil mid point (Celsius)
22+m	$ET_5(t)$	temperature at primary/secondary coil connection
23+m	$ET_6(t)$	temperature at secondary coil mid point (Celsius)
24+m	$ET_7(t)$	temperature at secondary coil down point (Celsius)
25+m	$ET_8(t)$	temperature at tertiary coil up point (Celsius)
26+m	$ET_9(t)$	temperature at tertiary coil midpoint (Celsius)
27+m	$ET_{10}(t)$	temperature at tertiary coil down point (Celsius)
28+m	$ET_{11}(t)$	temperature at internal oil up point (Celsius)
29+m	$ET_{12}(t)$	temperature at internal oil down point (Celsius)
30+m	$ET_{13}(t)$	temperature at transformer tank front point (Celsius)

Table 6 – 4 continued

Index	Variable	Description
31+m	$ET_{14}(t)$	temperature at transformer tank rear point (Celsius)
32+m	$Q_{core,1}(t)$	heat generated at core up point (W)
33+m	$Q_{core,2}(t)$	heat generated at core down point (W)
34+m	$Q_{coil\_pri,1}(t)$	heat generated at primary coil up point (W)
35+m	$Q_{coil\_pri,2}(t)$	heat generated at primary coil down point (W)
36+m	$Q_{coil\_sec,1}(t)$	heat generated at secondary coil up point (W)
37+m	$Q_{coil\_sec,2}(t)$	heat generated at secondary coil down point (W)
38+m	$Q_{coil\_ter,1}(t)$	heat generated at tertiary coil up point (W)
39+m	$Q_{coil\_ter,2}(t)$	heat generated at tertiary coil down point (W)
40+m	g_x	Thermal conductance between $Core-Coil$ $(ET_1 - ET_3)$
41+m	g_y	Thermal conductance between $Coil-Oil$ $(ET_3 - ET_{11})$
42+m	g_z	Thermal conductance between $Tank-Amb$ $(ET_{13} - ET_{amb})$

Table 6 - 5. Through variables of auto-transformer

Index	Variable	Description
0	$i_1(t)$	current through transformer primary side (A)
1	$i_2(t)$	current through transformer secondary side (A)
2	$i_3(t)$	current through transformer tertiary side (A)
3	$i_4(t)$	current through transformer tertiary neutral (A)
4	$i_5(t)$	current through transformer primary neutral (A)

These actual measurements together with the transformer model which are treated as virtual measurements, contribute 46+m measurements for the state estimator, while the state estimator has 48+m states. Besides, two additional pseudo measurements (Phase N voltages) and three temperature measurements (temperature at the tank, oil and primary coil) are available, which giving the parameter calibration problem a degree of freedom equals three. Therefore, we have enough observability to realize the parameter calibration of auto-transformer. By applying a multi-step dynamic state estimation, the degree of freedom would increase again. The reason to implement this approach is that the dynamic state estimator runs at high rates and the physical parameters of the auto-transformer can be assumed to be constant within 2-3 consecutive time steps. For example, consider a two time step case where we will have (48+m) + (45+m) = 93+2m states (for the second time step the 3 physical parameters are considered the same as in the first time step). In contrast, we have (49+m) *2 =98 + 2m measurements, which will make the state estimator more observable.

6.3 Autotransformer Parameters Identification – Numerical Results

In this section, a 300MVA, 765/345/13.8 kV single-phase auto-transformer with tertiary winding is selected to validate the performance of the proposed method. The test system consists of a generator source, several transformers and transmission lines, as shown in Figure 6-2. At time 29.9 sec, a single-phase line to ground fault is generated at the bus LINE345 to generate some transients for the purpose of better calibration.

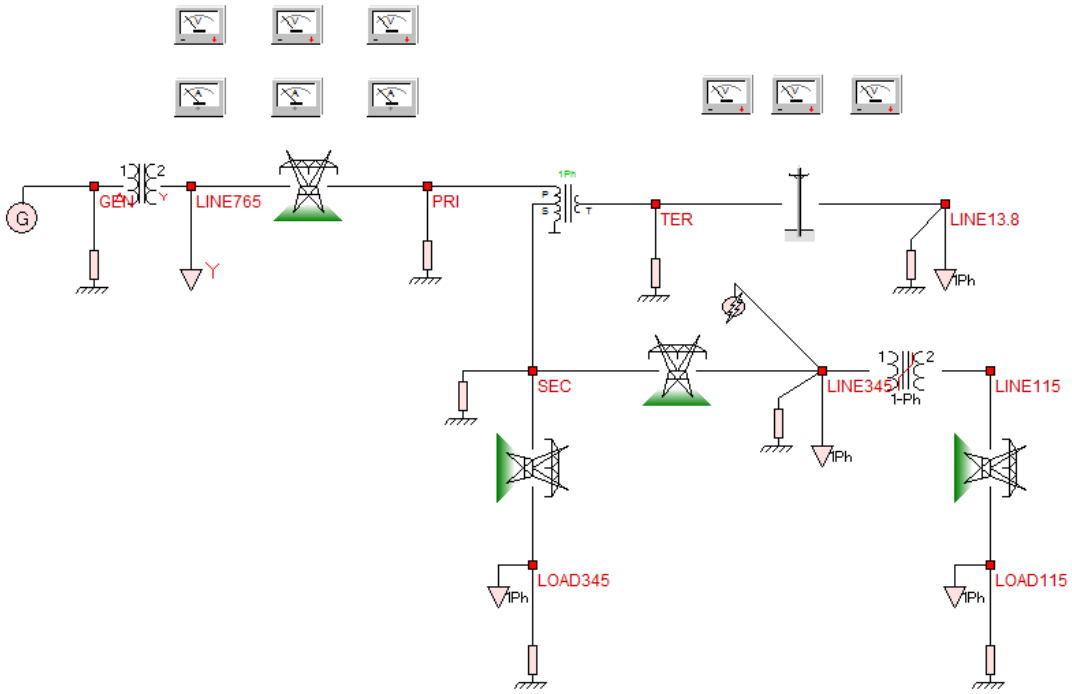

Figure 6 - 2. Auto-transformer parameter calibration test system

The waveforms of the measurements are illustrated in Figure 6-3.

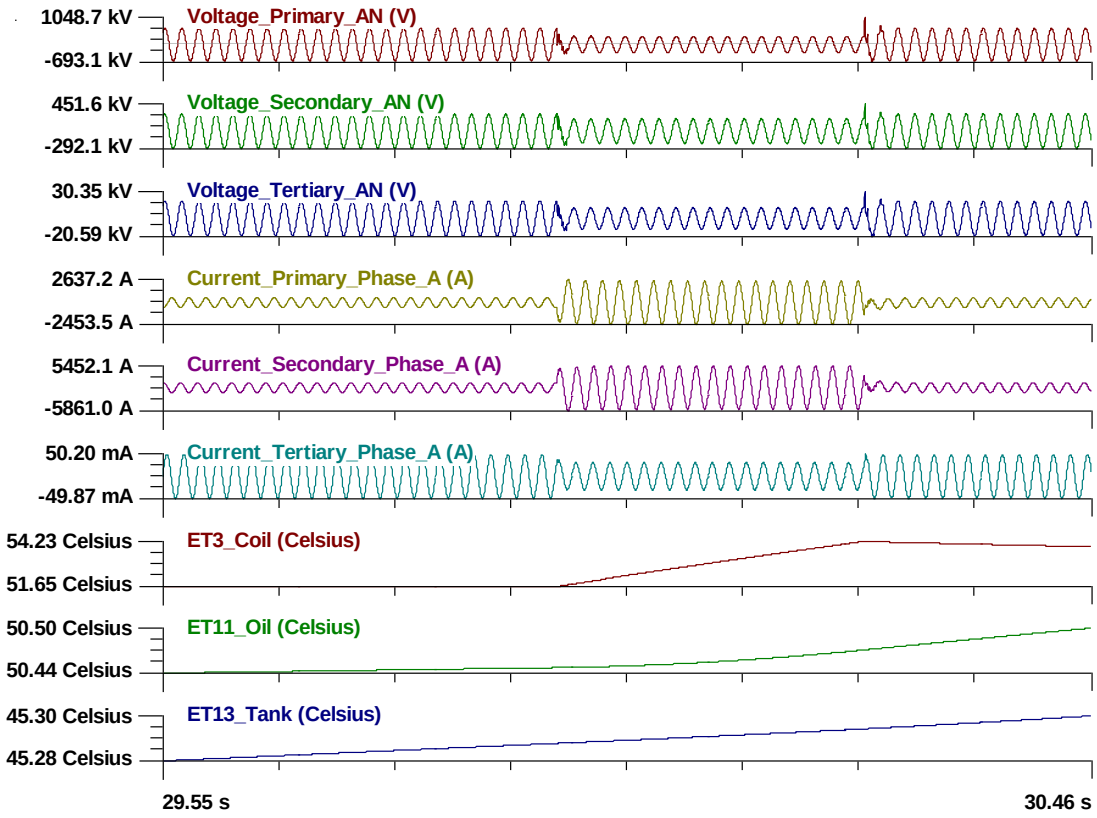

Figure 6 - 3. Auto-transformer measurements

There are six voltage and current measurements for the primary, secondary and tertiary terminals, as well as three temperature measurements: primary coil (ET_3), oil (ET_{11}) and tank (ET_{13}). The above measurements are used for auto-transformer parameter calibrations. The real and estimated parameters are presented in Table 6-6.

Table 6 - 6. Parameters calibration results

Parameters	Actual Value (kJ/Celsius)	Estimated Value (kJ/Celsius)	Error
g_x	72.54	72.51	0.41%
g_y	130.57	132.36	1.37%
g_z	29.02	29.53	1.76%

From the above Table, it is known that the estimation errors for these auto-transformer physical parameters are below 2%, which verifies the effectiveness of the

proposed parameter calibration method.

6.4 Summary

In this chapter, the proposed DSE-based method is used to calibrate transformer physical parameters. The independent physical parameters are modeled as state variables in the estimation process. The mathematical formulation of a single-phase autotransformer physical parameters identification problem is presented to illustrate the procedure. Numerical results validate the feasibility of using DSE method to calibrate transformer physical parameters.

CHAPTER 7 DEMONSTRATING EXAMPLES: DSE-BASED TRANSFORMER PROTECTION

7.1 Overview

In this chapter, proposed DSE-based transformer protection scheme is compared with the legacy protection schemes to test the security and dependability.

The example test system comprises a 35MVA, 115/35kV three-phase delta-wye saturable-core transformer with impedance Z = *j*0.10 pu, designated as T1 in Figure 7-1. The ambient temperature is 25 ˚C, the transformer is 50% loaded and it is protected with six aforementioned legacy schemes: (a) percentage differential protection; (b) harmonic-restraint differential protection; (c) negative-sequence differential protection; (d) overcurrent protection; (e) volts-over-hertz protection and (f) thermal protection. The performance of the legacy protection functions is compared with the performance of proposed DSE-based protection relay.

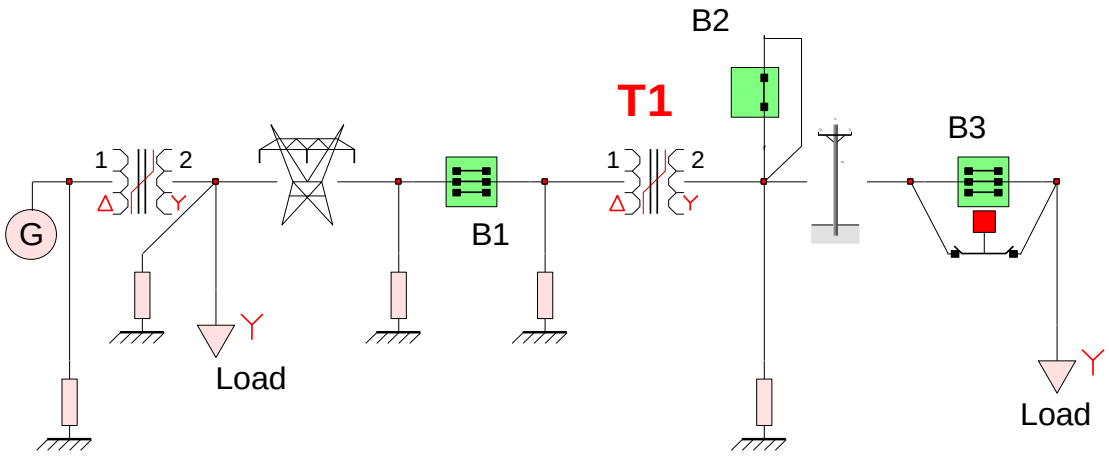

Figure 7 - 1. Transformer testing system.

The legacy protection functions have the following settings: (a) *percentage differential protection*: the percent differential threshold setting is 20%, the minimum

pickup operating current is 10A (referred to primary side); (b) *harmonic-restraint differential protection*: the percent differential threshold setting is 20%, the minimum pickup operating current is 10A (referred to primary side) and the 2nd harmonic blocking level I_{op2nd} / I_{op} is 20%; (c) *negative-sequence differential protection*: the percent differential threshold setting is 20%, the minimum pickup operating current is 1.0A (referred to primary side); (d) *time-overcurrent protection*: the pickup current referred to primary side is 900A and the time dial is 0.1 and very inverse; (e) *volts-over-hertz protection*: the time characteristic related to the ratio of volts-over-hertz is shown in Figure 7-2 ; (f) *thermal protection*: the temperature limit at the hot-spots is 105℃.

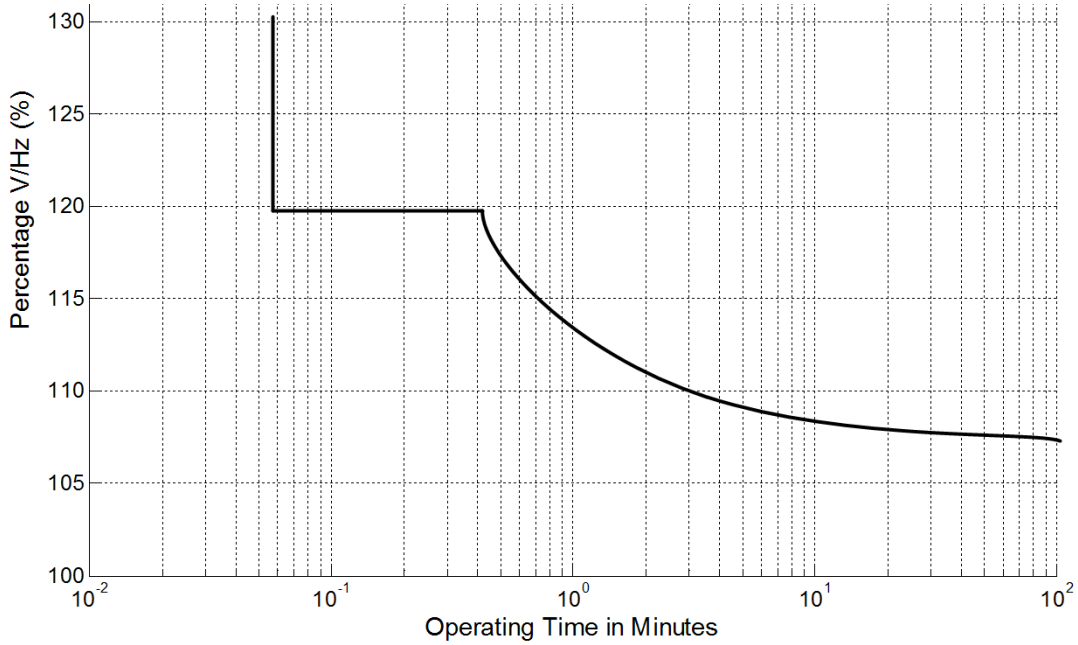

Figure 7 - 2. Transformer time characteristic related to volts-over-hertz.

7.2 Event One: Transformer Energization

In this event, transformer energization is presented. Breakers B1 and B2 are

initially open while the breaker B3 is closed. At time t = 5.2s the breaker B1 is suddenly closed and the transformer is energized, as shown in Figure 7-3.

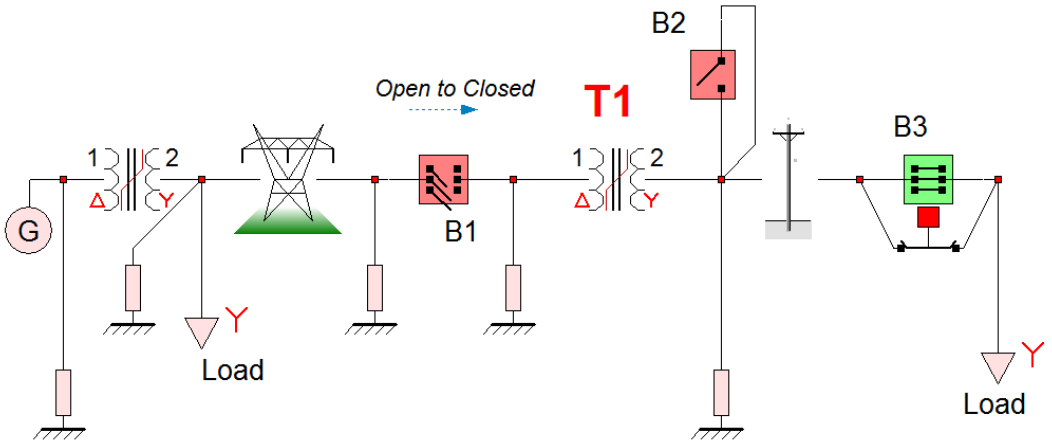

Figure 7 - 3. Transformer energization situation

The terminal voltages and currents in this event are shown in Figure 7-4 for the time period [5.10-5.30] seconds. Note that the first set of traces show the voltages at the two ends of the transformer and the second set of traces show the currents at the two sides of the transformer. Note obvious inrush currents occur on the primary side terminal currents when the breaker B1 is suddenly closed. The results of legacy protection functions as well as the proposed DSE-based method are presented next:

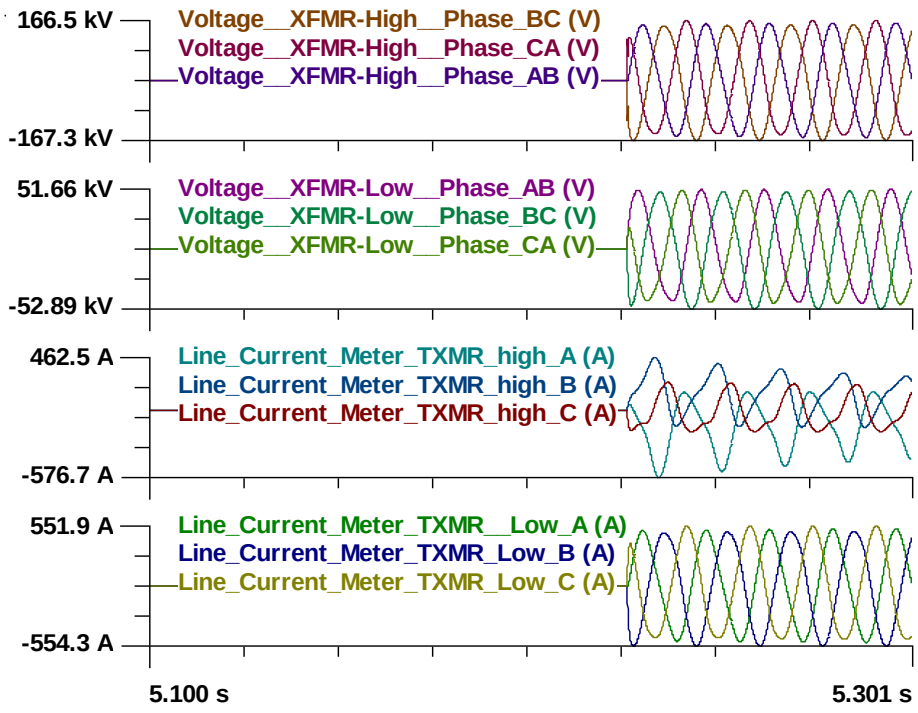

Figure 7 - 4. Terminal voltages and currents for transformer energization

(a) *Percentage Differential Protection*

The results of the percentage differential protection are shown in Figure 7-5. When the energization happens, because of the inrush currents, the operating current referring to the primary side is about 240 A, which is larger than the 10A setting. The restraining current is about 185A, and the differential percent is 141%, and it is also more than the 20% setting. Because both settings are exceeded, a tripping command is issued. As a consequence, the percentage differential function would falsely trip the transformer in this energization situations.

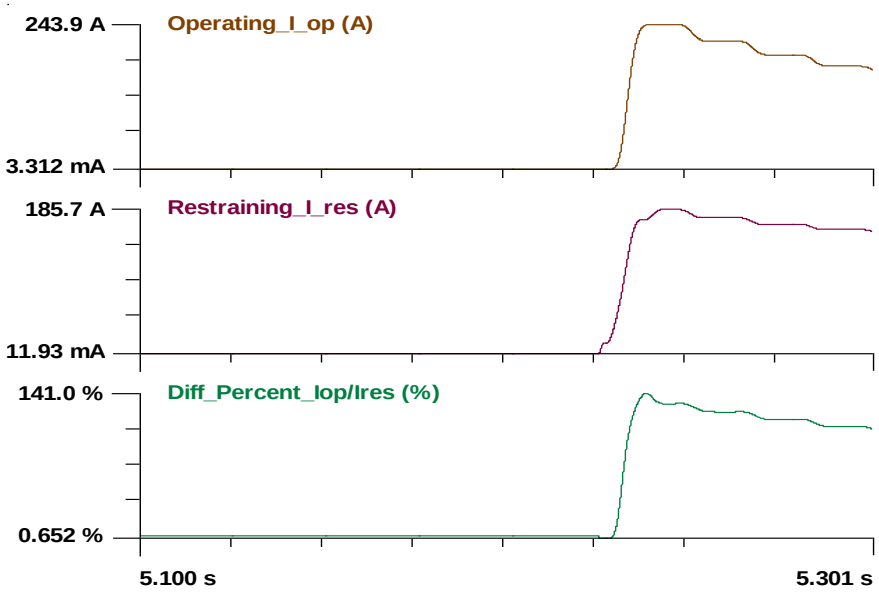

Figure 7 - 5. Percentage differential protection results for energization

(b) *Harmonic-restraint differential protection*

Except for the operating current, restraining current and differential percent, the harmonic-restraint differential function also monitors the second-harmonic of the operating-current, as shown in Figure 7-6. The values of operating current, restraining current and the differential percent are the same as those in Figure 7-5. The second-harmonic current is about 69A, and the measured second-harmonic level is 30%. This value is larger than the 20% setting. Therefore, the harmonic-restraint differential function would block trip signals, and the transformer would not be falsely tripped in this energization situation.

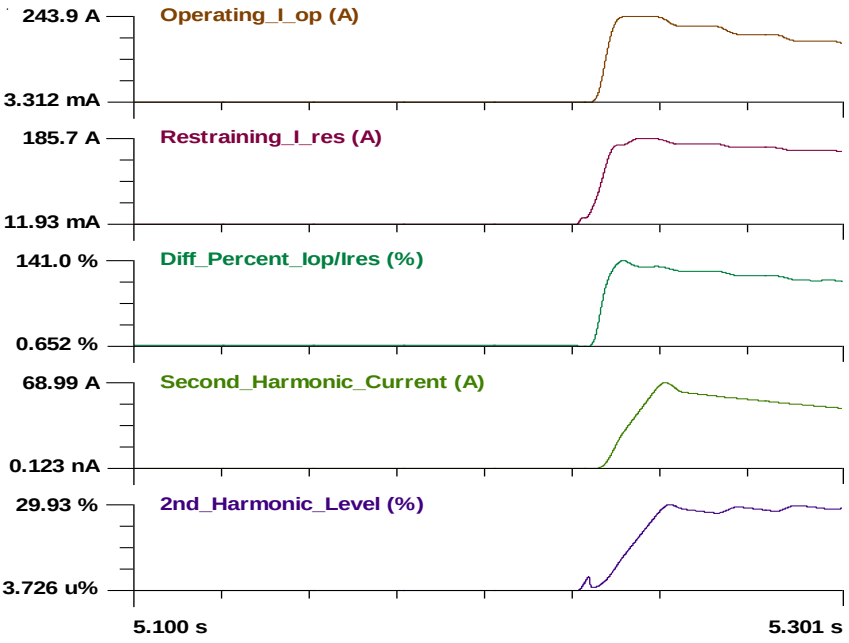

Figure 7 - 6. 2nd harmonic level for transformer energization

(c) *Negative-sequence differential protection*

The results of negative-sequence differential protection are shown in Figure 7-7. When the energization happens, the negative-sequence of operating current referring to the primary side is 95 A, which is higher than the 5 A setting. The negative-sequence restraining current is 104 A. The negative-sequence differential percent is 89%, which is also larger than the 20% setting. Because both settings are exceeded, a tripping command is issued. As a consequence, the negative-sequence differential function would falsely trip the transformer in this energization situations.

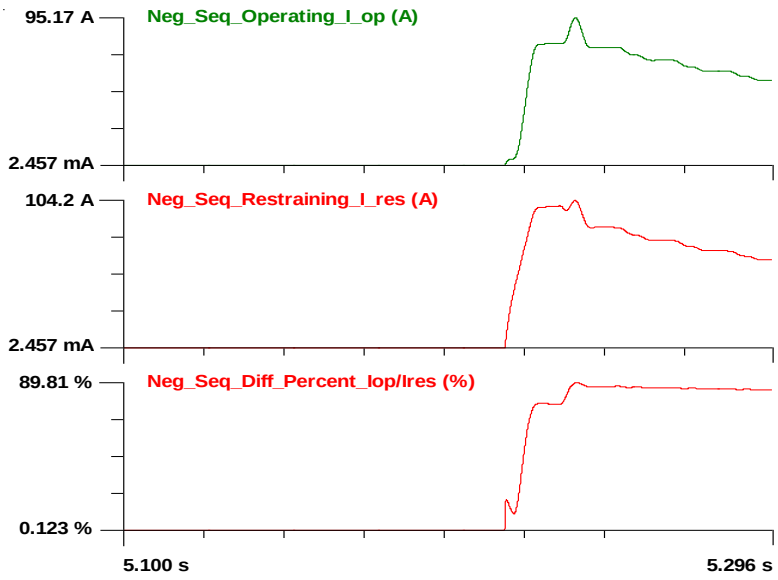

Figure 7 - 7. Negative-sequence differential protection results

(d) *Time-overcurrent protection*

The result of time-overcurrent protection is shown in Figure 7-8. The RMS value of transformer primary-side current is about 293 A and it is less than the setting (900A). Therefore, the transformer would not be falsely tripped by the time-overcurrent protection function in this energization situation.

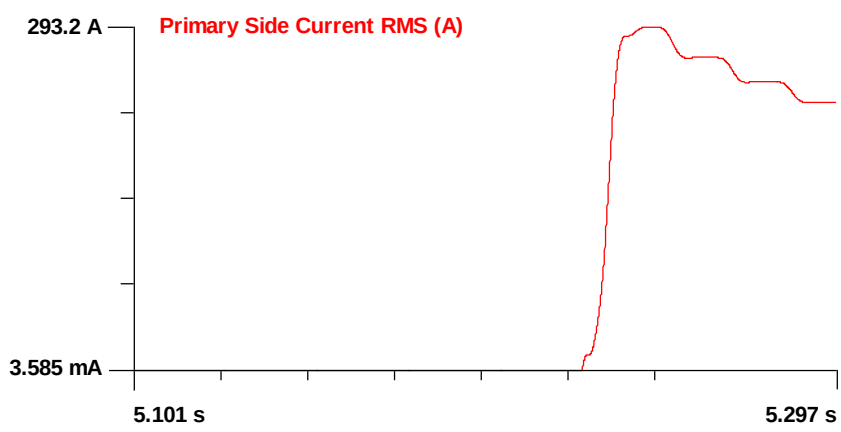

Figure 7 - 8. Time-overcurrent protection for transformer energization

(e) *Volts-over-hertz protection and thermal protection*

The volts-over-hertz protection function and thermal protection function are not for this situation.

(f) *Proposed DSE-based protection*

The results of proposed DSE-based protection scheme are shown in Figure 7-9. When the energization happens, the currents at both ends of transformer change from zero to large values. Though large inrush currents occur to the primary side terminal currents, the residuals of terminal currents remain at very small values. The chi-square value is also very small, while the confidence level stays around 100%. This high confidence level means there is nothing wrong inside the transformer so that the DSE-based protection scheme will not falsely trip the transformer, thus avoiding the mis-operation under energization situations.

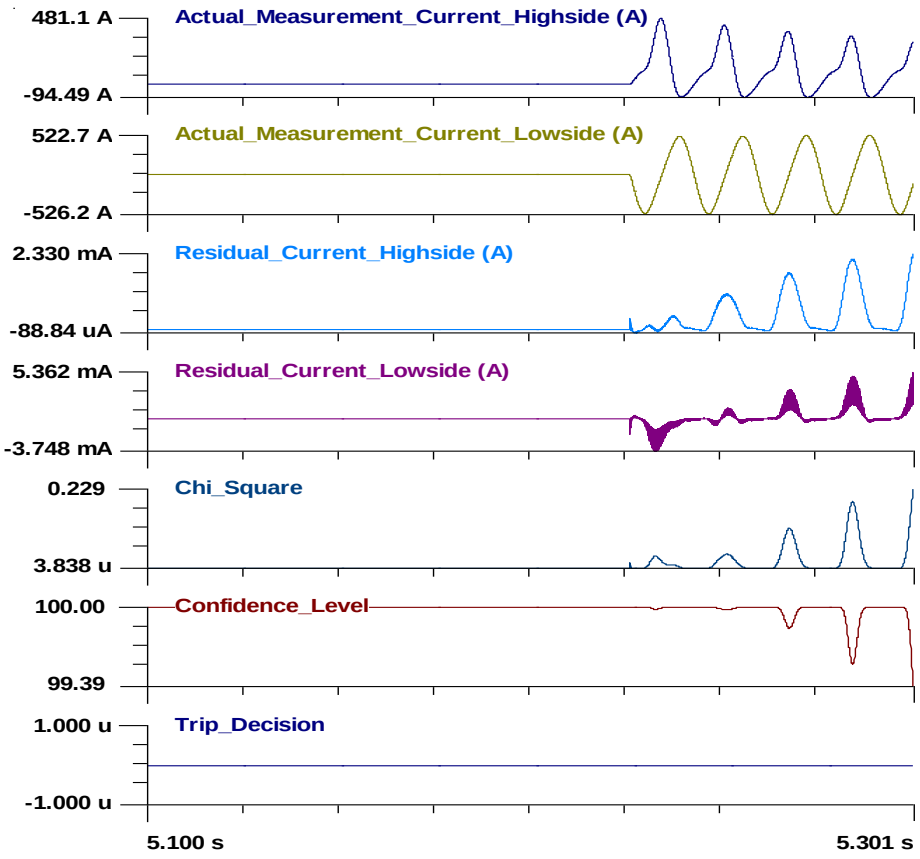

Figure 7 - 9. Proposed DSE-based protection for transformer energization

(h) *Summary of Event One*

A summary of the protection method results for Event One is shown in Table 7-1. In this event with transformer energization, some legacy functions such as the percentage differential and negative-sequence differential protection methods tend to falsely trip the transformer, which means they are insecure. In contrast, proposed DSE-based method guarantees 100% security when transformer is energized in this event.

Table 7 - 1. Summary of Event One: Energization

Protection Methods	Falsely Trip	
Percentage differential	Yes	Insecure
Harmonic-restraint differential	No	Secure
Negative-sequence differential	Yes	Insecure
Time-overcurrent	No	Secure
Volts-over-hertz	NA	NA
Thermal	NA	NA
Proposed DSE-based	No	Secure

7.3 Event Two: Secondary Side Coil Fault, 5% from Neutral

In this event an internal fault happens to the transformer. Breakers B1 and B3 are initially closed while the breaker B2 is open. At time t = 20.20s the breaker B2 is suddenly closed and a 5% coil-neutral fault happens to the phase A of secondary windings, as shown in Figure 7-10.

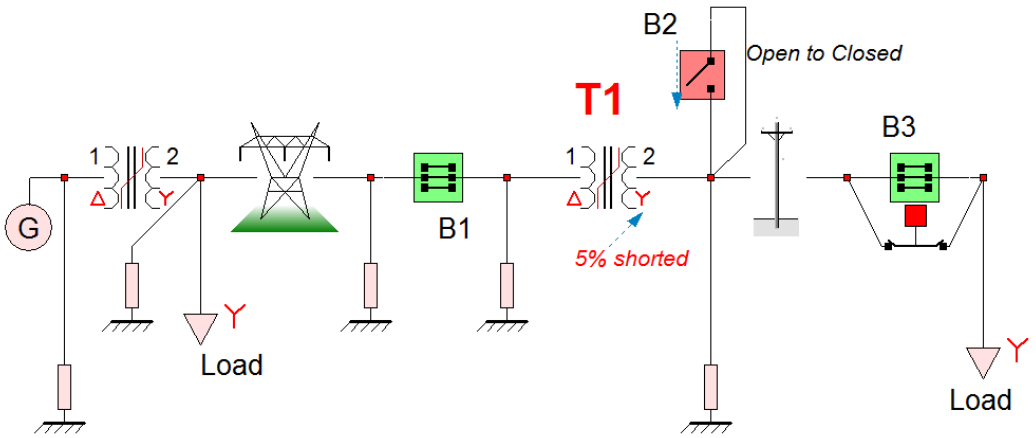

Figure 7 - 10. Transformer 5% fault near neutral situation

The terminal measurements are shown in Figure 7-11 for the time period [21.07-21.30] seconds. Note the first set of traces show the voltages at the two ends of the transformer and the second set of traces show the currents at the two sides of the transformer. Note that very little change occurs to the terminal voltages and currents due to this internal fault. The results of legacy protection functions as well as the proposed method are presented next:

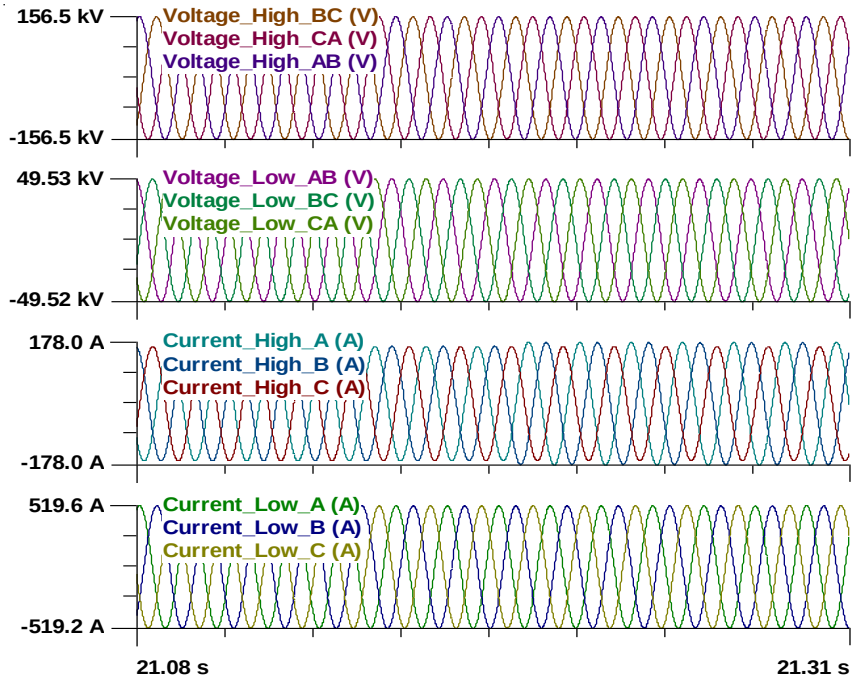

Figure 7 - 11. Terminal voltages and currents for transformer internal faults

(a) *Percentage Differential Protection*

The results for percentage differential protection are shown in Figure 7-12. When the internal fault happens, the operating-current referring to the primary side is about 6.51 A, which is smaller than the 10 A setting. The restraining current is about 121 A. The differential percent is 5.4%, and it is also less than the 20% setting. Because neither setting is exceeded, the percentage differential function would not send a trip signal, so the transformer is not protected by this function regarding this internal fault.

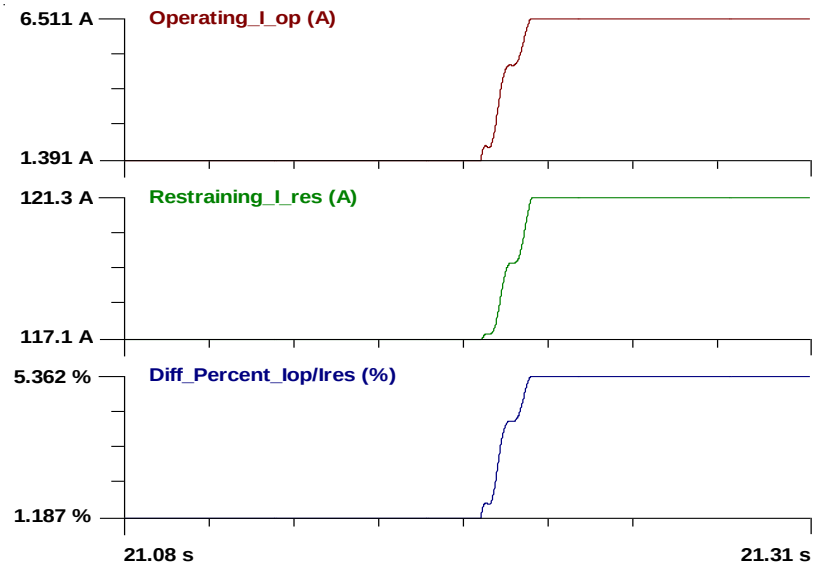

Figure 7 - 12. Percentage differential protection results

(b) *Harmonic-restraint differential protection*

The results of the harmonic-restraint differential protection are shown in Figure 7-13. The values of operating current, restraining current and the differential percent are the same as those in Figure 7-12. The second-harmonic current is about 1.36A. The measured second-harmonic level is around 22%, which is almost the same as the setting. However, because the other settings are not exceed, no trip signal will be sent. Therefore, the transformer is not protected by the harmonic-restraint differential function regarding this internal fault.

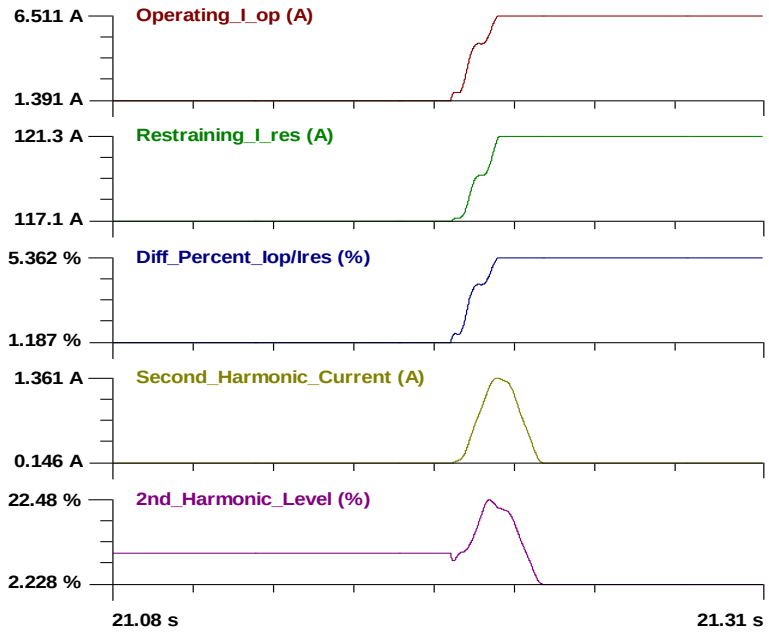

Figure 7 - 13. 2nd harmonic level for transformer internal faults

(c) *Negative-sequence differential protection*

The results for negative-sequence differential protection are shown in Figure 7-14. When the fault happens, the negative-sequence operating-current is 5.4 A (larger than setting). The negative-sequence restraing current is 6.84A and the negative-sequence differential percent is 66% (larger than setting). Because both settings are exceeded, a trip signal will be sent. Therefore, the negative-sequence differential function is able to protect the transformer against this internal fault. This function detects the fault at 21.206 s and it will trip the transformer at 21.216 s.

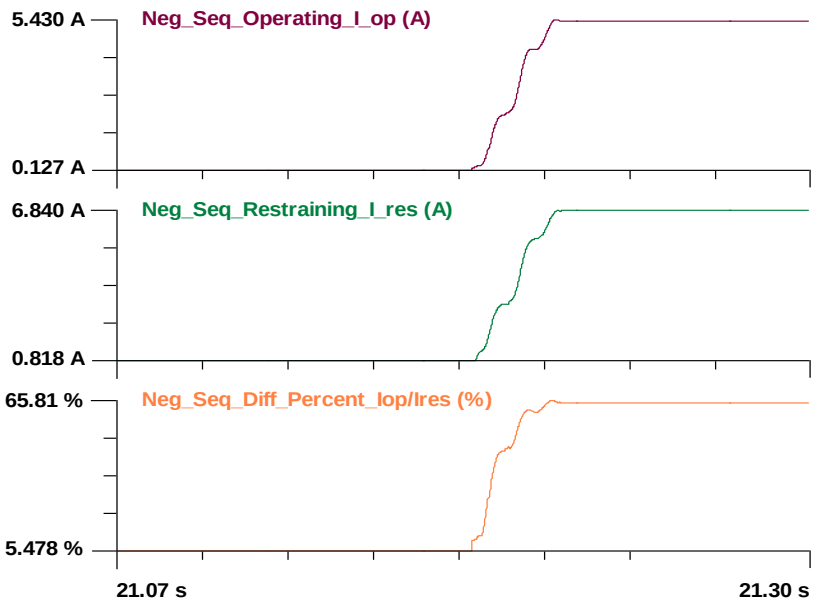

Figure 7 - 14. Negative-sequence differential protection results

(d) *Time-overcurrent protection*

The result of time-overcurrent protection is shown in Figure 7-15. The RMS value of transformer primary-side current is about 126 A when the fault happens. This value is less than the setting (900A) so no trip signal is sent. Therefore, the time-overcurrent scheme would fail to protect the transformer.

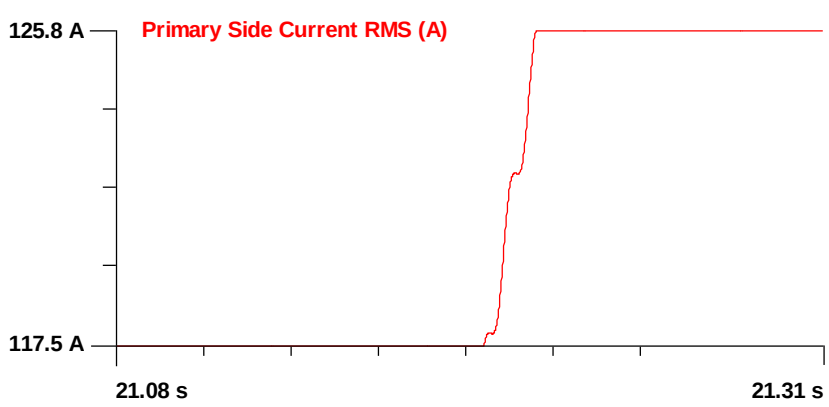

Figure 7 - 15. Time-overcurrent protection for transformer internal faults

(e) *Volts-over-hertz protection and thermal protection*

The volts-over-hertz protection function and thermal protection function are not for this situation.

(f) *Proposed DSE-based protection*

The results of proposed DSE-based protection are shown in Figure 7-16. When the internal fault happens, there are not obvious changes in the terminal currents. However, the residuals of terminal currents increase from zero to considerable values. The chi-square value also increase from zero to 152, while the confidence level drops from 100% to zero immediately. This zero confidence level indicates abnormalities inside the transformer and protection actions would be taken. It is noticed that confidence level is oscillating during the fault period since the internal fault is too small. An integral function is applied to accumulate the confidence level values and a trip decision is taken to protect the transformer, as shown in the figure. The DSE-based protection scheme detects the faults at 21.2002 s and it trips the transformer at 21.2082 s.

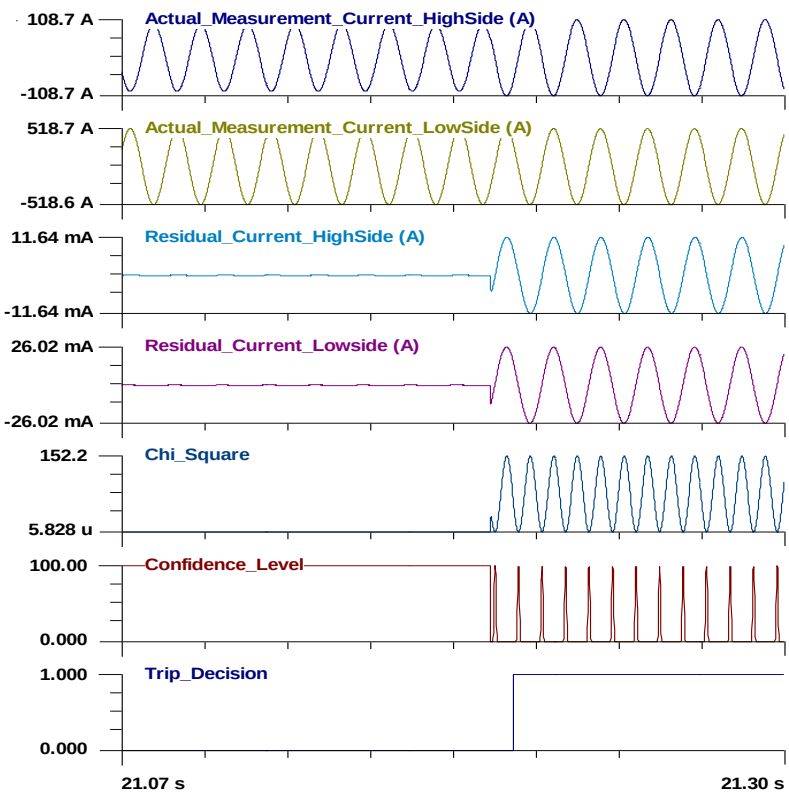

Figure 7 - 16. Proposed DSE-based protection for transformer internal faults

(h) ***Summary of Event Two***

A summary of the protection method results for Event Two is shown in Table 7-2. In this event where a fault near neutral happens, none of the legacy function could successfully detect the existence of fault except for the negative-sequence differential function, which means most of them are undependable. In contrast, the proposed DSE-based scheme is able to detect it dependably. Moreover, the speed of the proposed scheme is much faster than that of negative-sequence differential function.

Table 7 - 2. Summary of Event Two: Internal Fault

Protection Methods	Trip	
Percentage differential	No	Undependable
Harmonic-restraint differential	No	Undependable
Negative-sequence differential	Yes	Dependable
Time-overcurrent	No	Undependable
Volts-over-hertz	NA	NA
Thermal	NA	NA
Proposed DSE-based	Yes	Dependable

7.4 Event Three: 5% Secondary Side Coil Fault during Energization

In this event the transformer energization happens first, following an internal fault. Breakers B1 and B2 are initially open while the breaker B2 is closed. At time t = 1.31s the B1 is suddenly closed and the transformer is energized. One cycle later at time t = 1.326s, the breaker B2 is also closed and a 5% coil-neutral fault happens to the phase

A of secondary windings, as shown in Figure 7-17.

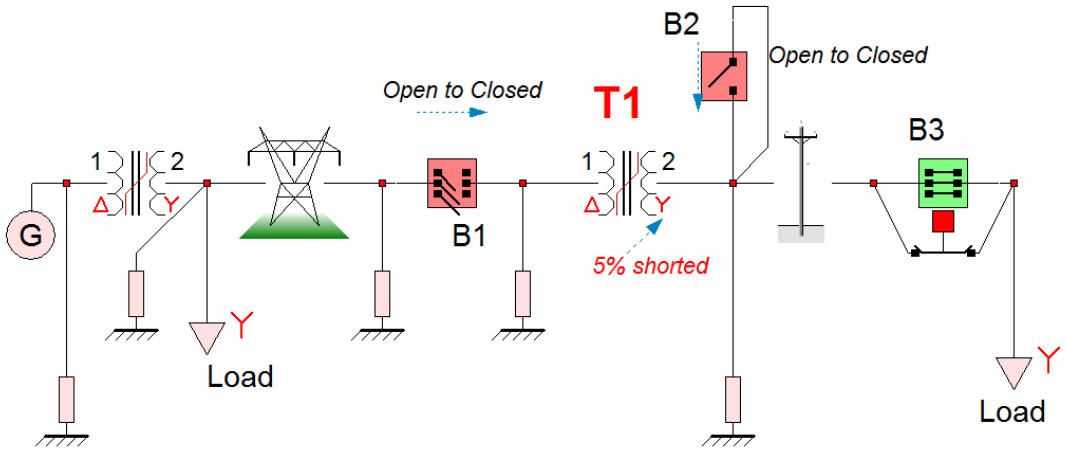

Figure 7 - 17. Transformer 5% fault during transformer energization

The terminal measurements are shown in Figure 7-18 for the time period [1.23-1.38] seconds. Note that the first set of traces show the voltages at the two ends of the transformer and the second set of traces show the currents at the two sides of the transformer. Note obvious inrush currents occur on the primary side terminal currents when the energization happens. The results of legacy protection functions as well as the proposed method are presented next:

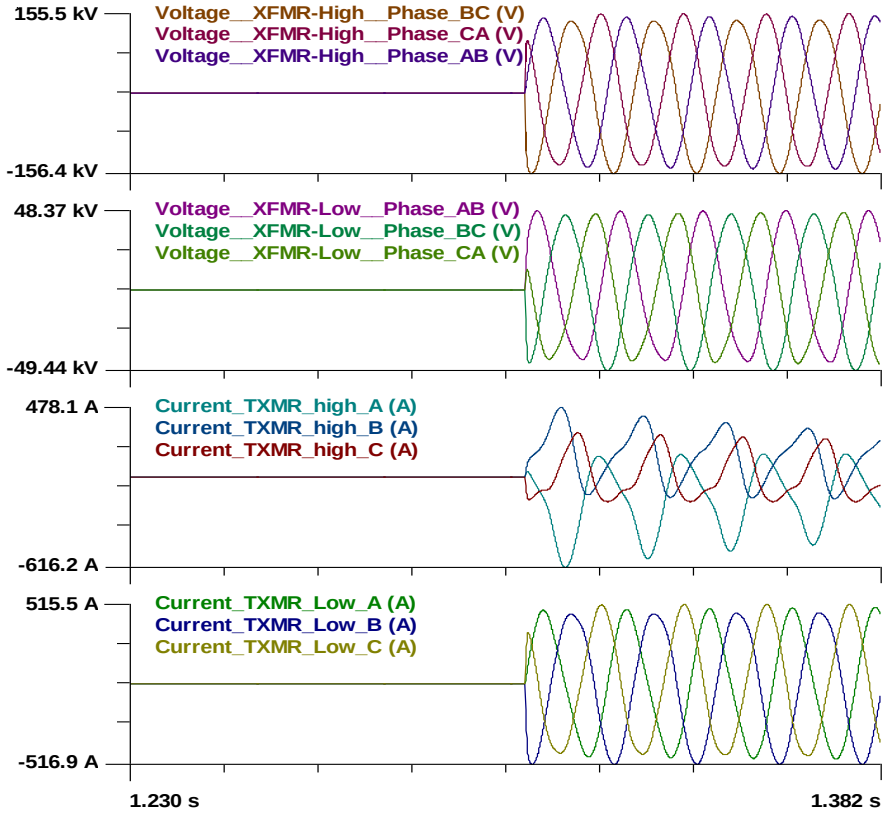

Figure 7 - 18. Terminal voltages and currents for transformer internal faults under energization

(a) *Percentage Differential Protection*

The results of the percentage differential protection are shown in Figure 7-19. When the energization happens, the operating current is about 278 A, which is larger than the 10A setting. The restraining current is about 190A. The differential percent is 154%, and it is also more than the 20% setting. Because both settings are exceeded, a tripping command is issued and transformer will be falsely tripped because of the energization.

One cycle later when the internal fault happens, there are not much change to the above values, thus the tripping decision is still effective. Though the percentage differential function would send a trip signal, it does not necessary mean this function is able to detect the internal fault. The large operating current and high different percent

are actually caused by the inrush currents. The percentage differential function dose not perform the correct reaction regarding the transformer energization in this event.

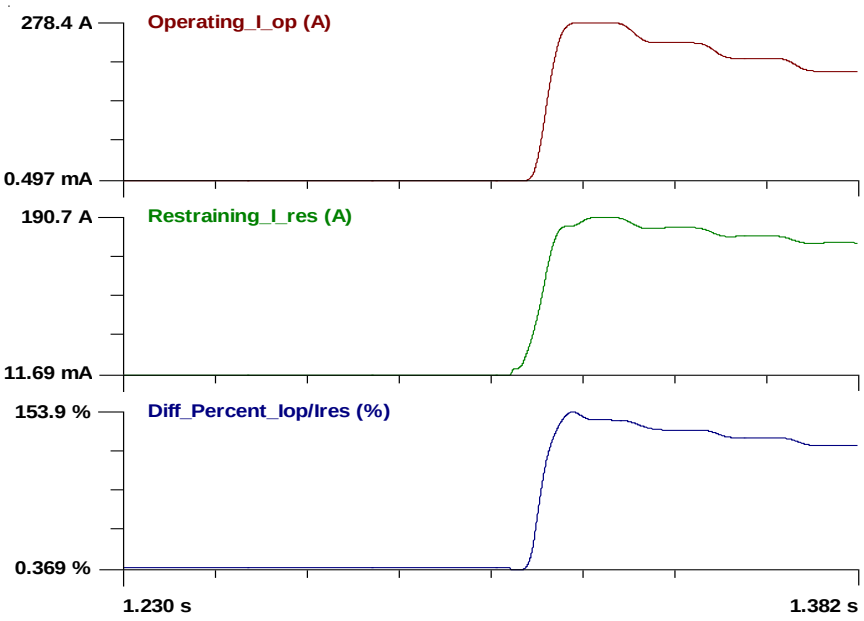

Figure 7 - 19. Percentage differential protection results for internal faults under energization

(b) *Harmonic-restraint differential protection*

Except for the operating-current, restraining-current and differential percent, the harmonic-restrained differential function also monitors the second-harmonic of the operating-current, as shown in Figure 7-20. The values of operating current, restraining current and the differential percent are the same as those in Figure 7-19. The second-harmonic current is about 72 A, and the measured second-harmonic level is 27% (larger than setting). Therefore, the harmonic-restrained differential function will block any false trip during transformer energization in this event.

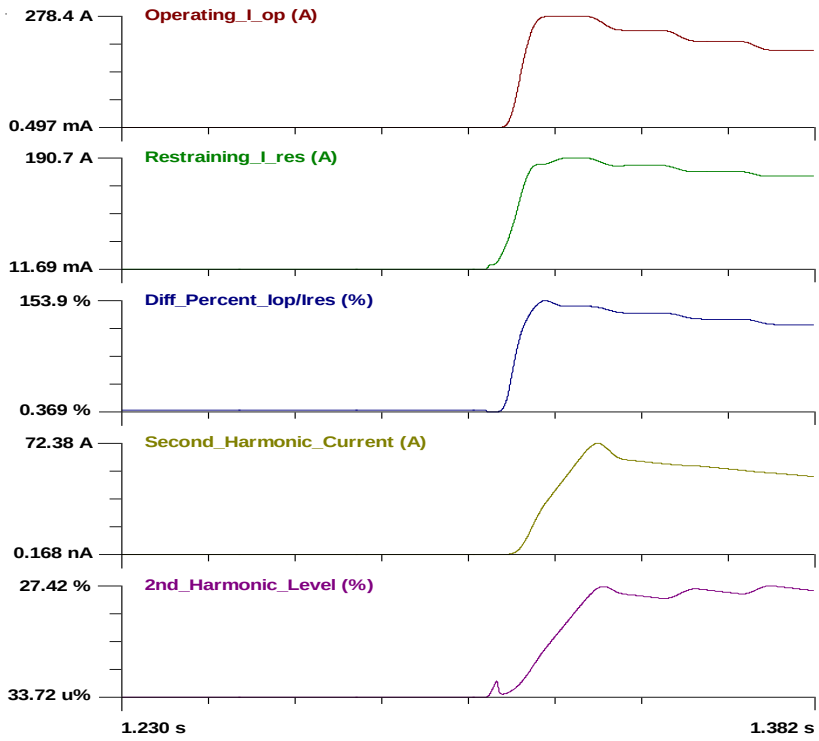

Figure 7 - 20. 2nd harmonic level for internal faults under energization

One cycle later when the internal fault happens, there are no much change to the above values. Therefore, any trip signal will be still blocked, even when the internal fault happens. As a consequence, the transformer is not protected when the internal fault happens in this situation.

(c) *Negative-sequence differential protection*

The results of negative-sequence differential protection are shown in Figure 7-21. When the energization happens, the negative-sequence operating-current is 100 A, which is higher than the 5 A setting. The negative-sequence restraining current is 108 A. The negative-sequence differential percent is 91%, which is also larger than the 20% setting. Therefore, the negative-sequence differential protection would falsely trip the transformer when the energization happens in this event.

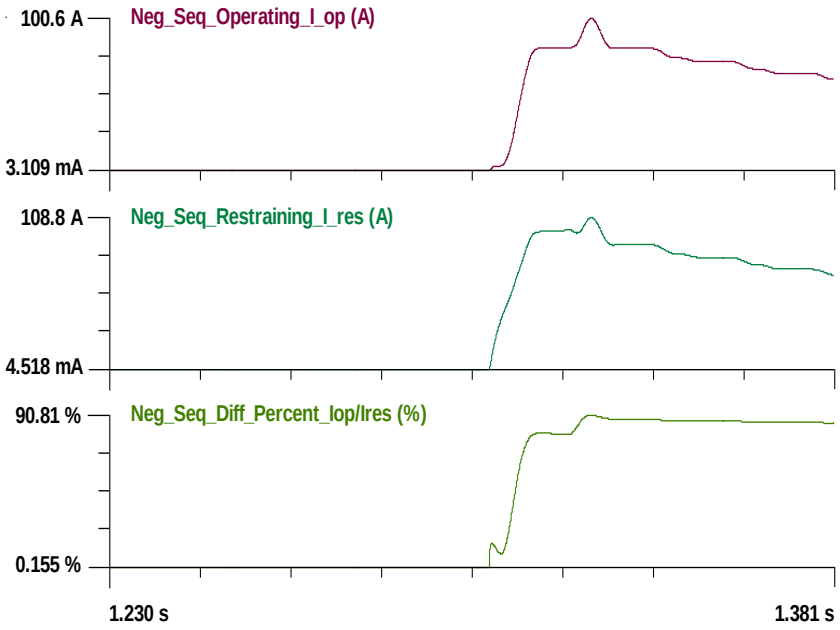

Figure 7 - 21. Negative-sequence differential protection results

One cycle later when the internal fault happens, there are not much change to the above values. So this function would trip the transformer when internal fault happens. However, this function dose not perform the correct reaction for transformer energization in this event. Moreover, if the harmonic-restraint differential protection function is also implemented, the trip signal would be blocked (the reason has been explained in the former protection function) and the transformer would not be protected.

(d) *Time-overcurrent protection*

The result of time-overcurrent protection is shown in Figure 7-22. When the energization happens, the RMS value of transformer primary-side current is about 317 A and it is less than the setting (900A). Therefore, the transformer would not be falsely protected during energization. When the internal fault happens, the RMS value is still below the setting. Therefore it cannot protect the transformer for the internal fault in this event.

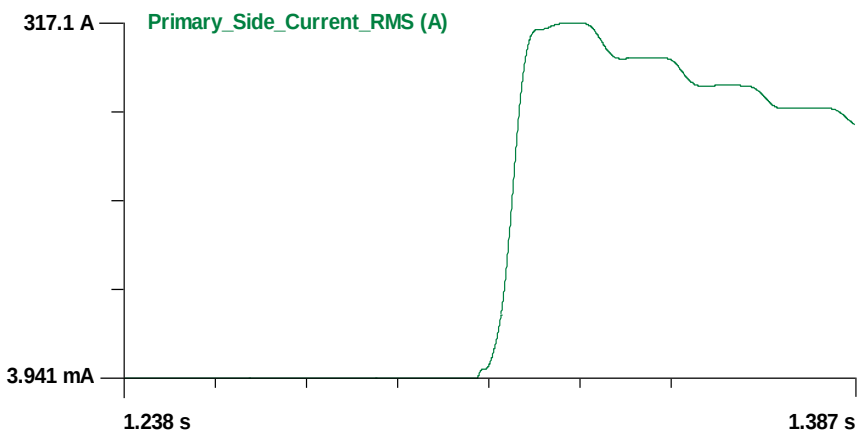

Figure 7 - 22. Time-overcurrent protection for internal faults under energization

(e) *Volts-over-hertz protection and thermal protection*

The volts-over-hertz protection function and thermal protection function are not for this situation.

(f) *Proposed DSE-based protection*

The results of proposed DSE-based protection scheme are shown in Figure 7-23. At first, when the energization happens, the currents at both ends of transformer change from zero to large values. Though a large inrush current occurs to the primary side terminal current, the residuals of terminal currents remains at very small values. The chi-square value is small and the confidence level stays around 100%. This high confidence level means there is nothing wrong inside the transformer during the first cycle. The DSE-based protection scheme will not falsely trip the transformer, thus avoiding the mis-operation under energization situations.

One cycle later when the internal fault happens, there are not much change at the terminal currents and the inrush current still exists. However, the residuals of terminal currents change from zero to considerable values. The chi-square value also increase

from zero to 139, while the confidence level drops from 100% to zero immediately. This zero confidence level indicates abnormalities inside the transformer and protection actions would be taken. It is noticed that confidence level is oscillating during the fault period since the internal fault is too small. An integral function is applied to accumulate the confidence level values and a trip decision is taken to protect the transformer, as shown in the figure. The DSE-based protection scheme makes the correct response for both the energization period and internal fault period in this event. It detects the fault at 1.3262 s and trips the transformer at 1.3342 s.

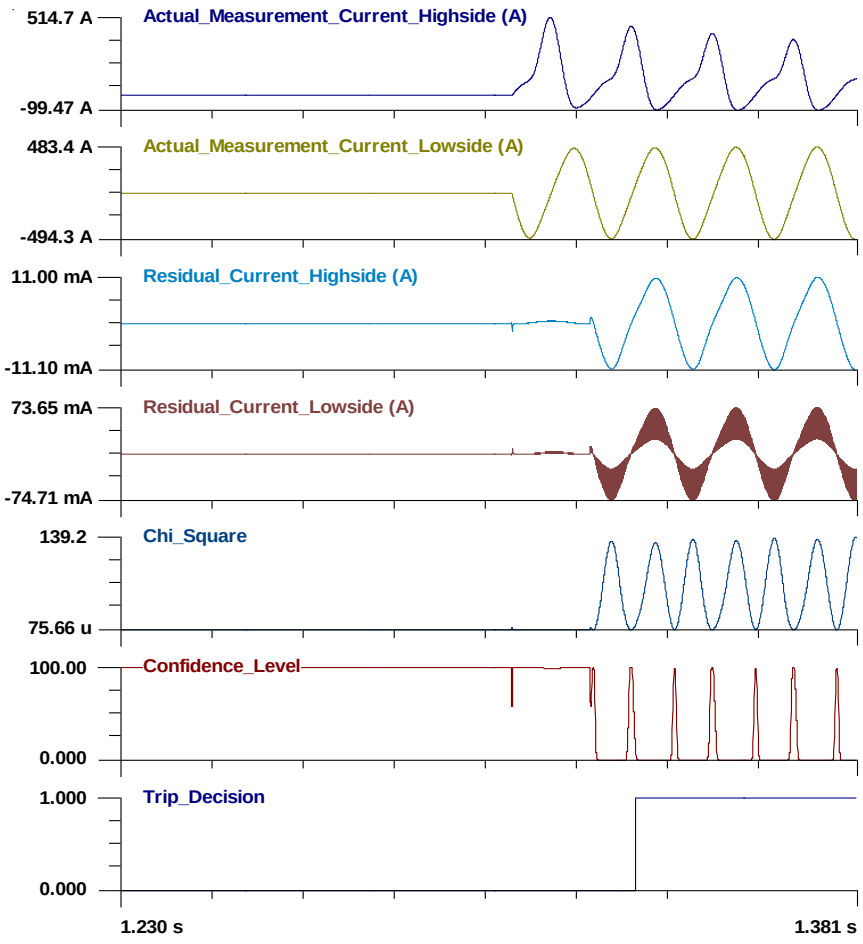

Figure 7 - 23. Proposed DSE-based protection for internal faults under energization

(h) ***Summary of Event Three***

A summary of the protection method results for Event Three is shown in Table 7-3. In this event where both internal fault and transformer energization happen in a short time interval, none of the legacy function could successfully make the right response for both situation. In contrast, the proposed scheme is able to stay inactive during transformer energization, while making the right trip decision when it detect the existence of internal fault with high dependability and sensitivity. Moreover, the speed of the proposed scheme is so fast that it can trip the transformer before the fault escalate to more server situation.

Table 7 - 3. Summary of Event Three: Energization and Internal Fault

Protection Methods	**Falsely Trip at Energization**	**Correct Trip at Internal Fault**	
Percentage differential	Yes	Yes	Insecure
Harmonic-restraint differential	No	No	Undependable
Negative-sequence differential	Yes	Yes	Insecure
Time-overcurrent	No	No	Undependable
Volts-over-hertz	NA	NA	NA
Thermal	NA	NA	NA
Proposed DSE-based	No	Yes	Secure and Dependable

7.5 Event Four: Transformer 1% Inter-turn Fault

In this event a transformer inter-turn fault is presented. Breakers B1 and B3 are

initially closed while the breaker B2 is open. At time t = 30.20s the breaker B2 is suddenly closed and a 1% inter-turn fault happens to the phase A of transformer secondary side windings, as shown in Figure 7-24.

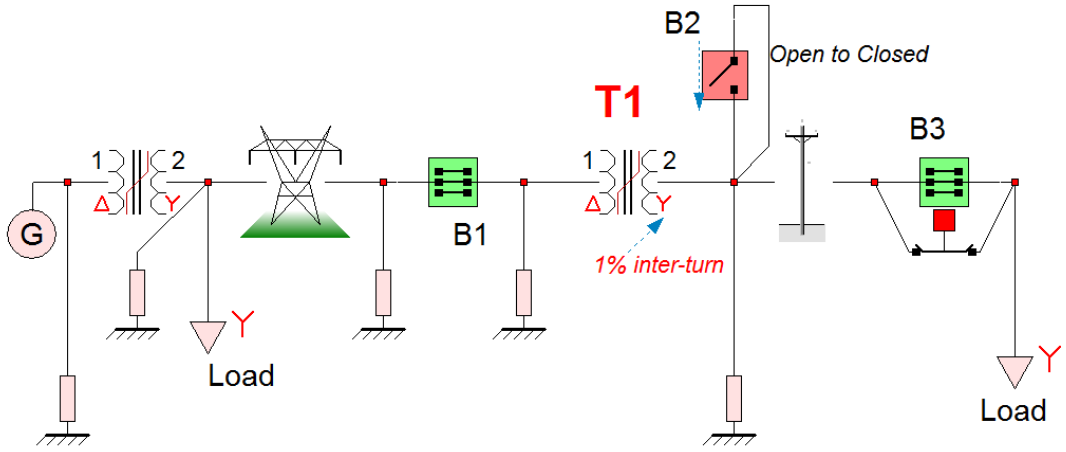

Figure 7 - 24. Transformer 1% inter-turn fault situation

The terminal measurements are shown in Figure 7-25 for the time period [30.10-30.27] seconds. Note that the first set of traces show the voltages at the two ends of the transformer and the second set of traces show the currents at the two sides of the transformer. Note that very little change occurs to the terminal voltages and currents due to this inter-turn fault. The results of legacy protection functions as well as the proposed method are presented next.

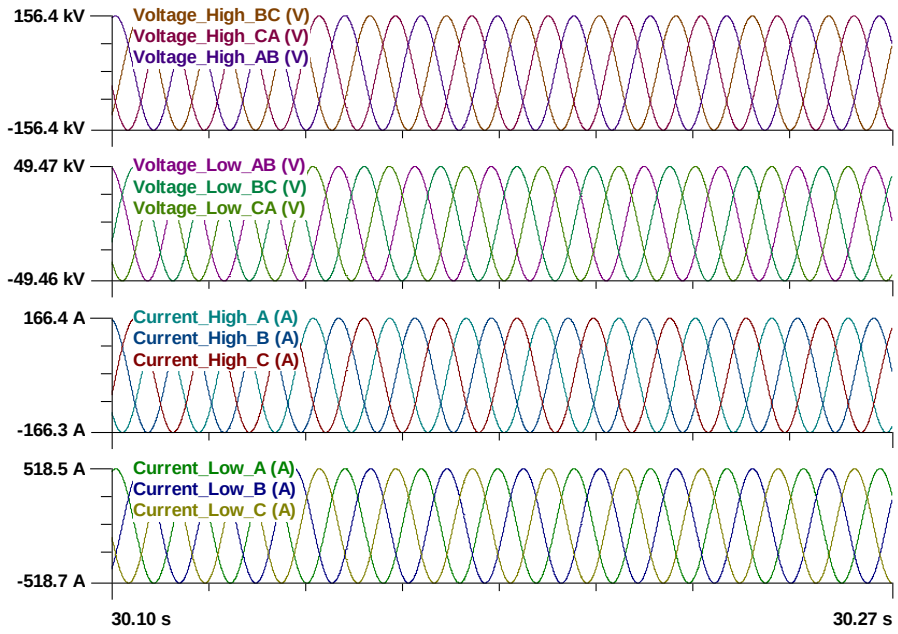

Figure 7 - 25. Terminal voltages and currents for transformer internal faults

(a) *Percentage Differential Protection*

The results for percentage differential protection are shown in Figure 7-26. When the internal fault happens, the operating-current is about 0.52 A, which is smaller than the 10 A setting. The restraining current is about 123A. The differential percent is 0.43%, and it is also less than the 20% setting. Because neither setting is exceeded, the percentage differential function would not send a trip signal, so the transformer is not protected by this function regarding this inter-turn fault.

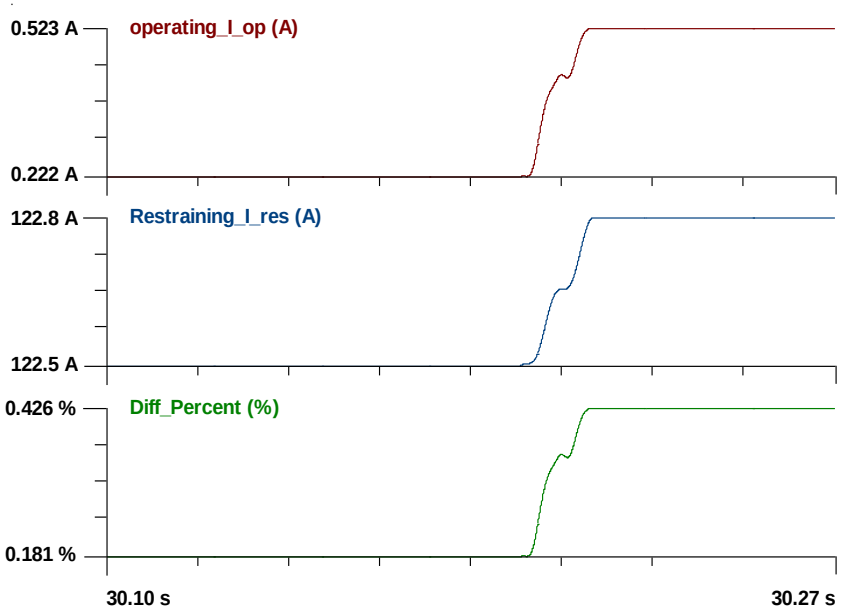

Figure 7 - 26. Percentage differential protection results

(b) *Harmonic-restrained differential protection*

Except for the operating-current, restraining-current and differential percent, the harmonic-restrained differential function also monitors the second-harmonic of the operating-current, as shown in Figure 7-27. The values of operating current, restraining current and the differential percent are the same as those in Figure 7-26. The second-harmonic of operating current is about 0.07A, and the measured second-harmonic level is around 16%, which is smaller than the setting. Because neither setting is exceeded, no trip signal will be sent when the inter-turn fault happens. Therefore, the transformer is not protected by the harmonic-restrained differential function regarding the inter-turn fault in this event.

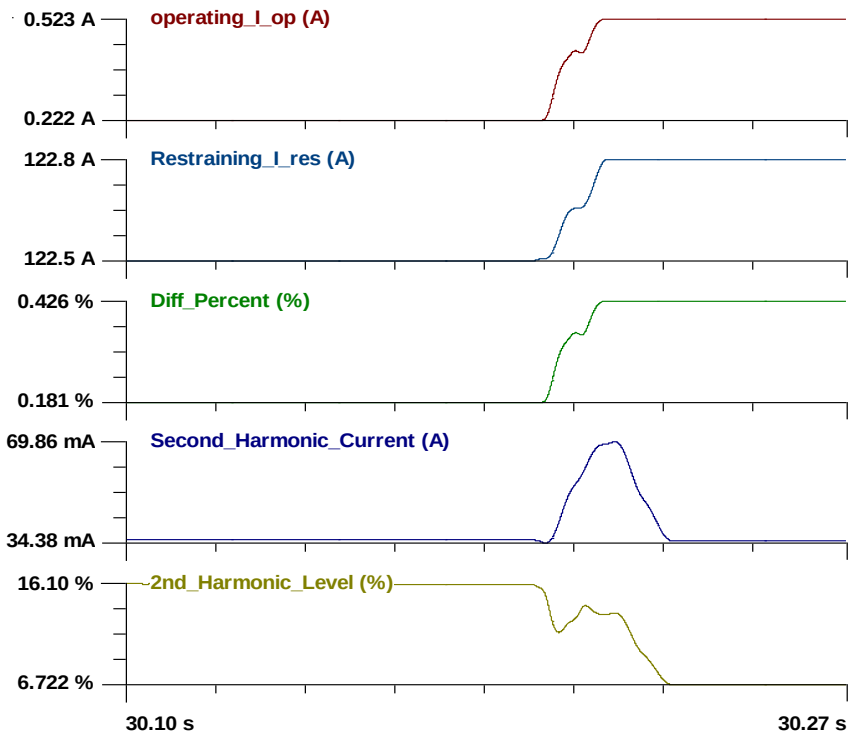

Figure 7 - 27. 2nd harmonic level for transformer internal faults

(c) *Negative-sequence differential protection*

The results for negative-sequence differential protection are shown in Figure 7-28. When the inter-turn fault happens, the negative operating-current is about 0.243 A, which is smaller than the 0.75 A setting. The negative-sequence restraining current is 1.81 A. The negative sequence differential percent is 14.68%, and it is also less than the 20% setting. Because neither setting is exceeeded, no trip signal would be sent. Therefore, the transformer is not protected by the negative-sequence differential function regarding the inter-turn fault in this event.

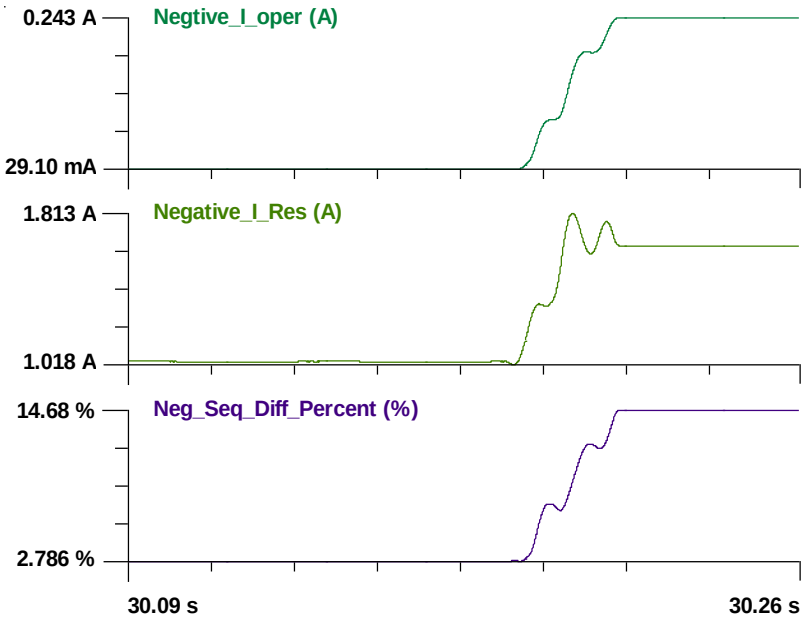

Figure 7 - 28. Negative-sequence differential protection results

(d) *Time-overcurrent protection*

The result of time-overcurrent protection is shown in Figure 7-29. The RMS value of transformer primary-side current is about 122 A when the fault happens. This value is less than the setting (900A) so no trip signal is sent. Therefore, the time-overcurrent scheme would fail to protect the transformer regarding the inter-turn fault in this event.

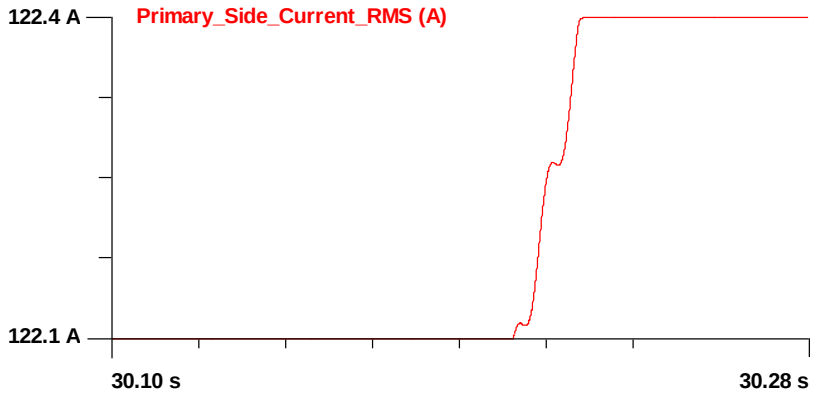

Figure 7 - 29. Time-overcurrent protection for transformer internal faults

(e) *Volts-over-hertz protection and thermal protection*

The volts-over-hertz protection function and thermal protection function are not for

this situation.

(f) *Proposed DSE-based protection*

The results of proposed DSE-based protection are shown in Figure 7-30.

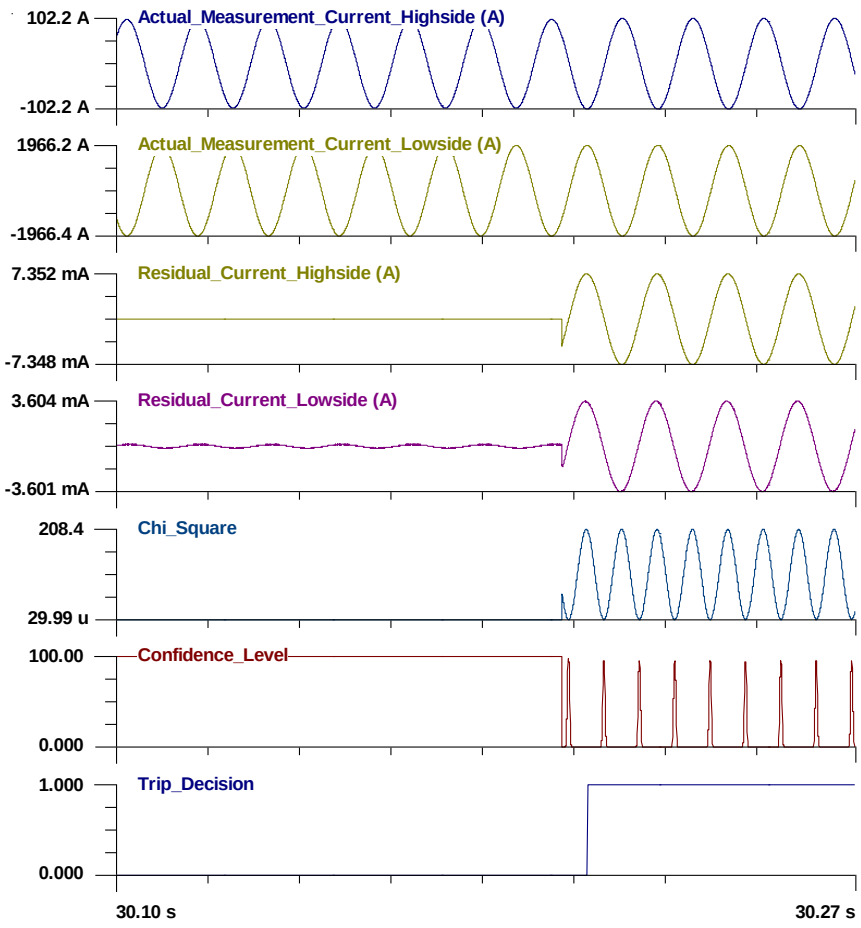

Figure 7 - 30. Proposed DSE-based protection for transformer internal faults

When the inter-turn fault happens, there are not obvious changes in the terminal currents. However, the residuals of terminal currents increase from zero to considerable values. The chi-square goes from a very small value to 208, while the confidence level drops from 100% to zero immediately. This zero value indicates abnormalities inside the transformer and protection actions would be taken as soon as possible. It is noticed that confidence level is oscillating during the fault period because the fault is too small. An integral function is applied to accumulate the confidence level values, and a trip

decision is taken to protect the transformer. It detects the fault at 30.2002 s and trips the transformer at 30.2082 s.

(h) ***Summary of Event Four***

A summary of the protection method results for Event Four is shown in Table 7-4. In this event where a 1% inter-turn fault happens, none of the legacy function could successfully detect the existence of fault. In contrast, the proposed scheme is able to detect it dependably with high sensitivity. Moreover, the speed of the proposed scheme is very fast and it only take 0.2ms to detect the existence of fault.

Table 7 - 4. Summary of Event Four: Internal Fault

Protection Methods	Trip	
Percentage differential	No	Undependable
Harmonic-restraint differential	No	Undependable
Negative-sequence differential	No	Undependable
Time-overcurrent	No	Undependable
Volts-over-hertz	NA	NA
Thermal	NA	NA
Proposed DSE-based	Yes	Dependable

7.6 Event Five: Auto-Transformer 1% Fault near Neutral

In this event, the regular transformer T1 is replaced with an auto-transformer T2

(the capacity and voltage ratings are unchanged). Breakers B1 and B3 are initially closed while the breaker B2 is open. At time t = 38.0s the breaker B2 is suddenly closed and a 1% fault near neutral happens to the phase B of transformer secondary side windings, as shown in Figure 7-31.

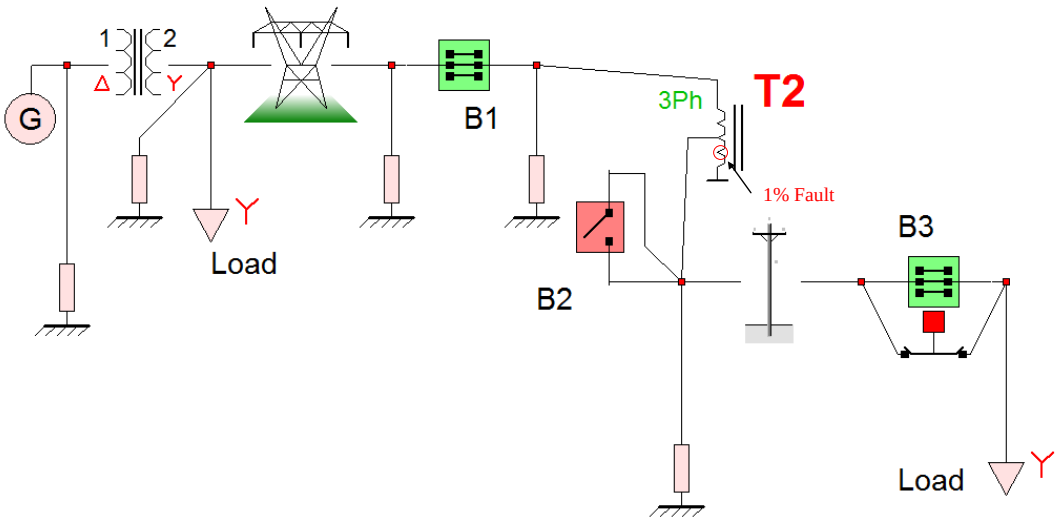

Figure 7 - 31. Autotransformer 1% inter-turn fault situation

The terminal measurements are shown in Figure 7-32 for the time period [37.90-38.05] seconds. Note that the first set of traces show the voltages at the two ends of the transformer and the second set of traces show the currents at the two sides of the transformer. Note that very little change occurs to the terminal voltages and currents due to this internal fault. The results of legacy protection functions as well as the proposed method are presented next.

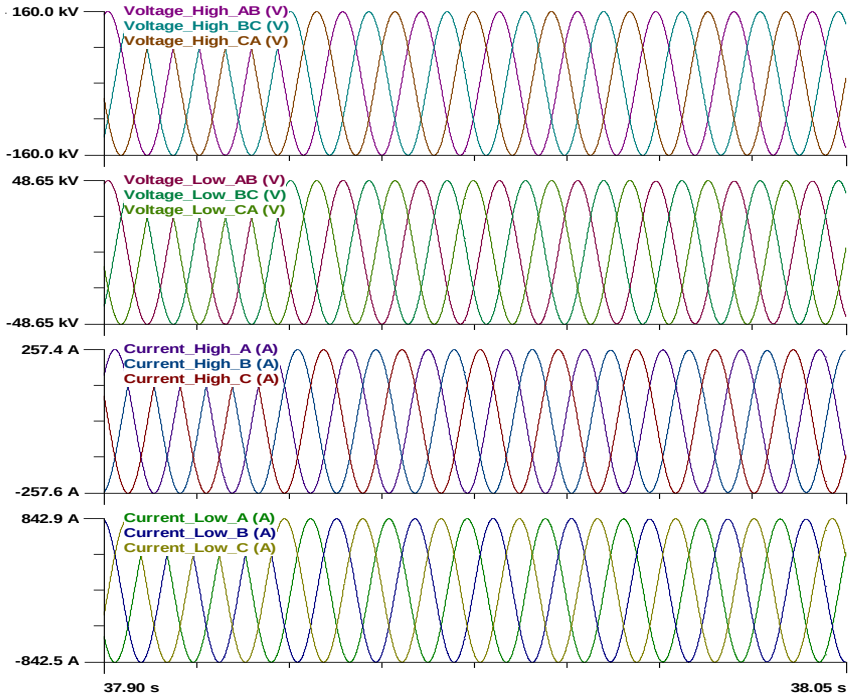

Figure 7 - 32. Terminal voltages and currents for auto-transformer internal faults

(a) *Percentage Differential Protection*

The results for percentage differential protection are shown in Figure 7-33. When the internal fault happens, the operating-current is about 0.75 A, which is smaller than the 10 A setting. The restraining current is about 180A. The differential percent is 0.41%, and it is also less than the 20% setting. Because neither setting is exceeded, the percentage differential function would not send a trip signal, so the transformer is not protected by this function regarding the internal fault in this event.

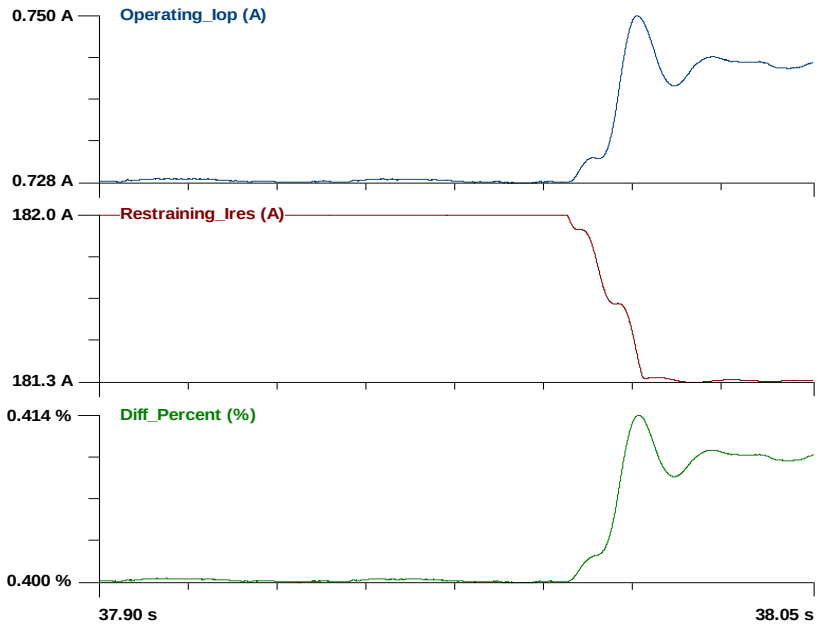

Figure 7 - 33. Percentage differential protection results

(b) *Harmonic-restrained differential protection*

Except for the operating-current, restraining-current and differential percent, the harmonic-restrained differential function also monitors the second-harmonic of the operating-current, as shown in Figure 7-34. The values of operating current, restraining current and the differential percent are the same as those in Figure 7-33. The second-harmonic current is about 3.8mA, and the measured second-harmonic level is around 0.5%, which is smaller than the setting. Because neither setting is exceeded, no trip signal will be sent. Therefore, the transformer is not protected by Harmonic-restrained differential function regarding the internal fault in this event.

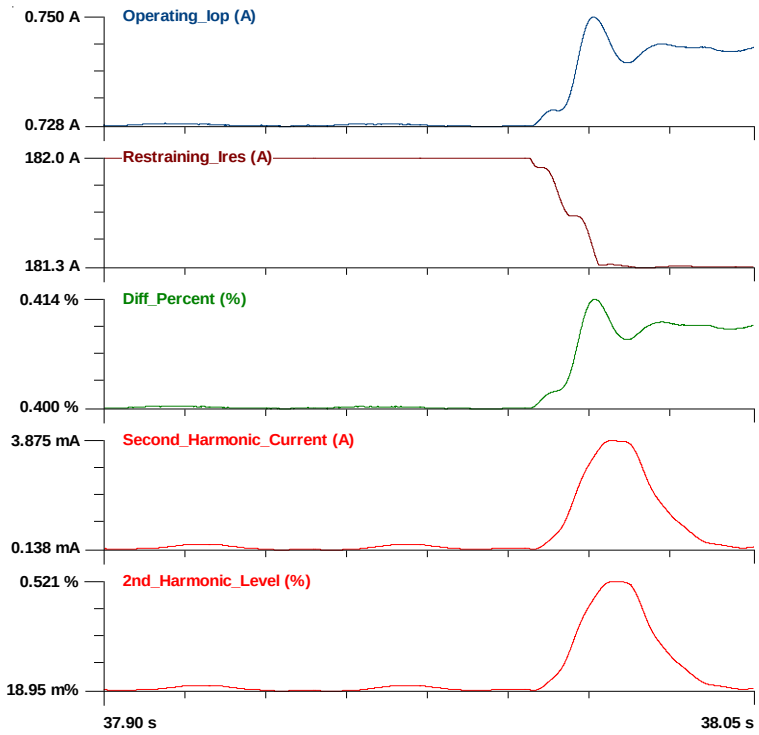

Figure 7 - 34. 2nd harmonic level for transformer internal faults

(c) *Negative-sequence differential protection*

The results for negative-sequence differential protection are shown in Figure 7-35. When the internal fault happens, the negative operating-current is about 0.54 A, which is a little smaller than the 0.75 A setting. The negative-sequence restraining current is 2.77 A. The negative sequence differential percent is 19.56%, and it is more or less the 20% setting. Because the minimun pickup current setting is not exceeeded, no trip signal would be sent. Therefore, the transformer is not protected by the negative-sequence differential function regarding the internal fault in this event.

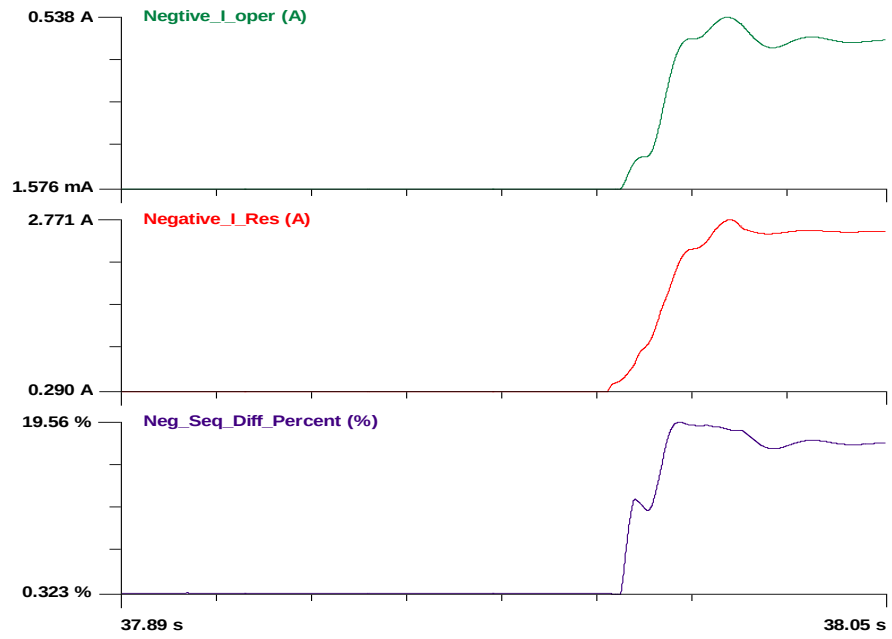

Figure 7 - 35. Negative-sequence differential protection results

(d) *Time-overcurrent protection*

The result of time-overcurrent protection is shown in Figure 7-36. The RMS value of transformer primary-side current is about 182 A when the fault happens. This value is less than the setting (900A) so no trip signal is sent. Therefore, the time-overcurrent scheme would fail to protect the transformer in this event.

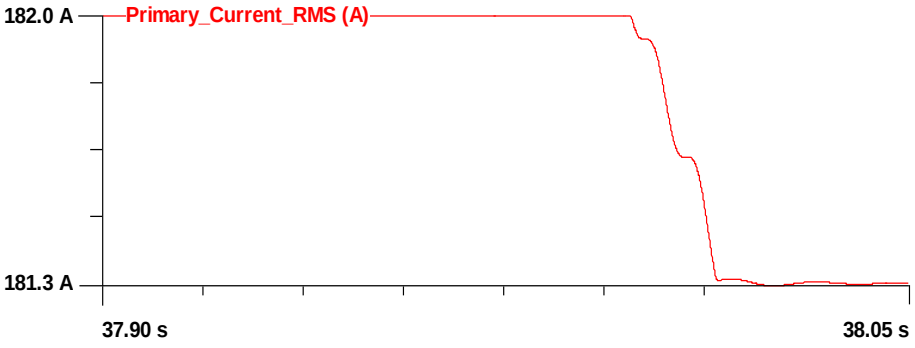

Figure 7 - 36. Time-overcurrent protection for transformer internal faults

(e) *Volts-over-hertz protection and thermal protection*

The volts-over-hertz protection function and thermal protection function are not for this situation.

(f) *Proposed DSE-based protection*

The results of proposed DSE-based protection are shown in Figure 7-37. When the inter-turn fault happens, there are not obvious changes in the terminal currents. However, the residuals of terminal currents increase from zero to considerable values. The chi-square goes from a very small value to 36, while the confidence level drops from 100% to zero immediately. This zero value indicates abnormalities inside the auto-transformer and protection actions would be taken as soon as possible. It is noticed that confidence level is oscillating during the fault period because the fault is too small. An integral function is applied to accumulate the confidence level values, and a trip decision is taken to protect the auto-transformer. It detects the fault at 38.0002 s and trips the transformer at 38.0082 s.

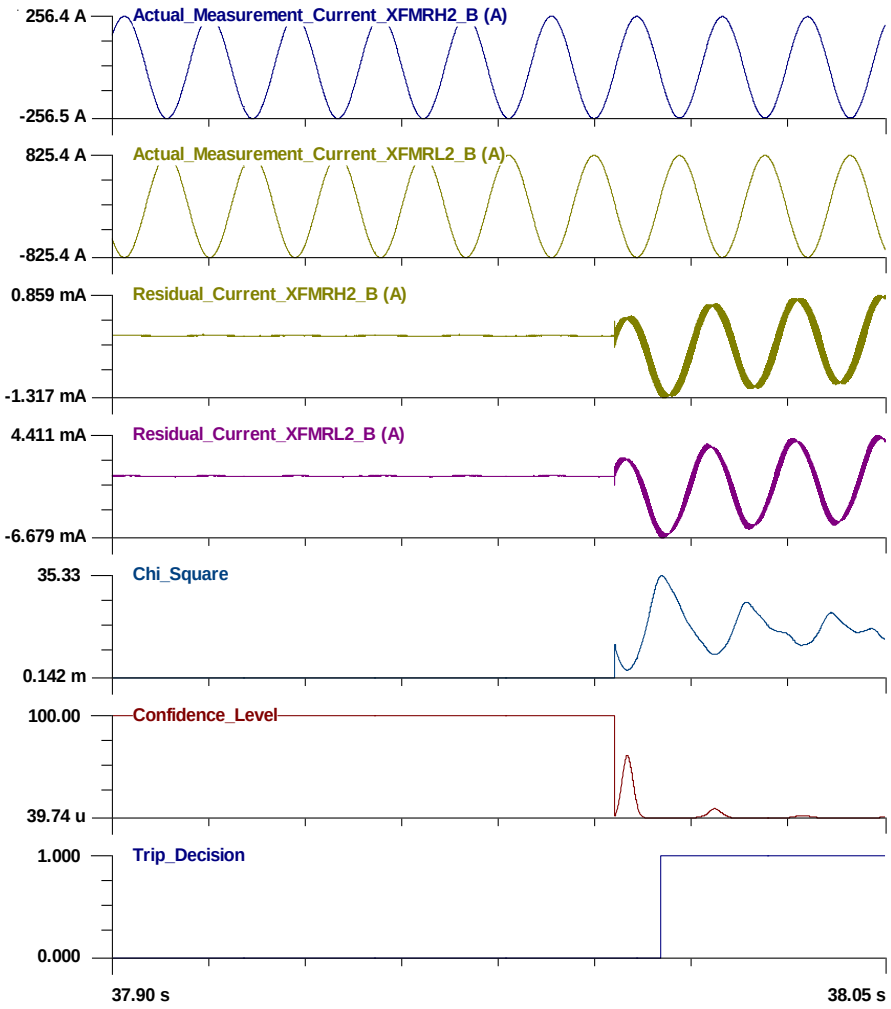

Figure 7 - 37. Proposed DSE-based protection for transformer internal faults

(h) *Summary of Event Five*

A summary of the protection method results for Event Five is shown in Table 7-5. In this event where a 1% internal fault happens to the auto-transformer, none of the legacy function could successfully detect the existence of inter-turn fault. In contrast, the proposed DSE-based scheme is able to detect it dependably with high sensitivity. Moreover, the speed of the proposed scheme is very fast and it only take 0.2ms to detect the existence of fault.

Table 7 - 5. Summary of Event Five: Internal Fault

Protection Methods	Falsely Trip	
Percentage differential	No	Undependable
Harmonic-restraint differential	No	Undependable
Negative-sequence differential	No	Undependable
Time-overcurrent	No	Undependable
Volts-over-hertz	NA	NA
Thermal	NA	NA
Proposed DSE-based	Yes	Dependable

7.7 Event Six: Auto-Transformer Over-Excitation

In this event, the auto-transformer T2 is over-excited during the simulation, as shown in Figure 7-38. The autotransformer is 35MVA 115kV/35kV/3.8kV and it is around 112% over-excited. The simulation time is 2min 30 sec.

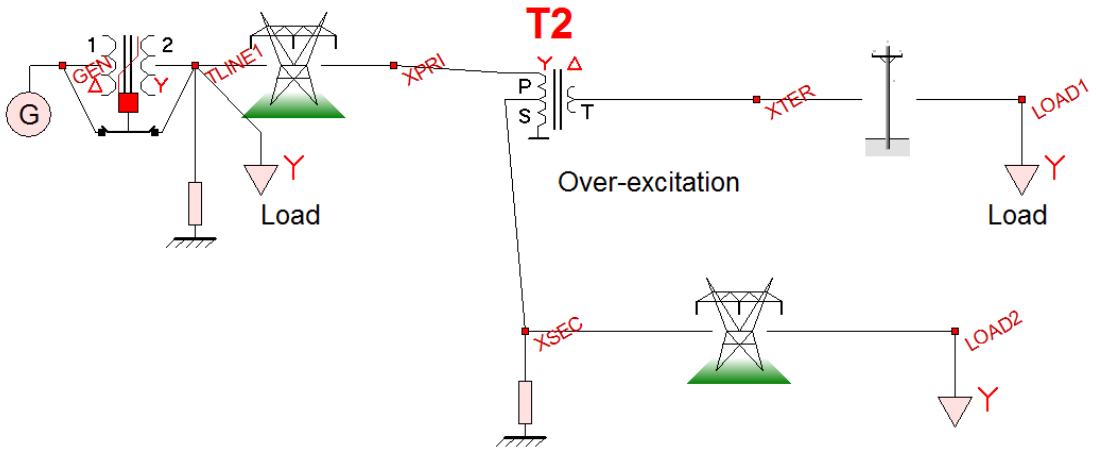

Figure 7 - 38. Auto-transformer over-excitation

The phase A terminal measurements of the autotransformer are shown in Figure 7-39. Note that the first three traces show the voltages at the primary, secondary and tertiary of the transformer and the second three traces show the currents. The results of legacy protection functions as well as the proposed method are presented next.

Figure 7 - 39. Auto-transformer phase A terminal measurements

(a) *Percentage differential protection, harmonic-restrained differential protection,*

negative-sequence differential protection and time-overcurrent protection

The percentage differential protection function, harmonic-restrained differential protection function, negative-sequence differential protection function and time-overcurrent protection function are not for this situation.

(b) *Volts-over-hertz protection*

The result of volts-over-hertz protection function is shown in Figure 7-40. The volts-over-hertz value is about 111.9%. According to the time characteristic of the autotransformer, this function would trip the transformer at time t = 120.0 sec.

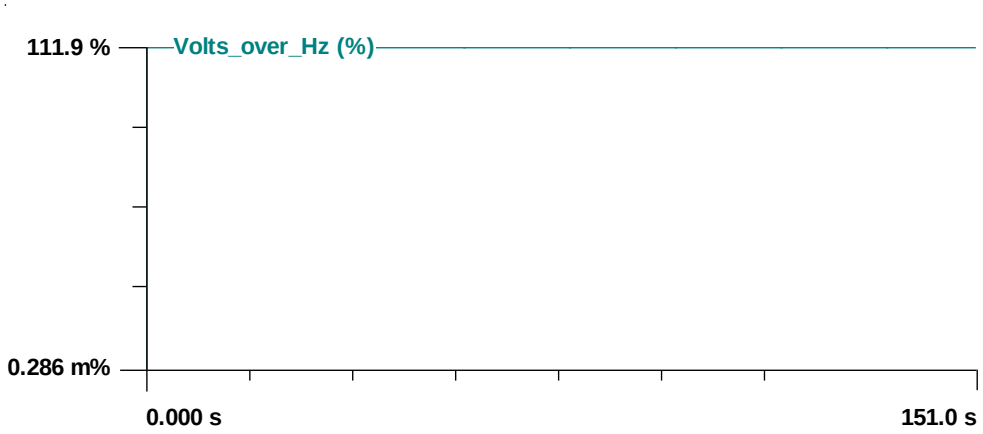

Figure 7 - 40. Volts-over-hertz protection for autotransformer over-excitation

(c) *Thermal protection*

The result of thermal protection function is shown in Figure 7-41. The hotspot temperature increases to 105.0 Celsius (the threshold) at time t = 111.2 sec, and it continues to increase. Therefore, the thermal protection function would trip the transformer at time t = 111.2 sec.

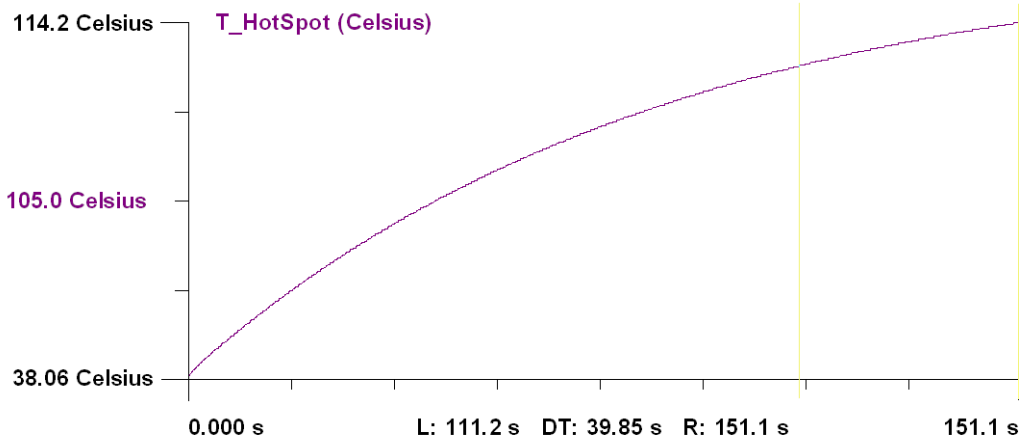

Figure 7 - 41. Thermal protection for autotransformer over-excitation

(e) *Proposed DSE-based protection*

The result of proposed DSE-based protection is shown in Figure 7-42. Based on the electro-thermal model, the DSE can estimate the temperature inside the auto-transformer. The estimated hottest temperature is the ET1 at the core, ant it reaches 105.0 Celsius (the threshold) at time t = 100.7 sec. Therefore, the DSE-based protection scheme will trip the transformer at time t = 100.7 sec.

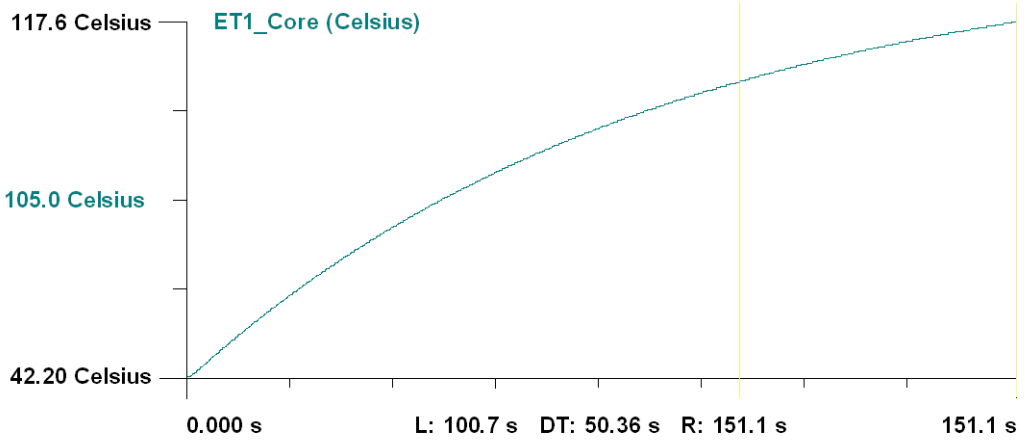

Figure 7 - 42. Proposed DSE-based protection for autotransformer over-excitation

(h) *Summary of Event Five*

A summary of the protection method results for Event Five is shown in Table 7-6. In this event where the autotransformer is 112% overexcited, the volts-over-hertz

protection function trips the transformer at t=120.0 s, the thermal protection function trips the transformer at t=111.2 s, and the DSE-based protection scheme trips the transformer at t=100.7 s. The DSE-based protection scheme takes less time to trip the transformer so that the transformer is better protected.

Table 7 - 6. Summary of Event Six: Transformer Over-excitation

Protection Methods	Trip Time
Volts-over-hertz	120.0 s
Thermal	111.2 s
Proposed DSE-based	100.7 s

7.8 Summary

In this chapter, the proposed DSE-based transformer protection scheme has been compared with six legacy protection schemes for different events. The results are summarized in Table 7-7 to Table 7-9.

According to the numerical results of different events, the proposed DSE-based scheme is secure, reliable, more sensitive and faster than legacy protection functions. In addition, the proposed method requires no coordination, and it has very few and simple settings. In this case, some unnecessary relay failures due to improper coordination, or improper settings, or even human errors can be avoided.

Table 7 - 7. Summary of Event 1~5: Fault Detection Time

Method / ***Event Number***	***Percentage Differential Protection***	***Harmonic Restrained Differential Protection***	***Negative Sequence Differential Protection***	***Time-Overcurrent Protection***	***DSE-Based Protection***
1	Falsely Trip	Correctly ignored	Falsely Trip	Correctly ignored	Correctly ignored
2	Wrongly ignored	Wrongly ignored	21.206 sec	Wrongly ignored	21.2002 sec
3	Falsely Trip	Wrongly ignored	Falsely Trip	Wrongly ignored	1.3262 sec
4	Wrongly ignored	Wrongly ignored	Wrongly ignored	Wrongly ignored	30.2002 sec
5	Wrongly ignored	Wrongly ignored	Wrongly ignored	Wrongly ignored	38.0002 sec

Table 7 - 8. Summary of Event 1~5: Fault Trip Time

Method / ***Event Number***	***Percentage Differential Protection***	***Harmonic Restrained Differential Protection***	***Negative Sequence Differential Protection***	***Time-Overcurrent Protection***	***DSE-Based Protection***
1	Falsely Trip	Correctly ignored	Falsely Trip	Correctly ignored	Correctly ignored
2	Wrongly ignored	Wrongly ignored	21.216 sec	Wrongly ignored	21.2082 sec
3	Falsely Trip	Wrongly ignored	Falsely Trip	Wrongly ignored	1.3342 sec
4	Wrongly ignored	Wrongly ignored	Wrongly ignored	Wrongly ignored	30.2082 sec
5	Wrongly ignored	Wrongly ignored	Wrongly ignored	Wrongly ignored	38.0082 sec

Table 7 - 9. Summary of Event 6: Time to Trip Overexcited Transformer

Method / *Event Number*	*Volts Over Hertz Protection*	*Thermal Protection*	*DSE-Based Protection*
6	120.0 sec	111.2 sec	100.7 sec

CHAPTER 8 CONCLUSION AND FUTURE WORK DIRECTION

8.1 Conclusion

The main contributions of this dissertation includes: (1) a new transformer protection scheme based on dynamic state estimation (DSE) has been proposed. The new scheme is secure, reliable, more sensitive and faster than legacy protection functions; (2) several protection gaps, such as transformer faults near the neutral, and inter-turn faults have been resolved with the proposed new method; (3) the electro-thermal models of several types of transformer are built in an object-oriented manner with the introduction of AQCF syntax; (4) the proposed DSE-based method uses the parameter calibration method to provide better models with validated parameters compared with traditional approaches; (5) the proposed method does not require coordination with other relays, and it only has very few and simple settings. Therefore, some unnecessary relay failures due to improper coordination, or improper settings, or even human errors can be avoided.

In particular, the proposed scheme is based on the dynamic state estimation using transformer dynamic model and the real-time measurements (terminal voltages, currents, temperatures, etc.). Three dynamic state estimation methods have been implemented to find the best estimates of transformer states, namely the unconstrained weighted least square (UCWLS) method, the constrained weighted least square (CWLS) method and the extended Kalman filter (EKF) method. With the output of the dynamic state estimator, a chi-square test is performed to determine how well the measured data

fit the dynamic model of the transformer. When the fit is within the accuracy of the meters by which the measurements are taking, the dynamic state estimator provides the true operating condition of the transformer. Any mismatch between the dynamic model and measurement indicates an internal abnormality.

There are many faults of transformer that are hard to be detected or correctly treated by the legacy protection functions, such as transformer faults near the neutral, internal faults during energization, and inter-turn faults, etc. In this dissertation, the proposed DSE-based protection are tested against six legacy methods (percentage-differential protection, harmonic-restraint differential protection, negative-sequence differential protection, overcurrent protection, volts-over-hertz protection, and thermal protection), for a number of "hard-to-be-detected" faults. Demonstration results show that new scheme is secure, reliable, more sensitive and faster than legacy protection functions. In some cases such as the 1% inter-turn fault of the transformer windings, neither legacy protection function is able to detect the existence of the fault, while the proposed method can quickly find out the fault. In conclusion, the proposed DSE-based scheme is capable to resolve the protection gaps of legacy methods.

To guarantee that the proposed DSE-based transformer protection scheme can be applied to any kind of transformers, an object-oriented model syntax is proposed and referred as the algebraic quadratic companion form (AQCF). This can be viewed as an advanced common information model. The measurements, obtained with traditional relaying instrumentations or via merging units, are also expressed in an object with

similar syntax as the AQCF. The proposed DSE-based protection scheme directly works with the model and measurements expressed in the above objects. To illustrate the implementation of this methodology, examples deriving of the AQCF electro-thermal models for both the regular single-phase saturable-core transformer and the single-phase auto-transformer are presented in the dissertation respectively.

Modeling accuracy and fidelity of the transformer are fundamental in this DSE-based approach. The actual transformer parameters used for state estimation are often quite different from the nameplate ratings, thus reliable transformer parameters calibration method are discussed in this dissertation. The basic approach of transformer parameters calibration is to expand the dynamic state estimation to include some independent parameters as state variables. Therefore the proposed method can also provide better models with validated parameters compared with traditional approaches. The dissertation provides an example of mathematical formulation of a single-phase autotransformer physical parameters identification problem to illustrate the procedure. Numerical results validate the feasibility of using dynamic state estimation to calibrate transformer physical parameters.

The numerical transformer relays are implemented with multiple protective functions that result in complex settings and even more complex coordination. This complexity increases the possibility of human error, and many times leads to inconsistencies and the possibility of improper protection actions. In contrast, the proposed DSE-based protection method does not require coordination with other relays,

and it only has very few and simple settings. This DSE-based method is almost "setting-less" comparing to the numerical relays. Failures due to improper coordination or settings can be avoided using the proposed method.

8.2 Future Work Directions

The proposed DSE-based protection method works really well in the laboratory for many different kinds of transformer models as well as for different events, but the proposed method has not been tested in the field yet. The next step is to test the DSE-based protection method on a real power transformer in the power system. Of course some problems are expected when applying this method on a real transformer, such as higher and non-Gaussian measurement noises or inaccurate model parameters. The original intention of proposed research is to develop a practical method to protect transformer with more sensitivity and reliability, so that some expected problems have already been taken into consideration when designing the protection algorithm. By continuously testing and refining the algorithm, practical DSE-based protection methods can be applied to protect the real power transformers.

The proposed method is object-oriented. It directly works with the model and measurements expressed in AQCF objects. Therefore, any protection zone, no matter it is a generator or transmission-line, can be protected similarly with the DSE-based method if the model and measurement are in AQCF objects. One of the future work direction includes testing the DSE-based method on other power system devices, or

other protection zones that consist of several devices. In fact, this method can be further implemented to protect an entire substation. The challenging problems of protecting a substation are (a) the dynamic model of substation could be too large for the real-time protection, (b) the configuration of a substation may change occasionally, which means the model may change. To solve the first problem, the quasi-domain dynamic state estimation can be used instead of the time-domain DSE. By using the quasi-domain DSE, the size of substation model is dramatically reduced. But the feasibility of applying the quasi-domain DSE should be further tested and verified. To solve the second problem, the autonomous operation and protection of the substation should be taken into serious consideration. More studies and tests are required to address this issue in the future work.

Nowadays many emerging technologies such as merging units with GPS synchronization, phasor measurement units (PMU), advanced metering infrastructures (AMI), remote terminal units (RTU) and other intelligent electronic devices (IED) have been implemented in modern power system, power system, there is an increasing cyber infrastructure in power systems which may be vulnerable to cyber-attacks. In addition, the increasing communications over utility networks coupled to public networks and multiple customer sites, the attack surface has drastically increased.

The proposed dynamic state estimation-based method in the dissertation could enable a cyber-physical modeling and simulation approach for situational awareness of the power system. Specifically, the DSE-based method can increase the cyber-security

of substations via data attack detection and context-based command authentication. Detection of maliciously altered data is enabled by the distributed dynamic state estimator and its tools, such as the chi-square test. The detection scheme provides the probability that a specific suspected datum is bad. A datum can be bad because of equipment malfunctioning, calibration, etc. However, additional information provided by the cyber-physical co-model can provide the probability whether the bad data are caused by a malicious data attack.

The command authentication is realized through three steps: (1) capture commands, (2) determine the effect of the captured commands on power system using a faster than real time simulation, and (3) authenticate or block the commands based on the faster than real-time simulation results.

The faster than real time simulation is achieved by constructing a subsystem model which comprises the substation of interest plus N-substations away. This model is constructed by simply retrieving the real-time model from these neighboring substations. Latencies are minimal. In addition, the rest of the system is represented with an equivalent with reduced size. The equivalent is computed at less frequent intervals and it does not have to be very accurate. Because this kind of simulation is performed at the substation level using high-end computers, it can be performed "faster than real time" to identify possible future vulnerabilities before they really occur.

PUBLICATIONS

1. Y. Liu, S. Choi, A.P.S. Meliopoulos, R. Fan, L. Sun and Z. Tan, "Dynamic State Estimation Enabled Predictive Inverter Control," *IEEE PES General Meeting, Boston*, MA, 2016.

2. A.P.S. Meliopoulos, G. Cokkinides, R. Fan, L. Sun and B. Cui, "Command Authentication via Faster Than Real Time Simulation," *IEEE PES General Meeting, Boston*, MA, 2016.

3. A.P.S. Meliopoulos, G. Cokkinides, Y. Liu, R. Fan, S. Choi and Paul T. Myrda, "Protection and Control of Converter Interfaced Generating (CIG)", *HICSS 2016, Hawaii*

4. R. Fan, A.P.S. Meliopoulos, G. Cokkinides, L. Sun and Y. Liu, "Dynamic State Estimation-based Protection of Power Transformers," *IEEE PES General Meeting*, Denver, CO, 2015.

5. Y. Liu, A.P.S. Meliopoulos, R. Fan and L. Sun, "Dynamic State Estimation-based Protection of Microgrid Circuits," *IEEE PES General Meeting*, Denver, CO, 2015.

6. P. Myrda, A.P.S. Meliopoulos, G. Cokkinides, L. Sun, R. Fan and R. Huang "Setting-less Dynamic State Estimation Based Protection," *Protection, Automation & Control (PAC) World Conference*, Zagreb, Croatia, June, 2014

7. A.P.S. Meliopoulos, L. Sun, R. Fan, and P. Myrda, "Update on Object-oriented DSE Based Protection", *Fault and Disturbance Conference*, Atlanta, GA, April 28-29, 2014.

8. R. Fan, D.Zhao, Z. Tan, L. Sun and A.P.S. Meliopoulos, "State space based modeling and sensitivity analysis of DFIG in an unbalanced network," *2013 North American Power Symposium*, Manhattan, KS, Sept. 22-24, 2013.

9. D. Zhao, A.P.S. Meliopoulos, Z. Tan and R. Fan, “Probability state sequence method for reliability analysis of wind farms considering wake effect,” *2013 North American Power Symposium*, Manhattan, KS, Sept. 22-24, 2013.

10. D. Zhao, A.P.S. Meliopoulos, Z. Tan, A. Umana and R. Fan, “A market-based operation method for distribution system with distributed generation and demand response,” *2013 North American Power Symposium (NAPS)*, Manhatan, KS, Sept. 22-24, 2013.

11. L. Sun, Z. Tan, R. Fan and A.P.S. Meliopoulos, “Transient response improvement of doubly-fed induction machine during unbalanced network,” *IEEE PES General Meeting*, Vancouver, Canada, July 21-25, 2013

12. D. Zhao, A.P.S. Meliopoulos, R. Fan, Z. Tan and Y. Cho, “Reliability evaluation with cost analysis of alternate wind energy farms and interconnections,” *2012 North American Power Symposium*, Champaign, IL, Sept. 09-11, 2012

APPENDICES

Appendix A: Quadratic Integration

Quadratic integration method is a numerical integration method that assumes that time domain functions vary quadratically within the integration time step. This assumption is illustrated in Figure A-1. Note that the three points, $x(t-h)$, x_m and $x(t)$ fully define the quadratic function in the interval $[t-h,t]$. The method is an implicit numerical integration method (it can be easily observed that it makes use of information at the unknown point $x(t)$) and therefore demonstrates the desired advanced numerical stability properties compared to explicit methods.

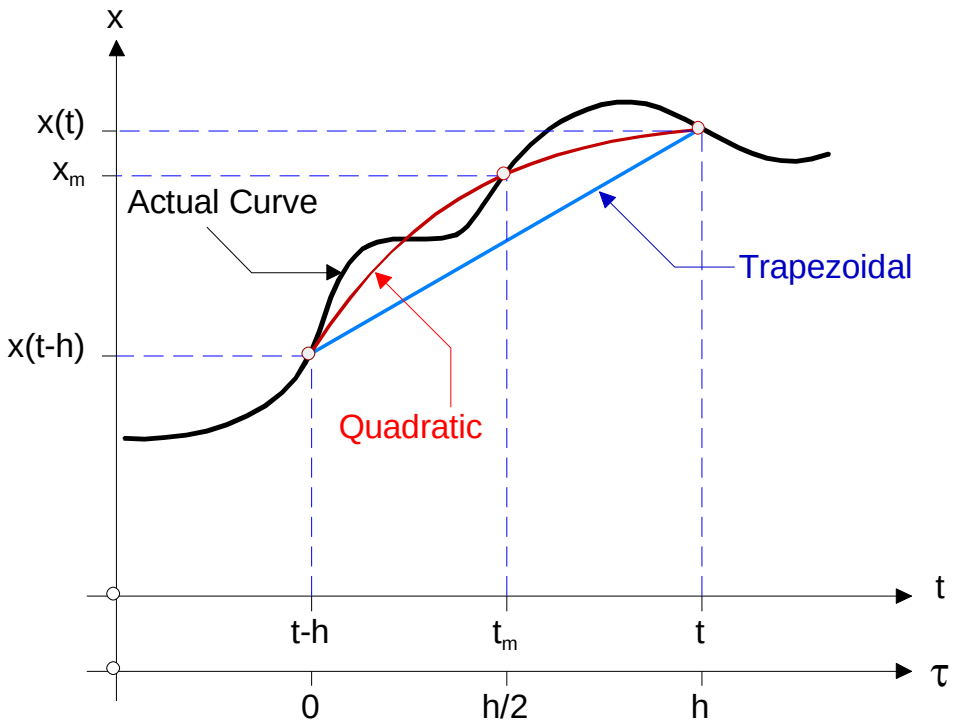

Figure A - 1. The quadratic integration method.

The general integration results are listed as follows,

Integration over time interval $[t-h,t_m]$:

$$\int_{t-h}^{t_m} x(\tau)d\tau = \frac{5h}{24}x(t-h) + \frac{h}{3}x_m - \frac{h}{24}x(t) \qquad \text{(A.1)}$$

Integration over time interval $[t-h, t]$:

$$\int_{t-h}^{t} x(\tau)d\tau = \frac{h}{6}x(t-h) + \frac{2h}{3}x_m + \frac{h}{6}x(t) \qquad \text{(A.2)}$$

Integration over time interval $t_m, t]$:

$$\int_{t_m}^{t} x(\tau)d\tau = -\frac{h}{24}x(t-h) + \frac{h}{3}x_m + \frac{5h}{24}x(t) \qquad \text{(A.3)}$$

Therefore, given the quadratized device model of a protection zone as:

$$i(t) = Y_{eqx1}\mathbf{x}(t) + Y_{equ1}\mathbf{u}(t) + D_{eqxd1}\frac{d\mathbf{x}(t)}{dt} + C_{eqc1}$$

$$0 = Y_{eqx2}\mathbf{x}(t) + Y_{equ2}\mathbf{u}(t) + D_{eqxd2}\frac{d\mathbf{x}(t)}{dt} + C_{eqc2}$$

$$0 = Y_{eqx3}\mathbf{x}(t) + Y_{equ3}\mathbf{u}(t) + \begin{Bmatrix} \vdots \\ \mathbf{x}(t)^T \left\langle F^i_{eqxx3} \right\rangle \mathbf{x}(t) \\ \vdots \end{Bmatrix} + \begin{Bmatrix} \vdots \\ \mathbf{u}(t)^T \left\langle F^i_{equu3} \right\rangle \mathbf{u}(t) \\ \vdots \end{Bmatrix} + \begin{Bmatrix} \vdots \\ \mathbf{u}(t)^T \left\langle F^i_{equx3} \right\rangle \mathbf{x}(t) \\ \vdots \end{Bmatrix} + C_{feqc3}$$

The model is obtained for a given time step h as follows:

1) Through variable equations:

$$i(t) = Y_{eqx1}\mathbf{x}(t) + Y_{equ1}\mathbf{u}(t) + D_{eqxd1}\frac{d\mathbf{x}(t)}{dt} + C_{eqc1}$$

After applying quadratic integration, we have

From time *t-h* to *t*,

$$i(t) = (\frac{4}{h}D_{eqxd1} + Y_{eqx1})\mathbf{x}(t) + Y_{equ1}\mathbf{u}(t) - \frac{8}{h}D_{eqxd1}\mathbf{x}(t_m) + (\frac{4}{h}D_{eqxd1} - Y_{eqx1})\mathbf{x}(t-h) + i(t-h) - Y_{equ1}\mathbf{u}(t-h)$$

From time *t-h* to t_m,

$$i(t_m) = \frac{1}{2h}D_{eqxd1}\mathbf{x}(t) + (\frac{2}{h}D_{eqxd1} + Y_{eqx1})\mathbf{x}(t_m) + Y_{equ1}\mathbf{u}(t_m) + (\frac{1}{2}Y_{eqx1} - \frac{5}{2h}D_{eqxd1})\mathbf{x}(t-h) - \frac{1}{2}i(t-h) + \frac{1}{2}Y_{equ1}\mathbf{u}(t-h) + \frac{3}{2}C_{eqc1}$$

2) Linear virtual equations:

$$0 = Y_{eqx2}\mathbf{x}(t) + Y_{equ2}\mathbf{u}(t) + D_{eqxd2}\frac{d\mathbf{x}(t)}{dt} + C_{eqc2}$$

After applying quadratic integration, we have

From time *t-h* to *t*,

$$0 = (D_{eqxd2} + \frac{h}{6}Y_{eqx2})\mathbf{x}(t) + \frac{h}{6}Y_{equ2}\mathbf{u}(t) + \frac{2h}{3}Y_{eqx2}\mathbf{x}(t_m) + \frac{2h}{3}Y_{equ2}\mathbf{u}(t_m) + (\frac{h}{6}Y_{eqx2} - D_{eqxd2})\mathbf{x}(t-h) + \frac{h}{6}Y_{equ2}\mathbf{u}(t-h) + hC_{eqc2}$$

From time *t-h* to t_m,

$$0 = -\frac{h}{24}Y_{eqx2}\mathbf{x}(t) - \frac{h}{24}Y_{equ2}\mathbf{u}(t) + (D_{eqxd2} + \frac{h}{3}Y_{eqx2})\mathbf{x}(t_m) + \frac{h}{3}Y_{equ2}\mathbf{u}(t_m) + (\frac{5h}{24}Y_{eqx2} - D_{eqxd2})\mathbf{x}(t-h) + \frac{5h}{24}Y_{equ2}\mathbf{u}(t-h) + \frac{h}{2}C_{eqc2}$$

3) Nonlinear equations

$$0 = Y_{eqx3}\mathbf{x}(t) + Y_{equ3}\mathbf{u}(t) + \begin{Bmatrix} \vdots \\ \mathbf{x}(t)^T \left\langle F^i_{eqxx3} \right\rangle \mathbf{x}(t) \\ \vdots \end{Bmatrix} + \begin{Bmatrix} \vdots \\ \mathbf{u}(t)^T \left\langle F^i_{equu3} \right\rangle \mathbf{u}(t) \\ \vdots \end{Bmatrix} + \begin{Bmatrix} \vdots \\ \mathbf{u}(t)^T \left\langle F^i_{equx3} \right\rangle \mathbf{x}(t) \\ \vdots \end{Bmatrix} + C_{eqc3}$$

These equations are the same under time t and time tm

$$0 = Y_{eqx3}\mathbf{x}(t) + Y_{equ3}\mathbf{u}(t) + \begin{Bmatrix} \vdots \\ \mathbf{x}(t)^T \left\langle F^i_{eqxx3} \right\rangle \mathbf{x}(t) \\ \vdots \end{Bmatrix} + \begin{Bmatrix} \vdots \\ \mathbf{u}(t)^T \left\langle F^i_{equu3} \right\rangle \mathbf{u}(t) \\ \vdots \end{Bmatrix} + \begin{Bmatrix} \vdots \\ \mathbf{u}(t)^T \left\langle F^i_{equx3} \right\rangle \mathbf{x}(t) \\ \vdots \end{Bmatrix} + C_{eqc3}$$

$$0 = Y_{eqx3}\mathbf{x}(t_m) + Y_{equ3}\mathbf{u}(t_m) + \begin{Bmatrix} \vdots \\ \mathbf{x}(t_m)^T \left\langle F^i_{eqxx3} \right\rangle \mathbf{x}(t_m) \\ \vdots \end{Bmatrix} + \begin{Bmatrix} \vdots \\ \mathbf{u}(t_m)^T \left\langle F^i_{equu3} \right\rangle \mathbf{u}(t_m) \\ \vdots \end{Bmatrix} + \begin{Bmatrix} \vdots \\ \mathbf{u}(t_m)^T \left\langle F^i_{equx3} \right\rangle \mathbf{x}(t_m) \\ \vdots \end{Bmatrix} + C_{eqc3}$$

REFERENCES

[1] J.L. Blackburn, and J.D. Thomas. *Protective relaying: principles and applications*. CRC press, 2014.

[2] B. Kasztenny, M. Thompson and N. Fischer, "Fundamentals of short-circuit protection for transformers," In *Protective Relay Engineers, 2010 63rd Annual Conference for*, pp. 1-13, 2010.

[3] A. P. Meliopoulos, and G. J. Cokkinides , "A Virtual Environment for Protective Relaying Evaluation and Testing," *IEEE Transactions on Power Systems*, Vol. 19, No. 1, pp. 104-111, February, 2004.

[4] A.P. Meliopoulos, L. Sun, R. Fan and P. Myrda, "Update on Object-oriented DSE Based Protection," *Proceedings of the 2014 Georgia Tech Fault and Disturbance Analysis Conference*, Atlanta, GA, 2014.

[5] North American Electric Reliability Corporation, *Misoperation Reports*, April 1, 2013.

[6] A. Guzman, H. Altuve, and D. Tziouvaras, "Power transformer protection improvements with numerical relays," *CIGRE Study Committee B5—Protection and Automation*, vol. 11, Sept. 14, 2015.

[7] V. Behjat, and A. Vahedi, "Numerical modelling of transformers interturn faults and characterizing the faulty transformer behavior under various faults and operating conditions," *IET electric power applications*, vol.5, no.5, pp.415-431, 2011.

[8] A. P. Meliopoulos, G. J. Cokkinides, R. Huang, E. Farantatos, S. Choi, Y. Lee and X. Yu, "Smart Grid Technologies for Autonomous Operation and Control," *IEEE Transaction on Smart Grid*, vol.2, no.1, pp.1-10, Mar. 2011.

[9] M. S. Sachdev, and M. A. Baribeau, "A new algorithm for digital impedance relays," *IEEE Transactions on Power Apparatus and Systems*, vol. 6, pp. 2232-2240, Nov. 1979.

[10] S. C. Sun, J. S. Wargo, and J. P. Garitty. "Electric power system with remote monitoring and control of protective relays," *U.S. Patent No. 4,972,290*, Nov. 1990.

[11] Y. Akimoto, T. Matsuda, K. Matsuzawa, M. Yamaura, R. Kondow, and T. Matsushima, "Microprocessor based digital relays application in TEPCO," *IEEE Transactions on Power Apparatus and Systems*, vol. 5, pp. 2390-2398, Nov. 1981.

[12] M. A. Rahman, and B. Jeyasurya, "A state-of-the-art review of transformer

protection algorithms," *IEEE Transactions on Power Delivery,* vol. 3, no. 2, pp. 534-544, 1988.

[13] P. Bastard, and H. Regal, "Differential protection device of a power transformer," *U.S. Patent No. 5,784,233*, Jul. 1998.

[14] R. E. Cordray, "Percentage-differential transformer protection," *Electrical Engineering*, vol. 50, no. 5, pp. 361-363, 1931.

[15] E. C. Wentz, and W. K. Sonnemann, "Current transformers and relays for high-speed differential protection, with particular reference to offset transient currents," *Electrical Engineering*, vol. 59, no. 8, pp. 481-488, 1940.

[16] C. R. Paul, "A comparison of the contributions of common-mode and differential-mode currents in radiated emissions," *IEEE Transactions on Electromagnetic Compatibility*, vol. 31, no. 2, pp. 189-193, 1989.

[17] W. E. Hyvarinen, and L. J. Rosell, "Parallel AC electrical system with differential protection immune to high current through faults," *U.S. Patent No. 4,173,774*, Nov. 1979.

[18] G. J Cokkinides, A. P. Meliopoulos and A.C. Westrom, "Method and apparatus for detecting and responding to downed conductors," *U.S. Patent No. 5,341,265*, Aug.. 1994.

[19] C.A. Mathews, "An improved transformer differential relay," *Electrical Engineering* vol.73, no.7, pp.648-648, 1954.

[20] K. Tian and P. Liu, "Improved Operation of Differential Protection of Power Transformers for Internal Faults Based on Negative Sequence Power," *Proceedings* of EMPD '98, vol. 2, pp. 422-425, 1998.

[21] H. T. Tseng, and J. F. Chen, "Voltage compensation-type inrush current limiter for reducing power transformer inrush current," *Electric Power Applications, IET* 6, no. 2, pp. 101-110, 2012.

[22] L. F. Kennedy, and C. D. Hayward, "Harmonic-current-restrained relays for differential protection," *Electrical Engineering*, vol. 57, no. 5, pp. 262-271, 1938.

[23] C. D. Hayward, "Harmonic-current-restrained relays for transformer differential protection," *Electrical Engineering*, vol. 60, no. 6, pp. 377-382, 1941.

[24] C. D. Hayward, "Prolonged inrush currents with parallel transformers affect differential relaying," *Transactions of the American Institute of Electrical Engineers*, vol. 60, no. 12, pp. 1096-1101, 1941.

[25] C. Concordia, C. N. Weygandt, and H. S. Shott, "Transient characteristics of current transformers during faults," *Electrical Engineering*, vol. 61, no. 5, pp. 280-285, 1942.

[26] J. Sykes, and I. Morrison, "A proposed method of harmonic restraint differential protecting of transformers by digital computer," *IEEE Transactions on Power Apparatus and System*s, vol. 3, no. PAS-91, pp. 1266-1272, 1972.

[27] W. Habib, and M. Marín, "A comparative analysis of digital relaying algorithms for the differential protection of three phase transformers," *IEEE Transactions on Power Systems*, vol.3, no. 3, pp. 1378-1384, 1988.

[28] N. Chiesa, and H. K. Høidalen, "Novel approach for reducing transformer inrush currents: laboratory measurements, analytical interpretation and simulation studies," *IEEE Transactions on Power Delivery,* vol. 25, no. 4, pp. 2609-2616, 2010.

[29] C.R. Mason, *Art & Science of Protective Relaying*, Vol. 195, Wiley, 1956.

[30] K. Tian and P. Liu, "Improved Operation of Differential Protection of Power Transformers for Internal Faults Based on Negative Sequence Power," *Proceedings of EMPD*, vol. 2, 1998.

[31] B. Kasztenny, N. Fischer,and H. J. Altuve, "Negative-sequence differential protection - principles, sensitivity, and security," *68th Annual Conference for Protective Relay Engineers*, pp. 364-379, 2015

[32] J. Rushton, "The fundamental characteristics of pilot-wire differential protection systems," *Proceedings of the IEE-Part A: Power Engineering*, vol. 108, no. 41, pp. 409-420, 1961.

[33] A. C. William, C. H. Martin, and P. C. Ronald, "Electrical protection systems," *U.S. Patent No. 3,225,256*, Dec., 1965.

[34] W. K. Sonnemann, "Universal sequence-current relaying means," *U.S. Patent 2,406,411*, Aug., 1946.

[35] T. S. Sidhu, and M. S. Sachdev, "Online identification of magnetizing inrush and internal faults in three-phase transformers," *IEEE Transactions on Power Delivery*, vol. 7, no. 4, pp. 1885-1891, 1992.

[36] M. M. Eissa, and O. P. Malik, "A new digital directional transverse differential current protection technique," *IEEE Transactions on Power Delivery*, vol. 11, no. 3, pp. 1285-1291, 1996.

[37] A. Guzmán, N. Fischer, and C. Labuschagne, "Improvements in transformer protection and control," *IEEE 62nd Annual Conference for Protective Relay*

Engineers, pp. 563-579, 2009.

[38] D. R. Parker, "Transformer Overcurrent Protection A Ten Point View", *IEEE Transactions on Power Apparatus and System*, vol. 101, no. 3, 00. 1723-1726, 1982.

[39] L. A. Kojovic, "Impact of current transformer saturation on overcurrent protection operation", *IEEE Power Engineering Society Summer Meeting*, vol. 3, pp. 1078-1083, 2002.

[40] R. W. Richard, and T. R. John, "High-speed self-restoring solid state overcurrent protection circuit," *U.S. Patent No. 3,386,005*, May 1968.

[41] K. Davy, "Overcurrent protection unit for alternating current machines," *U.S. Patent No. 3,119,951*, Jan. 1964.

[42] W. J. Premerlani, "Method for overcurrent protection," *U.S. Patent No. 4,432,031*, Feb. 1984.

[43] W. J. Carroll, "Overcurrent protection circuit utilizing peak detection circuit with variable dynamic response," *U.S. Patent No. 3,859,586*, Jan. 1975.

[44] R. Imazeki, M. Hattori, and S. Nakamura, "Overcurrent protection apparatus," *U.S. Patent No. 4,330,816*, May 1982.

[45] M. M. Giray, and M. S. Sachdev, "Off-nominal frequency measurements in electric power systems," *IEEE Transactions on Power Delivery*, vol. 4, no. 3, pp. 1573-1578, 1989.

[46] M. Kezunovic, and Y. Guo, "Modeling and simulation of the power transformer faults and related protective relay behavior," *IEEE Transactions on Power Delivery*, vol. 15, pp. 1, pp. 44-50, 2000.

[47] C. R. Mummert, "Excitation system limiter models for use in system stability studies," *IEEE Power Engineering Society 1999 Winter Meeting*, Vol. 1, 1999.

[48] C. H. Einvall, and J. R. Linders, "A three-phase differential relay for transformer protection," *IEEE Transactions on Power Apparatus and Systems*, vol. 94, no. 6, pp. 1971-1980, 1975.

[49] Benmouyal, Gabriel, "Design of a combined digital global differential and volt/hertz relay for step-up transformers," *IEEE Transactions on Power Delivery*, vol. 6, no. 3, pp. 1000-1007, 1991.

[50] Lee, D. C., P. Kundur, and R. D. Brown, "A high speed, discriminating generator loss of excitation protection," *IEEE Transactions on Power Apparatus and Systems*, vol. 6, pp. 1895-1899, 1979.

[51] G. W. Swift and S. E. Zocholl, M. Bajpai, J. F. Burger, C. H. Castro, S. R. Chano, F. Cobelo, S. P. De, E. C. Fennell, J. G. Gilbert, and S. E. Grier, "Adaptive transformer thermal overload protection", *IEEE Transaction on Power Delivery*, vol. 16, no. 4 pp. 516-52, 2001

[52] G. Swift, T. S. Molinski, and W. Lehn, "A fundamental approach to transformer thermal modeling. I. Theory and equivalent circuit," *IEEE Transactions on Power Delive*ry, vol. 16, no. 2, pp. 171-175, 2001.

[53] V. Galdi, L. Ippolito, A. Piccolo, and A. Vaccaro, "Neural diagnostic system for transformer thermal overload protection," *IEE Proceedings-Electric Power Application*s, vol. 147, no. 5, pp. 415-421, 2000.

[54] J. Perez, "Fundamental principles of transformer thermal loading and protection," *IEEE 63rd Annual Conference for Protective Relay Engineers*, pp. 1-14, May, 2010.

[55] A. M. Stoll, and M. A. Chianta, "A method and rating system for evaluation of thermal protection (No. NADC-MR-6809)," *Naval Air Development Center Warminster Pa Aerospace Medical Research Departmen*t, 1968.

[56] J. E. Pavlosky, and L. G. Stleger, "Apollo experience report: Thermal protection subsystem," 1974.

[57] R.P. Raj, "Transformer Core Fault Detection and Control," *Advance in Electronic and Electric Engineering*, vol. 3, no. 4, pp. 485-490, 2013.

[58] Brindisi, F, "Pressure relief valve unit," *U.S. Patent No. 3,844,310*, Oct. 1974.

[59] P. Osmokrović, "Mechanism of electrical breakdown of gases at very low pressure and interelectrode gap values," *IEEE Transactions on Plasma Science*, vol. 21, no. 6, pp. 645-653, 1993.

[60] J. R. Barr, "Pressure temperature relay," *U.S. Patent 2,553,291*, May, 1951.

[61] A. V. Riemsdijk, "Transformers and composite tap changers associated therewith," *U.S. Patent No. 3,546,535*, Dec., 1970.

[62] I. Jacques, "Method and device for supplying gas under pressure from a storage tank containing the said gas in liquefied state," *U.S. Patent No. 3,898,853*, Aug. 1975.

[63] R.R. Rogers, "IEEE and IEC codes to interpret incipient faults in transformers, using gas in oil analysis," *IEEE Transactions on Electrical Insulation*, vol. 5 pp. 349-354, 1978.

[64] O.P. Malik, P.K. Dash and G.S. Hope, "Digital protection of a power

transformer," *IEEE Transactions on Power Apparatus and System,* vol. 95, no. 3, pp. 763-763, 1976.

[65] M. A. Rahman, and P. K. Dash, "Fast algorithm for digital protection of power transformers," *Generation, Transmission and Distribution, IEE Proceedings,* vol. 129, no. 2, 1982.

[66] E. P. Dick, and C. C. Erven, "Transformer diagnostic testing by frequency response analysis," *IEEE Transactions on Power Apparatus and Systems,* vol.6, pp. 2144-2153, 1978.

[67] S. K. Pandy and L. Satish, "Multi-resolution signal decomposition: A new tool for fault detection in power transformers during impulse tests," *IEEE Transactions on Power Delivery*, vol. 13, no. 4, pp. 1194–1200, Nov. 1998.

[68] A. G. Phadke, J. S. Thorp, and M. G. Adamiak, "A new measurement technique for tracking voltage phasors, local system frequency, and rate of change of frequency," *IEEE Transactions on Power Apparatus and Systems*, vol. 5, pp. 1025-1038, 1983.

[69] A. G.Phadke, T. Hlibka, and M. Ibrahim, "A digital computer system for EHV substations: analysis and field tests," *IEEE Transactions on Power Apparatus and Systems*, vol. 95, no. 1, pp. 291-301, 1976.

[70] L. G. Perez, A. J. Flechsig, J. L Meador and Z. Obradovic, "Training an artificial neural network to discriminate between magnetizing inrush and internal faults," *IEEE Transactions on Power Delivery,* vol. 9, no. 1, pp. 434-441, 1994.

[71] J. Pihler, B. Grcar and D. Dolinar, "Improved operation of power transformer protection using artificial neural network," *IEEE Transactions on Power Delivery,* vol. 12, no. 3, pp. 1128-1136, 1997.

[72] H. P. Graf, and D. Henderson, "A reconfigurable CMOS neural network," *37th IEEE International Solid-State Circuits Conference, Digest of Technical Papers*, pp. 144-145, 1990.

[73] T. S. Sidhu, H. Singh, and M. S. Sachdev, "Design, implementation and testing of an artificial neural network based fault direction discriminator for protecting transmission lines," *IEEE Transactions on Power Delivery*, vol. 10, no. 2, pp. 697-706, 1995.

[74] P. Bastard, M. Meunier, and H. Regal, "Neural network-based algorithm for power transformer differential relays," *IEE Proceedings- Generation, Transmission and Distribution*. Vol. 142. No. 4. , 1995.

[75] Dalstein, Thomas, and Bernd Kulicke, "Neural network approach to fault classification for high speed protective relaying," *Power Delivery, IEEE Transactions on* 10.2 (1995): 1002-1011.

[76] Klir, George, and Bo Yuan. *Fuzzy sets and fuzzy logic*. Vol. 4. New Jersey: Prentice Hall, 1995.

[77] A. Wiszniewski and B. Kasztenny, "A multi-criteria differential transformer relay based on fuzzy logic," *IEEE Transactions on Power Delivery*, vol.10, pp. 1786–1792, Oct. 1995.

[78] A. Wiszniewski, and B. Kasztenny, "Fuzzy set approach to transformer differential relay," *IET Fifth International Conference on Developments in Power System Protection*, 1993.

[79] M. C. Shin, C. W. Park and J. H. Kim, "Fuzzy logic-based relaying for large power transformer protection," *IEEE Transactions on Power Delivery*, vol. 18, no. 3, pp. 718-724, 2003.

[80] A. Ferrero, S. Sangiovanni, and E. Zappitelli, "A fuzzy-set approach to fault-type identification in digital relaying," *IEEE Proceedings of the Power Engineering Society Transmission and Distribution Conference*, 1994.

[81] C. S. Burrus, R. A. Gopinath, and H. Guo, "Introduction to wavelets and wavelet transforms: a primer," 1997.

[82] M. G. Morante, and D. W. Nicoletti, "A wavelet-based differential transformer protection," *IEEE Transactions on Power Delivery*, vol. 14, no. 4, pp. 1351-1358, 1999.

[83] A. Saleh, and M. A. Rahman, "Modeling and protection of a three-phase power transformer using wavelet packet transform," *IEEE Transactions on Power Delivery*, vol. 20, no. 2, pp. 1273-1282, 2005.

[84] A. I. Megahed, A. Ramadan and W. ElMahdy, "Power transformer differential relay using wavelet transform energies," *2008 IEEE PES General Meeting-Conversion and Delivery of Electrical Energy*, pp. 1-6, 2008.

[85] O. Chaari, M. Meunier, and F. Brouaye, "Wavelets: a new tool for the resonant grounded power distribution systems relaying," *IEEE Transactions on Power Delivery*, vol. 11, no. 3, pp. 1301-1308, 1996.

[86] O. Chaari, and M. Meunier, "A recursive wavelet transform analysis of earth fault currents in Petersen-coil-protected power distribution networks," *Proceedings of the IEEE-SP International Symposium on Time-Frequency and Time-Scale*

Analysis, pp. 162-165, 1994.

[87] W. Zhang, Q. Tan, S. Mian, L. Zhou and P. Liu, "Self-adaptive transformer differential protection," *IET Proceedings on Generation, Transmission and Distribution*, vol. 7, no. 1, pp. 61-68, 2013.

[88] S. Dambhare, S. A. Soman, and M. C. Chandorkar, "Adaptive current differential protection schemes for transmission-line protection," *IEEE Transactions on Power Delivery*, vol. 24, no. 4, pp. 1832-1841, 2009.

[89] S. Sheng, K. Li, W. L. Chan, X. Zeng, D. Shi, and X. Duan, "Adaptive agent-based wide-area current differential protection system," *IEEE Transactions on Industry Applications*, vol. 46, no. 5, pp. 2111-2117, 2010.

[90] S. H. Horowitz, A. G. Phadke, and J. S. Thorp, "Adaptive transmission system relaying," *IEEE Transactions on Power Delivery*, vol. 3, no. 4, pp. 1436-1445, Oct. 1988.

[91] T. Hayder, U. Schaerli, K. Feser, and L. Schiel, "Universal adaptive differential protection for regulating transformers," *IEEE Transactions on Power Delivery*, vol. 23, no. 2, pp. 568-575, 2008.

[92] Z. Sun, and Y. Chen, "Transformer Differential Protection Based on the Characteristic Analysis of the First And Second Half Cycle of the Magnetizing In-Rush Current [J]," *Automation of Electric Power Systems*, vol. 4, 1996.

[93] H. Dashti, and M. S. Pasand, "Power Transformer Protection Using a Multiregion Adaptive Differential Relay," *IEEE Transactions on Power Delivery*, vol. 29, no. 2, pp. 777-785, 2014.

[94] A. P. Meliopoulos, G. J. Cokkinides, R. Fan, R. Huang, Y. Lee, L. Sun and Z. Tan, , "Setting-less Protection: Laboratory Testing", *PSERC Publication 14-03*, June 2014.

[95] *Chi-square tests*. Defense Technical Information Center, 1976.

[96] A. Fayed, W. Elgharbawy, and M. Bayoumi, "A data merging technique for high-speed low-power multiply accumulate units," *2004 IEEE International Conference on Acoustics, Speech, and Signal Processing*, Vol. 5, 2004.

[97] T. S. Sidhu, and Y. Yin, "Modelling and simulation for performance evaluation of IEC61850-based substation communication systems," *IEEE Transactions on Power Delivery*, vol. 22, no.3, pp. 1482-1489, 2007.

[98] R. E. Mackiewicz, "Overview of IEC 61850 and Benefits," *IEEE PES Power Systems Conference and Exposition*, 2006.

[99] L. Andersson, C. Brunner, and F. Engler, "Substation Automation based on IEC 61850 with new process-close Technologies," *IEEE Bologna Power Tech Conference Proceedings*, vol. 2, 2003.

[100] A.P. Meliopoulos, G. J. Cokkinides and G. K. Stefopoulos, "Quadratic integration method," *Proceedings of the 2005 International Power System Transients Conference, pp. 19-23,* 2005.

[101] G. K. Stefopoulos, G. J. Cokkinides, and A. P. Meliopoulos, "Quadratic integration method for transient simulation and harmonic analysis," *IEEE 13th International Conference on Harmonics and Quality of Power*, 2008.

[102] A. P. Meliopoulos, G. J. Cokkinides, and R.I. James, "Transformer Diagnostic System for Loss of Life and Coil Integrity," *Proceedings of the 1998 Georgia Tech Fault and Disturbance Analysis Conference*, Atlanta, GA,1998

[103] A. Sage, *Optimum systems control*. Southern Methodist University Dallas Information and Control Sciences Center, 1968.

[104] H. Sorenson, "Least-squares estimation: from Gauss to Kalman," *IEEE Spectrum*, vol. 7, no. 7, pp. 63-68, 1970.

[105] A. P. Meliopoulos, and F. Zhang, "Multiphase power flow and state estimation for power distribution systems," *IEEE Transactions on Power Systems*, vol. 11, no. 2, pp. 939-946, 1996.

[106] A. Abur, and A. Exposito. *Power system state estimation: theory and implementation*. CRC Press, 2004.

[107] D. L. Phillips, "A technique for the numerical solution of certain integral equations of the first kind," *Journal of the ACM*, vol. 9, pp. 97-101, 1962.

[108] B. R. Hunt, "The application of constrained least squares estimation to image restoration by digital computer." *IEEE Transactions on Computers*, vol. 100, no. 9, pp. 805-812, 1973

[109] G. Golub, and U. Matt, "Quadratically constrained least squares and quadratic problems," *Numerische Mathematik*, vol. 59, no. 1, pp. 561-580, 1991.

[110] S. S. Haykin, *Kalman filtering and neural networks*, pp. 221-269, New York: Wiley, 2001.

[111] Z. Huang, K. Schneider, and J. Nieplocha, "Feasibility studies of applying Kalman Filter techniques to power system dynamic state estimation," *IEEE International Power Engineering Conference*, pp. 376 - 382, 2007

[112] R. Fan, Z. Huang, S. Wang, R. Diao and D. Meng, "Dynamic state estimation and parameter calibration of a DFIG using the ensemble Kalman filter," *IEEE Power & Energy Society General Meeting*, Denver, 2015

[113] Y. Wang, and D. Lu, "On-line Correction of Transformer Parameter Based on Orthogonal Least Squares," *IEEE 3rd International Conference on Advanced Computer Theory and Engineering*, vol. 6, 2010.

[114] C. Borda, A. Olarte and H. Diaz, "PMU-based Line and Transformer Parameter Estimation," *IEEE PES Power Systems Conference and Exposition*, pp. 1-8, 2009.